Studies of Leading Catalysts for Olefin Metathesis: Evaluation of Synthetic Routes and Participation in Catalysis

Xinrui Ou

Thesis submitted to the University of Ottawa
in partial Fulfillment of the requirements for the degree of

Master of Science

Center for Catalysis Research and Innovation
Department of Chemistry and Biomolecular Science
Ottawa-Carleton Chemistry Institute
Faculty of Science
University of Ottawa

Table of Contents

List of Figures

List of Schemes

List of Tables

Abstract

Olefin metathesis is increasingly popular for the construction of carbon-carbon double bonds. In the past two decades, ruthenium metathesis catalysts have seen extensive development. Two marvelous early developments were the introduction of N-heterocyclic carbene (NHC) ligands, which greatly improved catalyst activity, and replacement of a nucleophilic stabilizing ligand (the alkylphosphine PCy_3) by a chelated benzylidene-ether. A more recent breakthrough is the introduction of cyclic alkyl amino carbene (CAAC) ligands as alternatives to the NHCs. Over the past 5 years, the CAAC catalysts have drawn much attention for their breakthrough productivity in challenging reactions, including ethenolysis and RCM macrocyclization.

Nevertheless, important challenges remain. As discussed in the first part of this thesis, these include the synthesis of key ligands (in particular, the styrenyl ether ligands $H_2C=^{13}CH\text{-}C_6H_4\text{-}2\text{-}O^iPr$ and $H_2C=^{13}CH\text{-}C_6H_3\text{-}2\text{-}O^iPr\text{-}5\text{-}NO_2$), which represent the source of the chelated benzylidene-ether noted above) and key catalysts (e.g., Hoveyda- and Grela-class catalysts bearing an H_2IMes or CAAC carbene ligand). A further challenge lies in understanding the behaviour of the styrenyl ether ligands – for example, how they contribute to catalyst partitioning between active, resting-state, and decomposed species, and the impact of the carbene ligand on that partitioning.

An initial objective was synthesis of labelled styrenyl ethers that would enable synthesis of Hoveyda and Grela catalysts with a ^{13}C-label at the alkylidene carbon. While $H_2C=^{13}CH\text{-}C_6H_4\text{-}2\text{-}O^iPr$ could be accessed, its nitro analogue could not, probably owing to attack on the NO_2 substituent. The remainder of Chapter 2 assessed reported routes to **HII/nG** and **HII-C1/nG-C1**, and reports on challenges and reproducibility issues. Difficulties in synthesis of the CAAC catalysts are attributed to the need for in situ-generated CAACs, and catalyst decomposition by the base required for deprotonation (i.e KHMDS or LiHMDS).

The second part of this thesis explores the impact of the NHC or CAAC ligands on initiation and "boomerang" recapture of the styrenyl ether ligands for Hoveyda- and Grela-class catalysts. Examination of the kinetics of initiation with bulky *t*-butyl vinyl ether (tBuVE) revealed a linear dependence of k_{obs} on [tBuVE], and faster reaction by the *p*-NO_2-substituted Grela catalyst. These data suggest an associative or interchange-associative (I_A) mechanism. A systematic comparison of initiation rate constants revealed the trend **HII** > **nG-C1** > **HII-C1** in chlorinated and aromatic solvents. Recapture of added styrenyl ether ligand was examined in macrocyclization (mRCM). Rate plots indicated inhibition by this ligand, even at the high dilutions required for mRCM, implying that boomerang re-uptake of the styrenyl ether is indeed operative for both Hoveyda- and Grela-class catalysts. However, inhibition was found to be more profound for **HII** than **HII-C1** or **nG-C1**. That is, the NHC catalysts are much more susceptible to partitioning into the off-cycle (precatalyst) form than are the CAAC catalysts. This higher commitment to the active cycle may be an important contributor to the impressive productivity of the CAAC catalysts. In addition, the slow initiation of these catalysts indicated above may be an asset, rather than a limitation, as it inhibits their susceptibility to bimolecular decomposition.

List of Contributions

Presentations (O = Oral, P = Poster; presenting author in bold)

P2. **X. Ou** and D. E. Fogg. "Assessing Initiation Rates for Key Metathesis Catalysts" 102nd Canadian Society for Chemistry Conference, Quebec City, QC, June 3rd, 2019.

O1. **X. Ou** and D. E. Fogg. "Examining the ligand impact on the Hoveyda/Grela precatalyst" Ottawa-Carleton Chemistry Institute (OCCI) Day, Ottawa, ON, May 23rd, 2019.

Publications

1. X. Ou, D. L. Nascimento, G. Occhipinti, V. R. Jensen and D. E. Fogg. "A Paradigm Inversion in Ru-Catalyzed Olefin Metathesis: Enhancing Metathesis Productivity by Slowing Catalyst Initiation" (Manuscript in preparation).

Acknowledgments

First of all, I would like to thank my supervisor Prof. Deryn Fogg for her guidance, support, and patience during my graduate studies. I really appreciate her guidance and help. I learned in the Fogg group important skills, knowledge and attitude that will help shape my future.

I have greatly valued the support of the uOttawa NMR staff, Dr. Glenn Facey and Dr. Peter Pallister. Dr. Pallister, I would like to thank you for your patience in NMR training and answering many questions on techniques.

To the members of the Fogg group: I would like to thank you all for your support, training and help. Alex, I would like to thank you for training on the use and maintenance of glovebox. Stephanie, I would like to thank you for communication on ideas and experimental tricks. Andrew, thanks for your help on experiments or life during my graduate study. Daniel, I would like to thank you for all your help and guidance. Nathan, thanks for bubble tea time. EJ and Christian, thanks for the joy that you bring to the lab.

To my family: Mom and Dad, I thank you for your support during my Master's degree. I gratefully appreciate your love and support over a period of immense challenges around the world.

List of Compounds

Organic and main-group compounds

Compound	Structure	Compound	Structure
H_2IMes	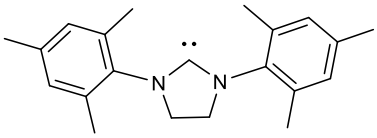	**C1**	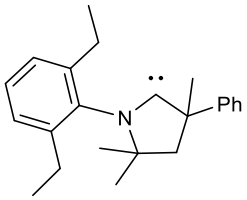
C2	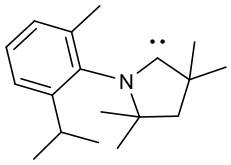	**C3**	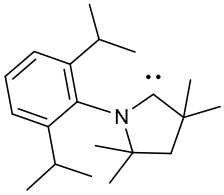
1	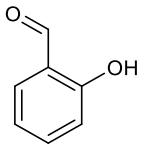	**1’**	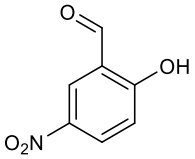
2	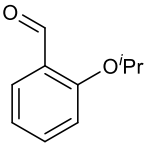	**2’**	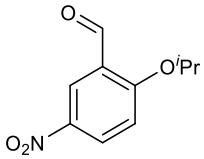
3	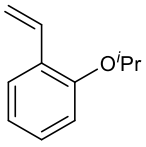	**3’**	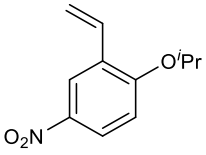
4	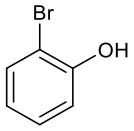	**4’**	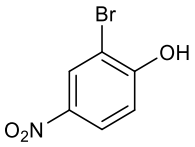
5	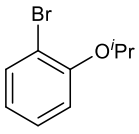	**5’**	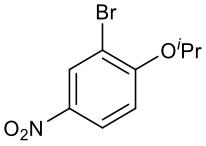
6	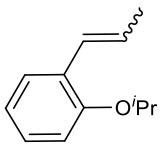	**6’**	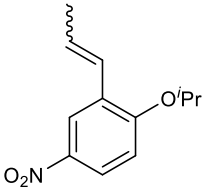

7	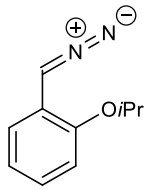	**8**	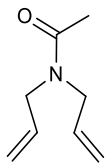
9	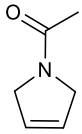	**10**	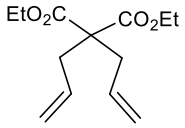
11	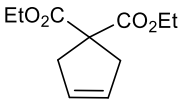	**12**	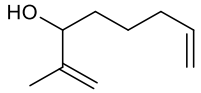
13	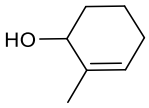	**14**	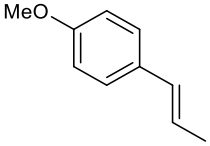
15	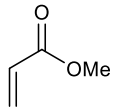	**16**	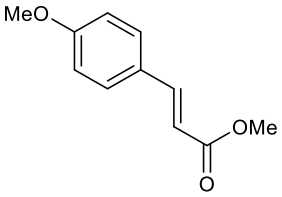
17	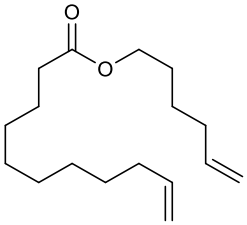	**18**	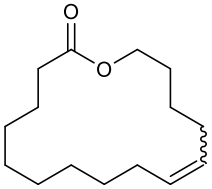
EVE	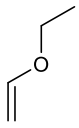	**tBuVE**	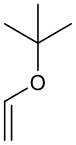
C1·BF_4	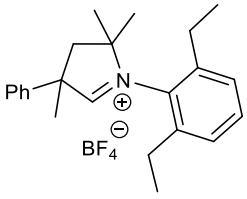	**LiHMDS**	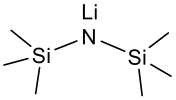
KHMDS	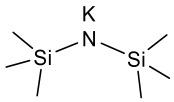		

Transition-metal complexes

Compound	Structure	Compound	Structure
Ta-1	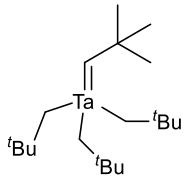	**MAP**	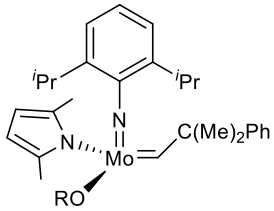
Mo-1	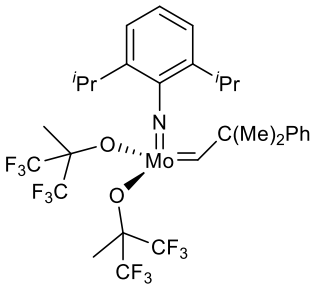	**GI**	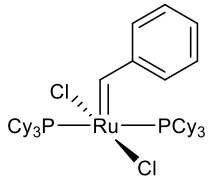
W-1	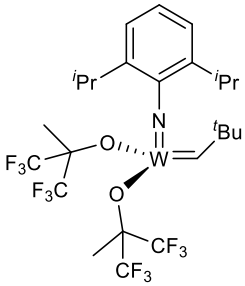	**GII**	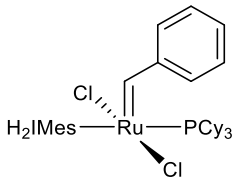
GIm	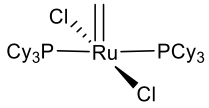	**GIIm**	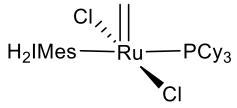
HI	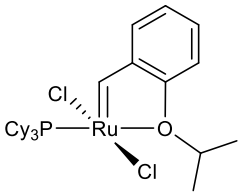	**nGI**	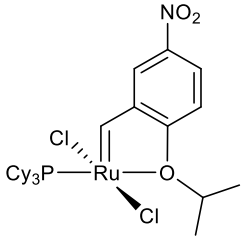
HII	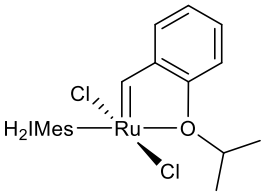	**nG**	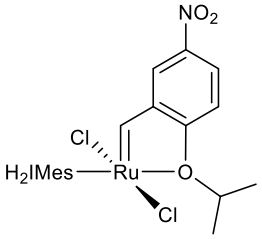

Ind-0	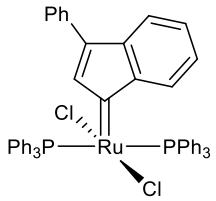	**Ind-I**	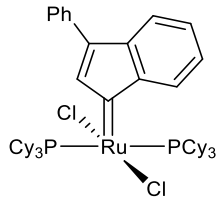
Ind-II	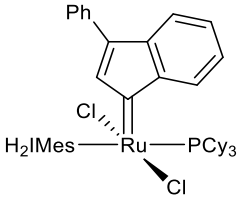	**UC-C1**	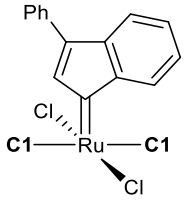
UC-dimer	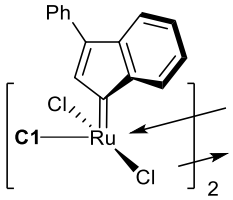	**HII-C1**	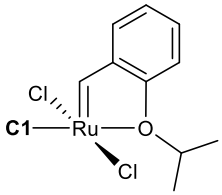
HII-C2	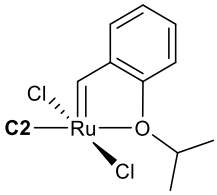	**nG-C1**	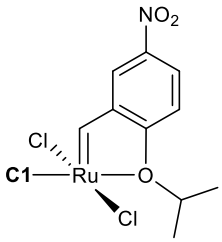
HII-PCy3	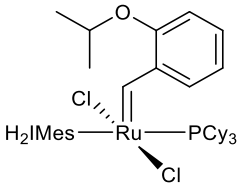	**HII'**	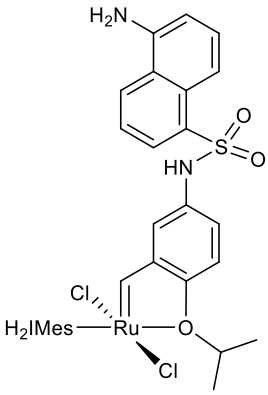
HII-*d*	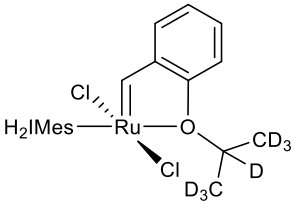	**Ru-1**	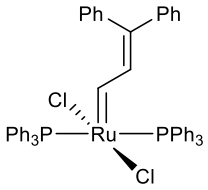
Ru-2	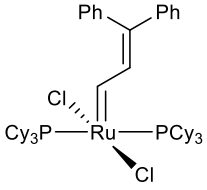	**Ru-3**	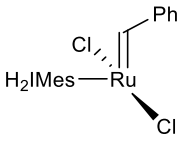

Ru-4	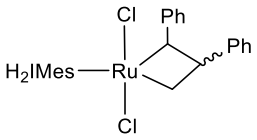	**Ru-5**	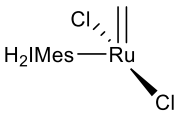
Ru-5'	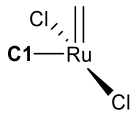	**Ru-6**	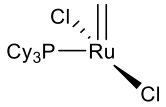
Ru-7	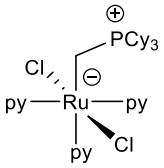	**Ru-8**	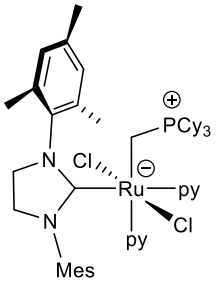
Ru-9	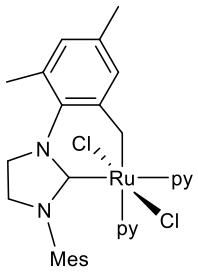	**Ru-10**	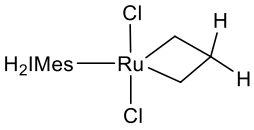
Ru-10'	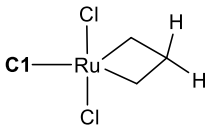	**Ru-11**	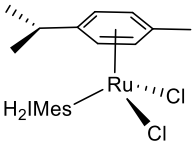
Ru-12	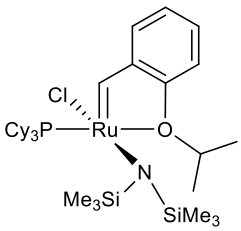	**Ru-13**	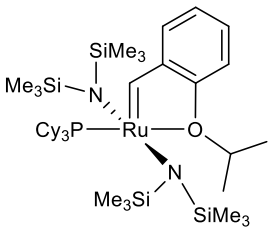
Ru-14	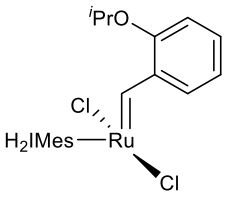	**Ru-15**	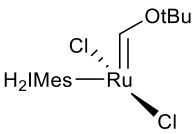
Ru-15'	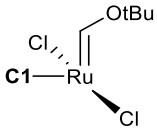		

List of Abbreviations

BMC	Bimolecular coupling
CAAC	Cyclic alkyl amino carbene
CM	Cross-metathesis
DMT	Dimethyl terephthalate
Equiv	Equivalents
EtOAc	Ethyl acetate
Et_2O	Diethyl ether
FID	Flame-ionization detector
GC	Gas chromatography
KHMDS	Potassium bis(trimethylsilyl)amide
KOtBu	Potassium tert-butoxide
KOtPe	Potassium tert-pentoxide
KTp	Potassium tris(1-pyrazolyl) borate
LDA	Lithium diisopropylamide
LiHMDS	Lithium bis(trimethylsilyl)amide
MAP	Monoaryloxide pyrrolide
MCB	Metallacyclobutane
MeOH	Methanol
mRCM	Macrocyclic ring-closing metathesis
NHC	N-heterocyclic carbene
NMR	Nuclear magnetic resonance
RCM	Ring-closing metathesis
ROMP	Ring-opening metathesis polymerization
THF	Tetrahydrofuran
TMB	1,3,5-trimethoxybenzene
TON	Turnover number

Chapter 1. Introduction

1.1 Background: Olefin metathesis

Olefin metathesis is one of the most versatile catalytic tools available for the construction of carbon-carbon bonds.[1] According to the Chauvin mechanism, the process is catalyzed by transition-metal alkylidene complexes (Scheme 1.1).[2] Thus, the olefin (alkene) substrate undergoes a [2+2] cycloaddition reaction with a metal alkylidene to form a metallacyclobutane (MCB) intermediate. The MCB then undergoes cycloreversion, either regenerating the starting alkene and alkylidene species, or redistributing the carbon-carbon double bond.

Scheme 1.1 The Chauvin mechanism for olefin metathesis

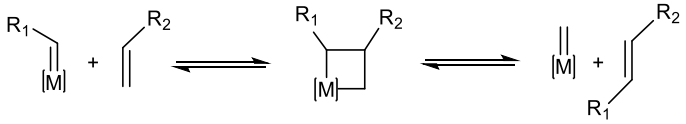

The three most important applications of this process, shown in Scheme 1.2, are ring-opening metathesis polymerization (ROMP), cross-metathesis (CM), and ring-closing metathesis (RCM). Each of these gives access to a key area of chemistry. ROMP opens the door to constructing specialty polymers using strained monomers.[3] CM has received most attention in "green chemistry", as a way to synthesize important compounds from renewable feedstocks, by metathesis of the internal olefins present in plant oils.[4] RCM, in particular, stands out for having brought organic chemists' attention to the potential of olefin metathesis. RCM has been recognized as a crucial strategy in total synthesis,[5] and is beginning to be used as a core methodology in pharmaceutical manufacturing, for the production of macrocycles as potential antiviral drugs.[6]

Scheme 1.2 Key applications of olefin metathesis

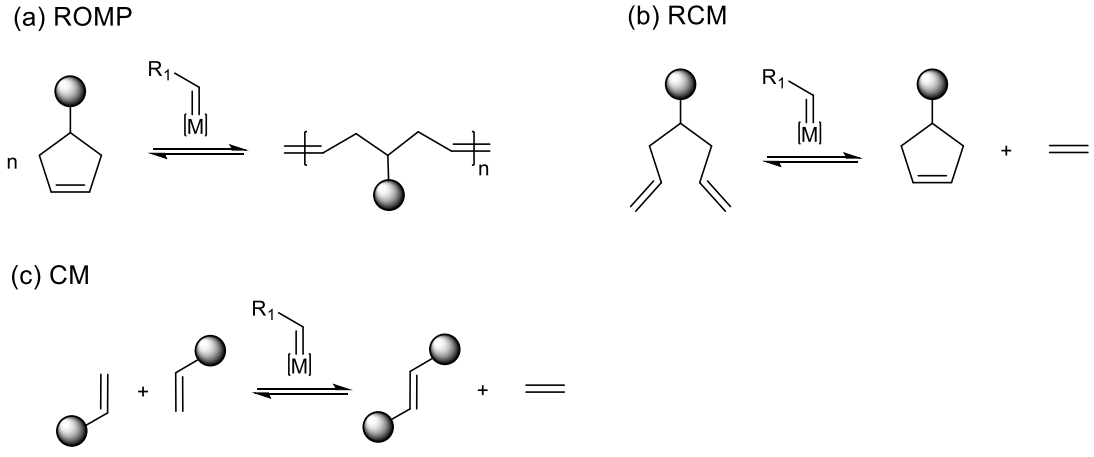

1.2 Olefin metathesis catalysts

1.2.1 Group 6 catalysts: Mo and W

A large number of olefin metathesis catalysts has been developed since Schrock and coworkers reported the first "well-defined" metal alkylidene complex **Ta-1** (Chart 1.1) in 1974.[7] Although this tantalum alkylidene complex was not very active in olefin metathesis, it is nevertheless a key structure, in that its synthesis demonstrated the feasibility of the all-carbon alkylidene ligand, and led to the synthesis and design of other group 6 metal catalysts.[8] The classic Schrock catalysts **Mo-1** and **W-1**, and current Schrock-Hoveyda monoalkoxidepyrrolide (**MAP**) catalysts are shown in Chart 1.1[9-11] These molybdenum and tungsten complexes are important for their very high metathesis activity. They are also easily tuned by modification of the ligands.[12] This tunability enables controlled reactions with substrates that have widely different reactivity, and has also permitted development of stereoselective and enantioselective metathesis reactions.

Chart 1.1 Selected Ta, Mo and W catalysts

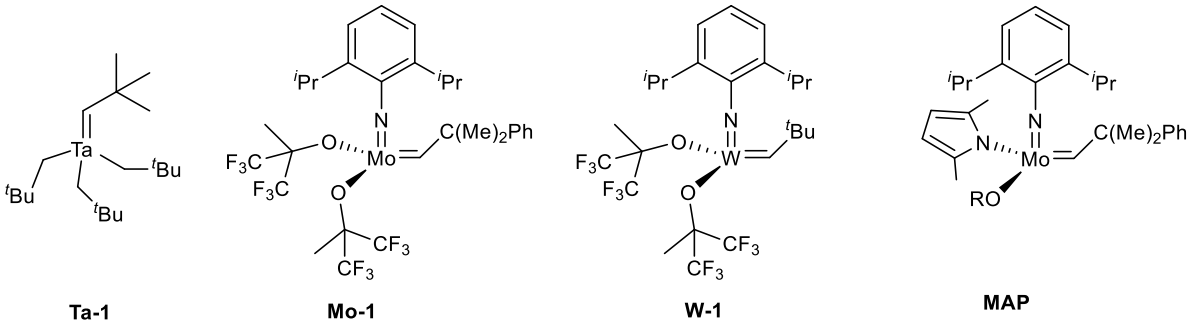

Ta-1 **Mo-1** **W-1** **MAP**

Despite these advantages, the group 6 catalysts are very sensitive to oxygen and water. The handling, use, and storage of these catalysts require inert atmosphere and rigorously anhydrous solvent.[13] Many are also thermally unstable, and must be stored at –30 °C in a glovebox.[13] Efforts to address the challenges to handling include using more stable precursors, with in situ generation of the active catalyst by chemical or thermal activation.[13]

Another limitation that is more difficult to overcome is the sensitivity to aldehydes, alcohols, and carboxylic acids.[12] On the other hand, while these catalysts are routinely described in the literature as less functional-group tolerant than the ruthenium catalysts, it is important to note that the Mo catalysts tolerate a number of functional groups (for example phosphines, thioethers and primary or secondary amines) that decompose the popular ruthenium catalysts, as described below.[12,14,15] Amine-tolerance is importance both because amines can be present as an impurity in aromatic solvents (for example, morpholine is reported as a contaminant in technical-grade toluene),[16] and also because amines are very common functional groups in pharmaceutical chemistry.[14]

1.2.2 Development of Ru catalysts

The first well-defined ruthenium catalyst, the vinylalkylidene complex **Ru-1** (Chart 1.2) was published by Grubbs and coworkers in 1992.[17] This PPh_3-stabilized complex was found to be active for ROMP of norbornene, even in the presence of water and alcohol. While slow initiation of **Ru-1** limited control over polymer chain lengths, the fact that the reaction proceeded indicates that the ruthenium complexes are much more stable to air and water than the Mo or W catalysts. However, it should also be noted that norbornene is a high-strain monomer that is readily polymerized, and this property allows ROMP to compete with decomposition by O_2 and water. In addition, because ROMP involves only internal olefins, the metathesis reaction proceeds via alkylidenes as the active species. That is, no vulnerable methylidene species are formed during ROMP, in contrast with CM or RCM of terminal olefins (see later).

Chart 1.2 First- and second-generation ruthenium catalysts for olefin metathesis

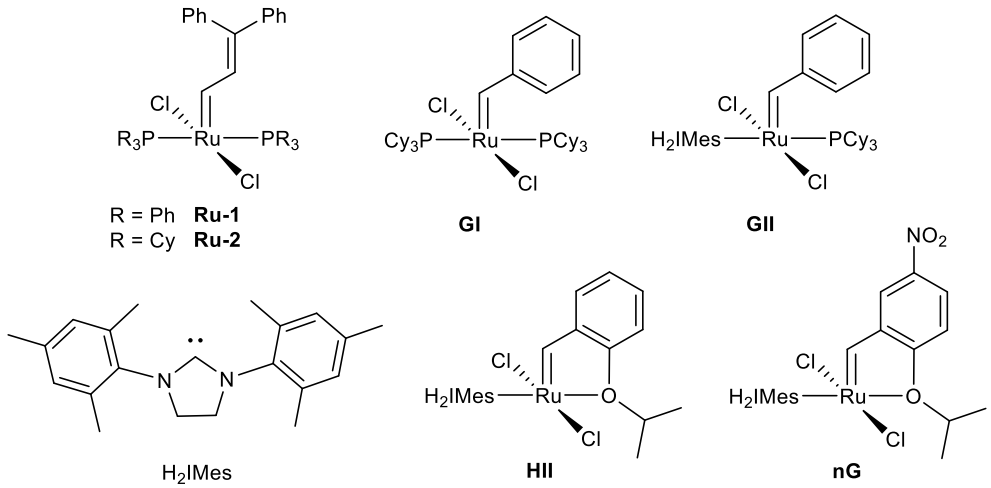

The PCy_3 analogue **Ru-2** was reported shortly afterwards.[18] The better donor ability of the alkylphosphine ligand was found to significantly increase the catalyst reactivity, expanding substrate scope beyond strained monomers. Catalyst **Ru-2** was therefore the first well-defined Ru catalyst that was reported to be able to effect RCM. Again, these reactions could be carried out in air with yields up to 93%, although the high catalyst loadings of 2 mol% (thousands of times higher than the ppm loadings now possible with Ru catalysts, see later) mask catalyst decomposition. Nevertheless, the tolerance of the ruthenium catalysts towards air, water, and protic media[17] was in very striking contrast to the sensitivity of the group 6 catalysts.

Subsequent research focused on modification of the alkylidene ligand. Ru catalysts bearing a benzylidene ligand were found to display greater metathesis activity and faster initiation, meaning they were capable of polymerizing low-strain monomers with relatively narrow polydispersity.[19,20] These advances came to major attention in 1996, with a full paper by Schwab and Grubbs describing the first-generation Grubbs catalyst (**GI**).[20] This was a breakthrough that, along with

reports on RCM,[21,22] led to the first recognition by organic chemists of the opportunities of olefin metathesis.

As applications expanded, however, the limitations of **GI** in terms of substrate scope began to emerge. With sterically bulky or electron-deficient substrates, for example, **GI** exhibits low or no activity.[23] As noted above, the activity of Ru metathesis catalysts increases as the donor ability of the phosphine ligand increases. N-heterocyclic carbenes (NHCs), as stronger σ-donors, are attractive substitutes for phosphines. The introduction of an NHC ligand in place of one phosphine ligand yielded more reactive catalysts, the most famous of which is the second-generation Grubbs catalyst bearing an H_2IMes ligand, **GII**.[24-26] Initial reports claimed that **GII** could even exhibit similar activity to **Mo-1** in RCM of bulky or electron-deficient substrates, while retaining higher stability to oxygen and water.[27,28] However, this claim probably involved commercial Schrock catalyst, and was based on comparison of rate curves, not total productivity in terms of maximum turnover numbers. The activity of many group 6 catalysts cannot be accurately estimated from commercially-produced catalysts, given their sensitivity to decomposition during transportation, storage, and handling.

The first-generation Hoveyda catalyst **HI**, a more robust phosphine-free ruthenium catalyst, was reported in 1999.[29] While **HI** was never widely used, its much more reactive H_2IMes analogue **HII (**Chart 1.2**)** was reported independently by the groups of Hoveyda[30] and Blechert[31] in 2000, and remains one of the most commonly used metathesis catalysts. **HII** is more stable to oxygen and water than **GII**, as indicated by the fact that it can be purified by chromatography in air.[30] However, **HII** is only robust when it is present as the precatalyst: that is, in the absence of olefin substrate. During metathesis, **HII** forms the same active species as other Ru catalysts such as **GII**, and is susceptible to the same decomposition pathways (other than those induced by PCy_3).[14,15,32,33] Nevertheless, the easy handling of **HII** (and its resistance to deactivation or decomposition by the strongly coordinating, nucleophilic PCy_3 ligand; see later) makes it a popular catalyst platform. Grela later developed the nitro-substituted analogue **nG**.[34] The NO_2 substituent para to the chelating ether donor in **nG** weakens the Ru-O dative bond, leading to a more active catalyst. Indeed, **nG** out-competes **GII** and **HII** in CM of electron-deficient substrates, as well as ethenolysis and macrocyclization (mRCM).[34,35]

A very recent breakthrough in Ru-catalyzed olefin metathesis has been the discovery of very high productivity for derivatives bearing cyclic alkyl amino carbene (CAAC) ligands. In these catalysts, one or two CAAC ligands replace the NHCs present in the second-generation catalysts.[36] The strong donor properties of CAACs make them excellent alternative ligands. In fact, the CAACs are both more σ-donating and more π-accepting than NHC ligands.[37] However, the first examples of these catalysts, developed by Grubbs and Bertrand in 2007, showed very poor activity.[38] The reasons for this low activity will be discussed in Section 1.3.2. The CAACs were dismissed until a 2015 report showing that a series of **HII-CAAC** catalysts exhibited almost unbelievably high productivity in the ethenolysis of methyl oleate to form linear α-olefins.[39] **HII-C2** (Chart 1.3) gave

the highest turnover number (TON), up to 340,000, orders of magnitude higher than the maximum TON achieved with H_2IMes catalysts.[40] However, this productivity required 99.995% pure ethylene. Our group, in collaboration with Apeiron Synthesis, showed that a **C1** catalyst performed better than the corresponding **C2** catalyst in the ethenolysis of methyl oleate using lower-grade 99.9% ethylene, and suggested that the phenyl group at the quaternary carbon of **C1** gives steric protection against decomposition by impurities.

Chart 1.3 Leading CAAC catalysts

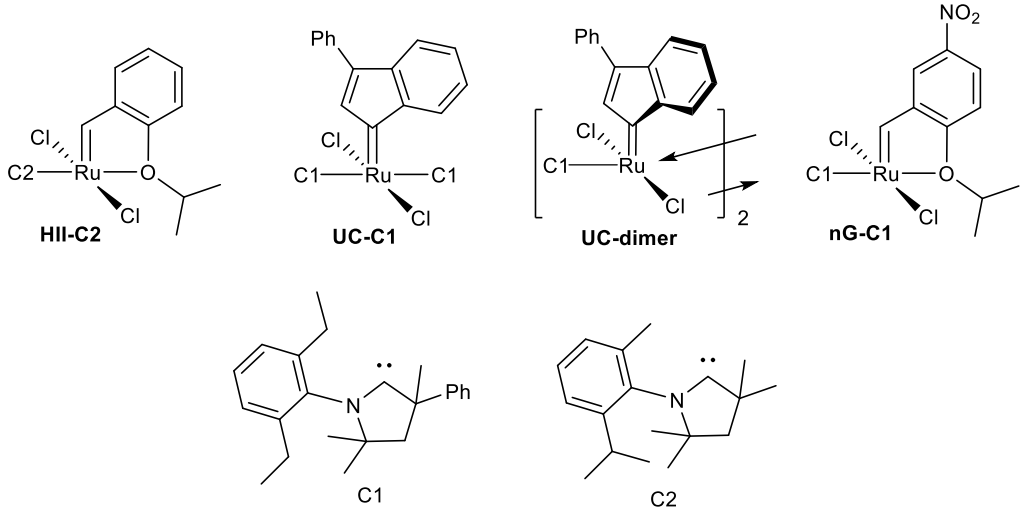

In 2017, Skowerski and co-workers reported a series of bis-CAAC indenylidene catalysts.[41] One example (**UC-C1**) is shown in Chart 1.3. One major drawback of bis-CAAC catalysts is the low lability of the second CAAC ligand, which must be lost to allow them to enter into the catalytic cycle. They usually require high temperature or added CuCl to help the CAAC to dissociate.[41] This limitation can be overcome by using the bis-CAAC indenylidene catalysts as an entry point to **nG-CAAC** catalysts.[42] **nG-C1** was found to be the best catalyst in both CM of acrylonitrile with ethyl 10-undecenoate (TON 28,500) and mRCM (TON 30,000), whereas its NHC analogue **nG** only show moderate productivity in mRCM (TON 2300). The reason for the higher performance of the CAAC catalysts than NHC catalysts will be discussed in Section 1.3.2.

Alternatively, **UC-C1** can be converted to a much more reactive indenylidene catalyst by removing one CAAC ligand. In collaborative work between our group and Skowerski's, the chloride-bridged indenylidene dimer (**UC-dimer**) was synthesized and shown to be more productive than **HII-C2** in ethenolysis using technical-grade (99.9% ethylene).[43] The high lability of **UC-dimer** makes it much more reactive than **UC-C1**. These indenylidene complexes are interesting for their much easier synthesis relative to the benzylidene analogues like **GII** and **HII**, which must be accessed via diazo reagents. This activity of **UC-dimer** was also striking in showing that the low reactivity of the indenylidene catalysts such as **Ind-II**, which was previously thought to be due to the bulk

of the disubstituted [Ru]=CRR' unit, is in fact only due to low ligand lability. The initiation rate of the dimer was 65 times faster than **UC-C1** and only 3.5 times slower than **nG-C1**.

1.3 Catalyst productivity

1.3.1 Catalyst deactivation

Major factors affecting catalyst productivity are initiation, deactivation, and decomposition. To better understand how these factors affect catalyst productivity, it is useful to start by elucidating all stages of the catalytic cycle, including entry and exit (Scheme 1.3). Unlike Mo catalysts, ruthenium catalysts usually require initiation via loss of a stabilizing ligand to form a four-coordinate active species. In the case of **GII**, for example, PCy_3 dissociation is necessary to enter the catalytic cycle. During metathesis, a vulnerable methylidene species will be formed. A major deactivation event involves trapping of this methylidene species by dissociated PCy_3 to form the off-cycle resting-state species **GIIm**. Justin Lummiss of this research group established that PCy_3 dissociation from **GIIm** is 275 times slower than **GII** at 80 °C in C_7D_8 (**GIIm**) or C_6D_6 (**GII**).[44,45] That is to say, once trapped, **GIIm** will accumulate during metathesis. The difficult re-entry into the catalytic cycle therefore limits the productivity of **GII**. The PCy_3 ligand also has more permanent negative impacts, as discussed in the next Section.

Scheme 1.3 Catalytic cycle of **GII**

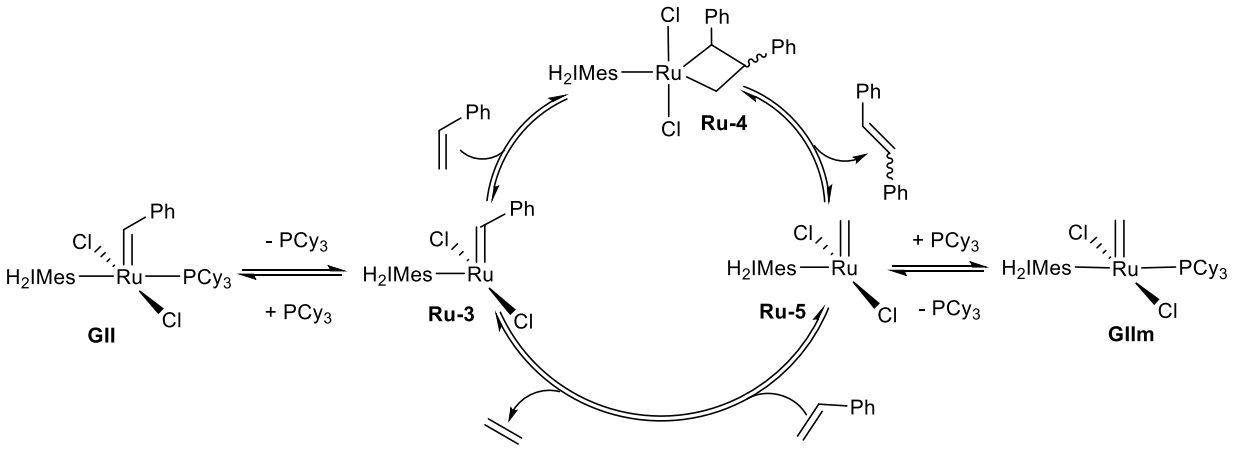

1.3.2 Intrinsic decomposition

Over the past decade, three major intrinsic decomposition pathways have been established for ruthenium catalysts. The first of these to be clearly outlined is a pathway relevant to phosphine-stabilized catalysts such as **GI** and **GII**. The nucleophilic free phosphine PCy_3 can attack the methylidene species to form a σ-alkyl intermediate.[46,47] If the latter can then deprotonate an adjacent ligand, it can eliminate a phosphonium salt $[MePCy_3]Cl$. For **GI**, which lacks a readily activated C–H bond, Justin Lummiss succeeded in trapping and crystallizing the σ-alkyl intermediate **Ru-7** in the presence of excess pyridine.[46] For **GII**, facile C-H activation of a mesityl

o-methyl group enabled rapid decomposition of the σ-alkyl intermediate **Ru-8**, liberating [$MePCy_3$]Cl.[47] It should be noted that the first clue for this pathway came from a Hong and Grubbs study noting formation of the phosphonium salt. The latter was not quantified, and the same paper proposed a detailed pathway for decomposition of **GIIm** to form a crystallographically characterized hydridic ruthenium dimer. This proposal captured most of the attention. The significance of the phosphonium salt was overlooked. However, this can now be recognized as the first real clue about the risks posed by the nucleophilic PCy_3 ligand.

Scheme 1.4 Nucleophilic attack of PCy_3 on the active methylidene intermediate

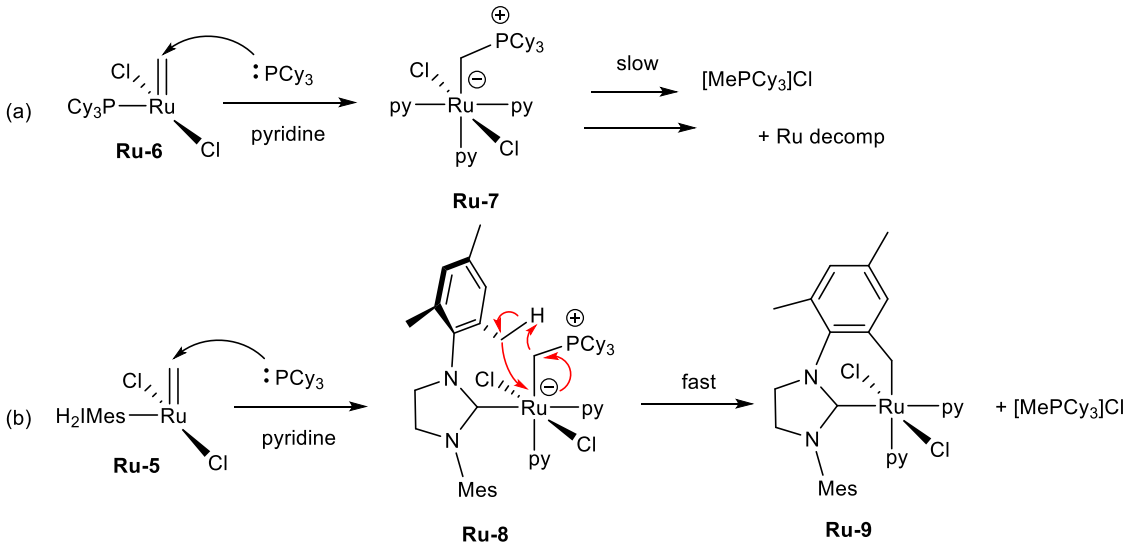

Two other intrinsic decomposition pathways are common for the majority of metathesis catalysts, with an exception noted below. First, as shown in Scheme 1.5, the metallacyclobutane (MCB) intermediate generated during metathesis decomposes via β-elimination, producing ruthenium hydride intermediate followed by eliminating propylene.[48-51] This will cause unwanted isomerization.[51] The vulnerability of the unsubstituted MCB to this decomposition pathway accounts for the high risks associated with the ethylene co-product in metathesis of terminal olefins.[48,49]

Scheme 1.5 Decomposition of MCB via β-elimination

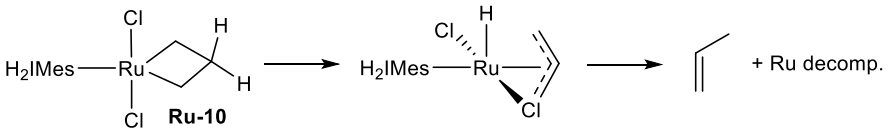

The other general decomposition pathway is biomolecular decomposition (BMC) of the [Ru]=CHR species.[52] The most vulnerable species in metathesis is the 14-electron methylidene intermediate **Ru-5**, which is not only susceptible to nucleophilic attack, but also readily couples with another [Ru]=CH_2 species, generating ethylene and losing the functional Ru=CH_2 moiety (Scheme 1.6). Identification of this decomposition pathway is critical to realizing that high catalyst loading (and hence high catalyst concentrations) in metathesis can limit catalyst productivity.

Scheme 1.6 Bimolecular decomposition of methylidene species

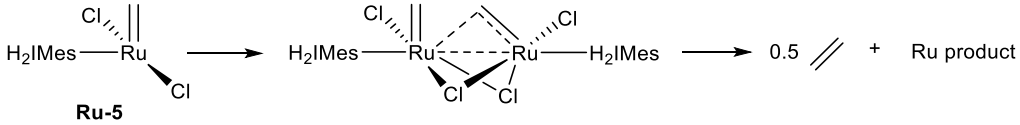

Large excesses of ethylene promote formation of both metallacyclobutane and methylidene species, and therefore promote decompositions. Ethenolysis is thus a very challenging reaction. However, as mentioned in Section 1.2, the CAAC catalysts show extremely high productivity in ethenolysis. Daniel do Nascimento of this research group recently showed that this is due to the resistance of the CAAC catalysts to β-hydride elimination.[53] He also showed that they are more susceptible to BMC, although the latter problem can be reduced by reducing catalyst loading.[53] The discovery that the CAAC catalysts are very susceptible to BMC explains the 2007 Grubbs-Bertrand report that CAAC catalysts showed poor activity. The catalyst loading was high (1-5 mol%),[38] and metathesis was carried out in a sealed NMR tube, precluding ventilation of ethylene.

1.4 Scope of thesis

As described in this introduction, Ru catalysts have seen tremendous development from generation to generation over the past 30 years. Along with catalyst developments, mechanistic studies of catalyst deactivation and decomposition are now emerging as important potential aids to new catalyst design. These developments indicate great opportunities for Ru-catalyzed olefin metathesis. However, synthetic advances aimed at facilitating access to new catalysts are less developed. Chapter 2 of this thesis focuses on synthetic strategies for the production of NHC and CAAC catalysts, as well as efforts toward production of isotopically-labelled catalysts for mechanistic study.

Our recent finding that CAAC catalysts resist β-elimination helps to explain why the CAAC catalysts are extremely productive in ethenolysis. Another key factor is catalyst deactivation. While catalyst deactivation or decomposition effects have now been well studied for Grubbs-class catalysts, particularly by Justin Lummiss of this research group, they are just beginning to be probed with CAAC catalysts. Chapter 3 examines how initiation and recapture of the active species affects the productivity of **HII-C1** and **nG-C1**, in comparison to their H_2IMes analogues **HII** and **nG**. Finally, Chapter 4 summarizes key findings and suggestions for future work.

1.5 References

(1) Trnka, T. M.; Grubbs, R. H., The development of $RuX_2L_2(=CHR)$ olefin metathesis catalysts: An organometallic success story. *Acc. Chem. Res.* **2001**, *34*, 18–29.

(2) Hérisson, J. L.; Chauvin, Y., Catalysis of olefin transformations by tungsten complexes. II. Telomerization of cyclic olefins in the presence of acyclic olefins. *Makromol. Chem.* **1971**, *141*, 161–176.

(3) Fogg, D. E.; Foucault, H. M., Ring-Opening Metathesis Polymerization. In *Comprehensive Organometallic Chemistry III*, Crabtree, R. H.; Mingos, D. M. P., Eds. Elsevier: Oxford, 2007; Vol. 11, pp 623–652.

(4) Pederson, R. L.; Fellows, I. M.; Ung, T. A.; Ishihara, H.; Hajela, S. P., Applications of olefin cross metathesis to commercial products. *Adv. Synth. Catal.* **2002**, *344*, 728–735.

(5) Nicolaou, K. C.; Bulger, P. G.; Sarlah, D., Metathesis reactions in total synthesis. *Angew. Chem., Int. Ed.* **2005**, *44*, 4490–4527.

(6) Higman, C. S.; Lummiss, J. A. M.; Fogg, D. E., Olefin Metathesis at the Dawn of Uptake in Pharmaceutical and Specialty Chemicals Manufacturing. *Angew. Chem., Int. Ed.* **2016**, *55*, 3552–3565.

(7) Schrock, R. R., Alkylcarbene Complex of Tantalum by Intramolecular alpha-Hydrogen Abstraction. *J. Am. Chem. Soc.* **1974**, *96*, 6796–6797.

(8) Schrock, R. R.; Copéret, C., Formation of High-Oxidation-State Metal–Carbon Double Bonds. *Organometallics* **2017**, *36*, 1884–1892.

(9) Schrock, R. R.; DePue, R. T.; Feldman, J.; Schaverien, C. J.; Dewan, J. C.; Liu, A. H., Preparation and reactivity of several alkylidene complexes of the type W(CHR')(N-2,6-C_6H_3-iso-Pr_2)$(OR)_2$ and related tungstacyclobutane complexes. Controlling metathesis activity through the choice of alkoxide ligand. *J. Am. Chem. Soc.* **1988**, *110*, 1423–1435.

(10) Schrock, R. R.; Murdzek, J. S.; Bazan, G. C.; Robbins, J.; DiMare, M.; O'Regan, M., Synthesis of molybdenum imido alkylidene complexes and some reactions involving acyclic olefins. *J. Am. Chem. Soc.* **1990**, *112*, 3875–3886.

(11) Schrock, R. R., Recent Advances in High Oxidation State Mo and W Imido Alkylidene Chemistry. *Chem. Rev.* **2009**, *109*, 3211–3226.

(12) Schrock, R. R.; Hoveyda, A. H., Molybdenum and tungsten imido alkylidene complexes as efficient olefin-metathesis catalysts. *Angew. Chem., Int. Ed.* **2003**, *42*, 4592–4633.

(13) Grela, K., *Olefin Metathesis-Theory and Practice*. Wiley: Hoboken, NJ, 2014.

(14) Nascimento, D. L.; Reim, I.; Foscato, M.; Jensen, V. R.; Fogg, D. E., Challenging Metathesis Catalysts with Nucleophiles and Bronsted Base: The Stability of State-of-the-Art Catalysts to Attack by Amines. *ACS Catal.* **2020**, *10*, 11623–11633.

(15) Ireland, B. J.; Dobigny, B. T.; Fogg, D. E., Decomposition of a Phosphine-Free Metathesis Catalyst by Amines and Other Nitrogen Bases: Metallacyclobutane Deprotonation as a Major Deactivation Pathway. *ACS Catal.* **2015**, *5*, 4690−4698.

(16) Nicola, T.; Brenner, M.; Donsbach, K.; Kreye, P., First Scale-Up to Production Scale of a Ring Closing Metathesis Reaction Forming a 15-Membered Macrocycle as a Precursor of an Active Pharmaceutical Ingredient. *Org. Process Res. Dev.* **2005**, *9*, 513–515.

(17) Nguyen, S. T.; Johnson, L. K.; Grubbs, R. H.; Ziller, J. W., Ring-Opening Metathesis Polymerization (ROMP) of Norbornene by a Group VIII Carbene Complex in Protic Media. *J. Am. Chem. Soc.* **1992**, *114*, 3974–3975.

(18) Fu, G. C.; Nguyen, S. T.; Grubbs, R. H., Catalytic ring-closing metathesis of functionalized dienes by a ruthenium carbene complex. *J. Am. Chem. Soc.* **1993**, *115*, 9856–9857.

(19) Schwab, P.; France, M. B.; Ziller, J. W.; Grubbs, R. H., A series of well-defined metathesis catalysts - synthesis of $RuCl_2(=CHR')(PR_3)_2$ and their reactions. *Angew. Chem., Int. Ed. Engl.* **1995**, *34*, 2039–41.

(20) Schwab, P.; Grubbs, R. H.; Ziller, J. W., Synthesis and Applications of $RuCl_2(=CHR')(PR_3)_2$: The Influence of the Alkylidene Moiety on Metathesis Activity. *J. Am. Chem. Soc.* **1996**, *118*, 100–110.

(21) Fu, G. C.; Grubbs, R. H., The application of catalytic ring-closing olefin metathesis to the synthesis of unsaturated oxygen heterocycles. *J. Am. Chem. Soc.* **1992**, *114*, 5426–5427.

(22) Fu, G. C.; Grubbs, R. H., The synthesis of nitrogen heterocycles via catalytic ring-closing metathesis of dienes. *J. Am. Chem. Soc.* **1992**, *114*, 7324–7325.

(23) Kirkland, T. A.; Grubbs, R. H., Effects of Olefin Substitution on the Ring-Closing Metathesis of Dienes: ADMET favoured over RCM for conformationally strained substrate? *J. Org. Chem.* **1997**, *62*, 7310–7318.

(24) Huang, J.; Stevens, E. D.; Nolan, S. P.; Petersen, J. L., Olefin Metathesis-Active Ruthenium Complexes Bearing a Nucleophilic Carbene Ligand. *J. Am. Chem. Soc.* **1999**, *121*, 2674–2678.

(25) Scholl, M.; Trnka, T. M.; Morgan, J. P.; Grubbs, R. H., Increased Ring Closing Metathesis Activity of Ruthenium-Based Olefin Metathesis Catalysts Coordinated with Imidazolin-2-Ylidene Ligands. *Tetrahedron Lett.* **1999**, *40*, 2247–2250.

(26) Weskamp, T.; Schattenmann, W. C.; Spiegler, M.; Herrmann, W. A., A Novel Class of Ruthenium Catalysts for Olefin Metathesis. *Angew. Chem., Int. Ed.* **1998**, *37*, 2490–2493.

(27) Ritter, T.; Day, M. W.; Grubbs, R. H., Rate Acceleration in Olefin Metathesis through a Fluorine-Ruthenium Interaction. *J. Am. Chem. Soc.* **2006**, *128*, 11768–11769.

(28) Scholl, M.; Ding, S.; Lee, C. W.; Grubbs, R. H., Synthesis and Activity of a New Generation of Ruthenium-Based Olefin Metathesis Catalysts Coordinated with 1,3-Dimesityl-4,5-dihydroimidazol-2-ylidene Ligands. *Org. Lett.* **1999**, *1*, 953–956.

(29) Kingsbury, J. S.; Harrity, J. P. A.; Bonitatebus, P. J.; Hoveyda, A. H., A Recyclable Ru-Based Metathesis Catalyst. *J. Am. Chem. Soc.* **1999**, *121*, 791–799.

(30) Garber, S. B.; Kingsbury, J. S.; Gray, B. L.; Hoveyda, A. H., Efficient and Recyclable Monomeric and Dendritic Ru-Based Metathesis Catalysts. *J. Am. Chem. Soc.* **2000**, *122*, 8168–8179.

(31) Gessler, S.; Randl, S.; Blechert, S., Synthesis and Metathesis Reactions of a Phosphine-Free Dihydroimidazole Carbene Ruthenium Complex. *Tetrahedron Lett.* **2000**, *41*, 9973–9976.

(32) Ton, S. J.; Fogg, D. E., The Impact of Oxygen on Leading and Emerging Ru-Carbene Catalysts for Olefin Metathesis: An Unanticipated Correlation Between Robustness and Metathesis Activity *ACS Catal.* **2019**, *9*, 11329−11334.

(33) Goudreault, A. Y.; Walden, D. M.; Nascimento, D. L.; Botti, A. G.; Steinmann, S. N.; Michel, C.; Fogg, D. E., Hydroxide-Induced Degradation of Olefin Metathesis Catalysts: A Challenge for Metathesis in Alkaline Media. *ACS Catal.* **2020**, *10*, 3838−3843.

(34) Michrowska, A.; Bujok, R.; Harutyunyan, S.; Sashuk, V.; Dolgonos, G.; Grela, K., Nitro-Substituted Hoveyda-Grubbs Ruthenium Carbenes: Enhancement of Catalyst Activity through Electronic Activation. *J. Am. Chem. Soc.* **2004**, *126*, 9318–9325.

(35) Higman, C. S.; Nascimento, D.; Ireland, B. J.; Audorsch, S.; Bailey, G. A.; Fogg, D. E., Chelate-Assisted Ring-Closing Metathesis: A Strategy for Accelerating Macrocyclization at Ambient Temperatures. *J. Am. Chem. Soc.* **2018**, *140*, 1604−1607.

(36) Montgomery, T. P.; Johns, A. M.; Grubbs, R. H., Recent Advancements in Stereoselective Olefin Metathesis Using Ruthenium Catalysts. *Catalysts* **2017**, *7*, 1–38.

(37) Melaimi, M.; Jazzar, R.; Soleilhavoup, M.; Bertrand, G., Cyclic (Alkyl)(amino)carbenes (CAACs): Recent Developments. *Angew. Chem., Int. Ed.* **2017**, *56*, 10046–10068.

(38) Anderson, D. R.; Lavallo, V.; O'Leary, D. J.; Bertrand, G.; Grubbs, R. H., Synthesis and Reactivity of Olefin Metathesis Catalysts Bearing Cyclic (Alkyl)(Amino)Carbenes. *Angew. Chem., Int. Ed.* **2007**, *46*, 7262–7265.

(39) Marx, V. M.; Sullivan, A. H.; Melaimi, M.; Virgil, S. C.; Keitz, B. K.; Weinberger, D. S.; Bertrand, G.; Grubbs, R. H., Cyclic Alkyl Amino Carbene (CAAC) Ruthenium Complexes as Remarkably Active Catalysts for Ethenolysis. *Angew. Chem., Int. Ed.* **2015**, *54*, 1919–1923.

(40) Schrodi, Y.; Ung, T.; Vargas, A.; Mkrtumyan, G.; Lee, C. W.; Champagne, T. M.; Pederson, R. L.; Hong, S. H., Ruthenium Olefin Metathesis Catalysts for the Ethenolysis of Renewable Feedstocks. *Clean Soil, Air, Water* **2008**, *36*, 669–673.

(41) Gawin, R.; Kozakiewicz, A.; Guńka, P. A.; Dąbrowski, P.; Skowerski, K., Bis(Cyclic Alkyl Amino Carbene) Ruthenium Complexes: A Versatile, Highly Efficient Tool for Olefin Metathesis. *Angew. Chem., Int. Ed.* **2017**, *56*, 981–986.

(42) Gawin, R.; Tracz, A.; Chwalba, M.; Kozakiewicz, A.; Trzaskowski, B.; Skowerski, K., Cyclic Alkyl Amino Ruthenium Complexes—Efficient Catalysts for Macrocyclization and Acrylonitrile Cross Metathesis. *ACS Catal.* **2017**, *7*, 5443–5449.

(43) Nascimento, D. L.; Gawin, A.; Gawin, R.; Guńka, P. A.; Zachara, J.; Skowerski, K.; Fogg, D. E., Integrating Activity with Accessibility in Olefin Metathesis: An Unprecedentedly Reactive Ruthenium-Indenylidene Catalyst Bearing a Cyclic Alkyl Amino Carbene. *J. Am. Chem. Soc.* **2019**, *141*, 10626–10631.

(44) Lummiss, J. A. M.; Higman, C. S.; Fyson, D. L.; McDonald, R.; Fogg, D. E., The Divergent Effects of Strong NHC Donation in Catalysis. *Chem. Sci.* **2015**, *6*, 6739–6746.

(45) Lummiss, J. A. M.; Perras, F. A.; Bryce, D. L.; Fogg, D. E., Sterically-Driven Metathesis: The Impact of Alkylidene Substitution on the Reactivity of the Grubbs Catalysts. *Organometallics* **2016**, *35*, 691–698.

(46) Lummiss, J. A. M.; McClennan, W. L.; McDonald, R.; Fogg, D. E., Donor-Induced Decomposition of the Grubbs Catalysts: An Intercepted Intermediate *Organometallics* **2014**, *33*, 6738–6741.

(47) McClennan, W. L.; Rufh, S. A.; Lummiss, J. A. M.; Fogg, D. E., A General Decomposition Pathway for Phosphine-Stabilized Metathesis Catalysts: Lewis Donors Accelerate Methylidene Abstraction. *J. Am. Chem. Soc.* **2016**, *138*, 14668−14677.

(48) Janse van Rensburg, W.; Steynberg, P. J.; Meyer, W. H.; Kirk, M. M.; Forman, G. S., DFT Prediction and Experimental Observation of Substrate-Induced Catalyst Decomposition in Ruthenium-Catalyzed Olefin Metathesis. *J. Am. Chem. Soc.* **2004**, *126*, 14332–14333.

(49) Romero, P. E.; Piers, W. E., Mechanistic Studies on 14-Electron Ruthenacyclobutanes: Degenerate Exchange with Free Ethylene. *J. Am. Chem. Soc.* **2007**, *129*, 1698–1704.

(50) Romero, P. E.; Piers, W. E., Direct Observation of a 14-Electron Ruthenacyclobutane Relevant to Olefin Metathesis. *J. Am. Chem. Soc.* **2005**, *127*, 5032–5033.

(51) Engel, J.; Smit, W.; Foscato, M.; Occhipinti, G.; Törnroos, K. W.; Jensen, V. R., Loss and Reformation of Ruthenium Alkylidene: Connecting Olefin Metathesis, Catalyst Deactivation, Regeneration, and Isomerization. *J. Am. Chem. Soc.* **2017**, *139*, 16609–16619.

(52) Bailey, G. A.; Foscato, M.; Higman, C. S.; Day, C. S.; Jensen, V. R.; Fogg, D. E., Bimolecular Coupling as a Vector for Decomposition of Fast-Initiating Olefin Metathesis Catalysts. *J. Am. Chem. Soc.* **2018**, *140*, 6931–6944.

(53) Nascimento, D. L.; Fogg, D. E., Origin of the Breakthrough Productivity of Ruthenium-CAAC Catalysts in Olefin Metathesis (CAAC = Cyclic Alkyl Amino Carbene). *J. Am. Chem. Soc.* **2019**, *141*, 19236–19240.

Chapter 2. Refining Routes to Leading Phosphine-Free Metathesis Catalysts

2.1 Introduction

As described in Chapter 1, Ru metathesis catalysts have become very popular since they were first discovered in the early 1990s.[1] Phosphine-free catalysts such as **HII** and **nG** (Chart 2.1), in particular, are beginning to be used in the most demanding contexts like pharmaceutical manufacturing.[2] NHC complexes[3] have received the most attention, but several reports show the CAAC catalysts can be much more productive in some metathesis reactions.[4-8] Accessibility to both of these classes of Ru-carbene metathesis catalysts is therefore important. This chapter will begin by presenting the current state of the art in synthesis of the phosphine-free Hoveyda and Grela catalysts. Then, experiments directed at assessing these various approaches, to identify the most robust and reliable methods, will be described.

Chart 2.1 Metathesis catalysts and carbene ligands discussed

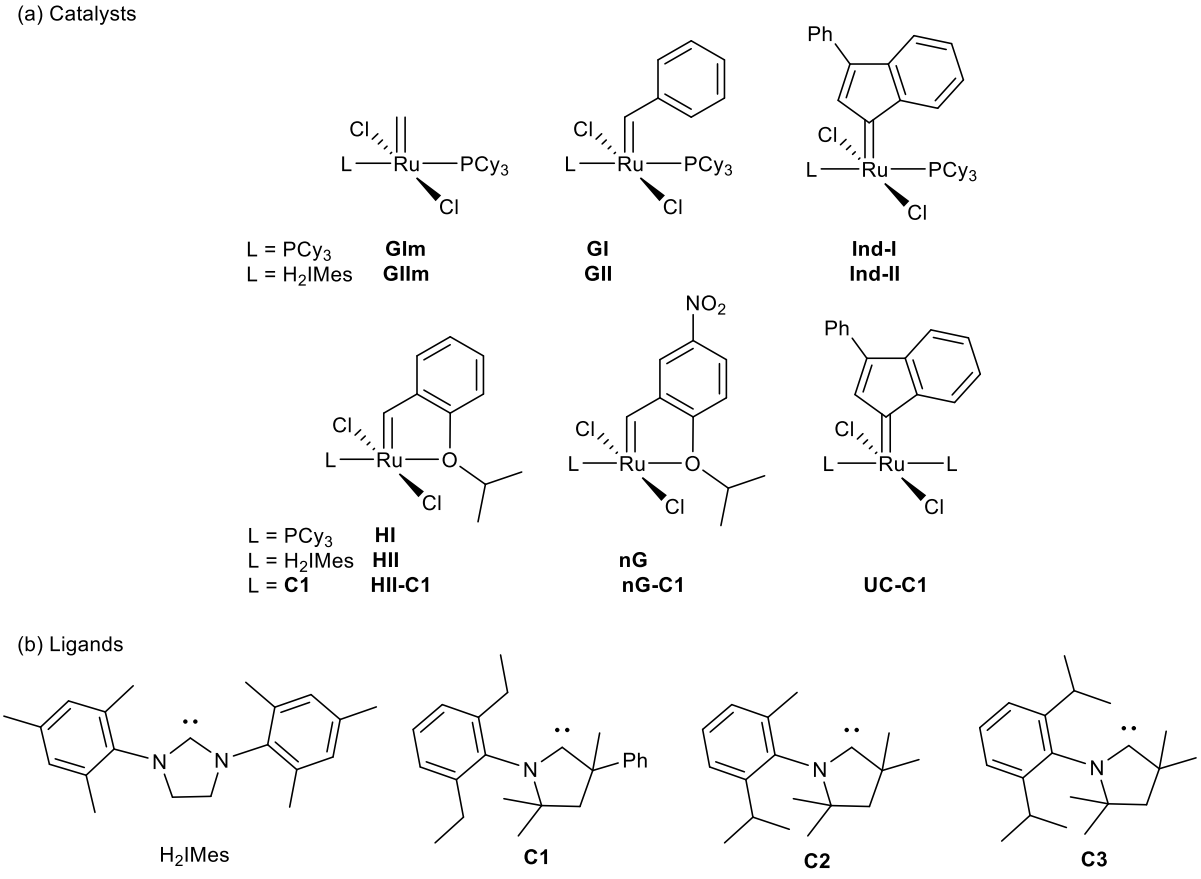

Over the past 20 years, most of the synthetic routes developed focused on the important "second-generation" Ru-NHC catalysts.[9-14] The original examples were reported in 1998 by the Herrmann[15] group and in 1999 by Grubbs[9,16] and Nolan,[17] by ligand exchange of the first-generation Grubbs

catalyst **GI** with an NHC ligand. One of the most important was the H_2IMes complex known as the second-generation Grubbs catalyst **GII** (Chart 2.1). In the initial chemistry, the NHC was generated in situ by reaction with a strong base. Nolan and coworkers later developed a route using free IMes.[18] The importance of free-carbene routes will be discussed below in the context of phosphine-free catalyst synthesis.

GII and other phosphine-stabilized catalysts dominated synthetic goals for many years. However, strong binding of the PCy_3 ligand limits their reactivity.[19,20] For example, Justin Lummiss showed that the PCy_3 is 41,000 less labile in resting-state species $RuCl_2(H_2IMes)(PCy_3)(=CH_2)$, **GIIm** than **GI** (Table 2.1).[19,20] The PCy_3 ligand also decomposes the catalyst by abstracting the methylidene ligand.[21] These problems became more widely recognized after Justin Lummiss developed a high-yield synthesis of **GIIm**[22] (and the ^{13}C-labelled isotopologue) by ligand exchange of **GIm** with free H_2IMes.[23] This enabled confirmation that $[MePCy_3]Cl$ is the major decomposition product, confirming that nucleophilic attack by PCy_3 on $[Ru]=CH_2$ is the major problem.[23-26] Gwendolyn Bailey later described nucleophilic attack of the free PCy_3 ligand on electron-deficient olefins such as acrylates.[27] All of these findings helped to turn attention to synthetic routes to phosphine-free catalysts.

Table 2.1 Lability of PCy_3 ligand in Grubbs type catalysts at 80 °C (Table reproduced from Ref. 20)

Catalyst	k_1 for PCy_3 loss (s^{-1})	k_{rel} (x times slower than **GI**)
GI	9.6	1
GII	0.13	148
GIm	-[a]	-[a]
GIIm	4.7×10^{-4}	41,000

[a] The rate of PCy_3 loss from **GIm** cannot be calculated, due to competing decomposition

The first phosphine-free catalyst was the first-generation Hoveyda catalyst **HI**. It was discovered accidentally when **GI** was used in metathesis reactions of 2-isopropoxystyrene **3**.[28] In 2000, the second-generation complex **HII** was reported by the groups of Hoveyda[11,29] and Blechert.[29] Their approaches illustrate two general routes, which can be classified as metathesis or ligand-exchange routes. The former involves cross-metathesis of a Grubbs catalyst with a styrenyl ether ligand, the latter involves ligand exchange of the first-generation catalyst. For example, Hoveyda carried out cross-metathesis of **GII** with styrenyl ether **3** (Scheme 2.1a), in the presence of CuCl to take up the released PCy_3. Silica-gel chromatography was required to remove the copper salts, decomposed Ru species, and other byproducts, but high yields of **HII** (85%) were reported.

Scheme 2.1 Synthesis of **HII** via metathesis with styrenyl ether **3**

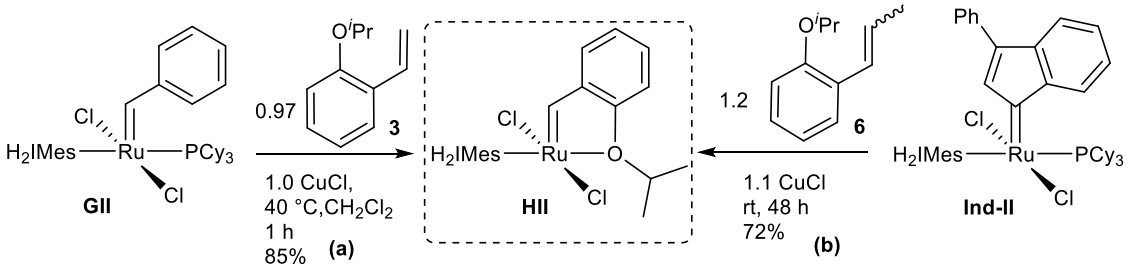

Grela and Slugovc reported a closely related approach to **HII** (Scheme 2.1 b),[30] but starting with the second-generation indenylidene catalyst (**Ind-II**). Attractive features of this route are the economy and convenience of **Ind-II** (reflecting the easy, diazo-free synthesis of the parent indenylidene complex **Ind-I**). However, one problem is the low lability of the PCy_3 ligand in **Ind-II**, due to the weak steric pressure of the rigid indenylidene ligand.[20] This results in slow reaction (48 h at RT). Another contributor to slow reaction is the use of an internal olefin, β-methyl isopropoxystyrene (**6**), as the source of the styrenyl ether ligand. This avoids the vulnerable [Ru]=CH_2 species, which is expected to reduce catalyst decomposition and improve yields. However, yields dropped to 72%,[30] perhaps because of the need for chromatography, which also adds to the inconvenience of the procedure.

In 2000, Blechert reported the first ligand-exchange route to **HII**, by reaction of the first-generation Hoveyda catalyst **HI** with H_2IMes generated in situ from H_2IMes·HCl (Scheme 2.2a).[29] Of note, even in refluxing toluene-THF, reaction stalled at the **HII**-PCy_3 adduct (Scheme 2.2). In the protocols above, where CuCl was present from the outset as a PCy_3 scavenger, no adduct formation was described. On stirring with chloroform, however, the PCy_3 ligand could be abstracted. The yield of **HII** was relatively low, only 75% yield from **HI**.

Scheme 2.2 Synthesis of **HII** via ligand exchange reactions of the first-generation Hoveyda catalyst with NHC sources

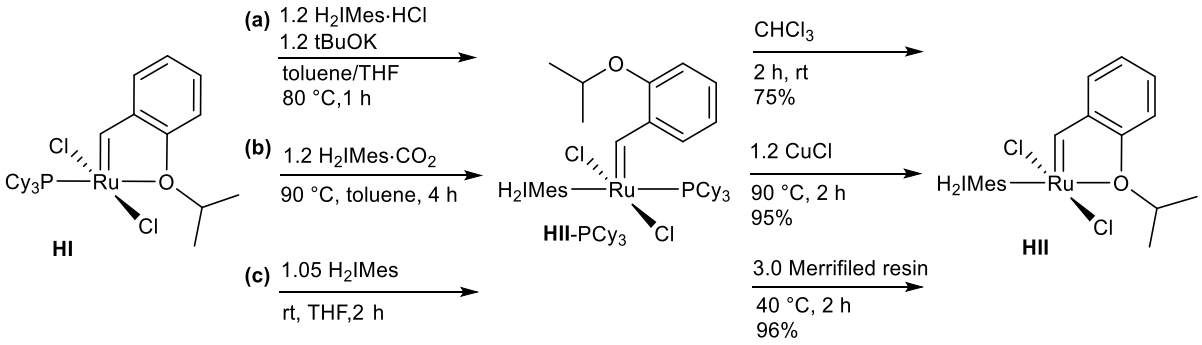

A 2009 report by Delaude and coworkers described an alternative source of H_2IMes (Scheme 2.2b).[12] The carboxylate adduct H_2IMes·CO_2 was used, instead of its HCl salt. The carboxylate reagent, which can be produced readily by bubbling CO_2 through a solution of the free NHC, is attractive because it is an air-stable, easily-handled compound from which the free NHC can be

released thermally, instead of requiring base. In the reported synthesis of **HII**, a slight excess of $H_2IMes{\cdot}CO_2$ (1.2 equiv) was stirred with **HI** for 4 h at 90 °C in toluene.[12] CuCl was then added and stirring was continued at 90 °C for another 2 h. Despite the expected advantage of cleanliness resulting from use of the zwitterionic NHC carboxylate, chromatography was still required to remove the CuCl-phosphine co-product, organic byproduct and possibly decomposed Ru. Yields of 95% were reported, but a Scifinder search suggests this route has not been widely adopted. A recent review[31] showed only one subsequent report using this method.[32] This may be due to the need to generate the free NHC to prepare the carboxylate, the high temperatures of the exchange reaction (which may cause decomposition), and the need for chromatography.

An alternative, milder ligand-exchange route involves reaction with free H_2IMes (Scheme 2.2c).[13,23,33,34] The free-carbene route was pioneered by Nolan and coworkers with IMes,[18] and expanded by our group to free H_2IMes, which is more widely used in metathesis but more difficult to generate cleanly.[13,33] Free NHCs are attractive for their mildness and their significantly improved cleanliness, meaning that the products are free of salts, bases, and byproducts resulting from in situ NHC generation. An additional focus has been workup to remove the PCy_3 released in the reaction without extraction or chromatography. Our original route[33] involved reaction of **HI**, **GI**, or **Ind-I** with the phosphine-scavenging resin Amberlyst. However, this highly acidic resin must be stored with care (especially if it is kept in a glovebox) to protect it from volatiles that can degrade the resin and enable side-reactions. Daniel do Nascimento of this research group[13] utilized a less aggressive, more selective Merrifield iodide resin to scavenge free PCy_3 (Scheme 2.2c). Workup involved simply filtering through Celite, and solvent removal, affording spectroscopically clean **HII** in 96% yield. Compared with CuCl/chromatography routes, the Merrifield route offers much more convenient purification. It is important to note that rigorously dry solvents are essential in all of this chemistry, given the extreme sensitivity of the free carbene to ring-opening hydrolysis by water.[33]

While all of these synthetic routes are reported to give good to excellent yields, both **GII** or **HI** are expensive precursors. Sigma prices at the time of writing are CAD $304 and $275 per gram, respectively. They must be synthesized in three relatively laborious steps from $RuCl_3{\cdot}xH_2O$ (net yields 50-53% and 37%, respectively). A shorter, more economical route to **HII** from piano-stool complex **Ru-11** was developed by Craig Day of this research group (Scheme 2.3).[14] It involves the reaction of **Ru-11** with chelating diazoalkane **7** to liberate the labile *p*-cymene ligand and install the benzylidene ligand. This is more economical in terms of both price and atom-efficiency, as **Ru-11** can be synthesized readily from commercial $[RuCl_2(p\text{-cymene})]_2$ ($86/g), or in two steps and 83% net yield from $RuCl_3{\cdot}xH_2O$.[14]

Scheme 2.3 Synthesis of **HII** via piano-stool–aryldiazomethane methodology

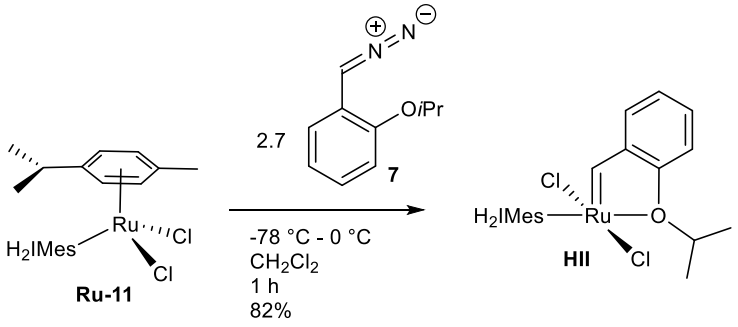

Fewer routes to CAAC catalysts have been reported, and their yields are often much lower. One reason for the lower yields may be in situ generation of CAAC ligands: the much higher yields and cleanliness of free-carbene routes to the NHC ligands were discussed above. Use of the free CAACs in the context of olefin metathesis has not been reported. Indeed, the only isolated free CAACs reported to date bear an N-diisopropyl group (N-DIPP).[35] The N-DIPP derivative is greatly stabilized by its bulk.[36,37] The CAAC **C3**, for example (Chart 2.1)[38] is not only stable against dimerization via the Wanzlick equilibrium, but is stable for up to two weeks in solution.

However, the free CAACs have not been isolated for the ligands that show maximum activity in olefin metathesis, i.e. **C1** (with N-diethylphenyl)[5-7,39] and **C2** (N-methylisopropylphenyl derivatives).[4] Bertrand has noted that a fundamental challenge is the weak acidity of the aldiminium proton in the CAAC salt. Strong base is required to deprotonate the cyclic aldiminium salts, enabling competing deprotonation at other sites. (It is for this reason that the sp^3-carbon adjacent to the nitrogen group must be a quaternary carbon). Similarly, reaction of an N-Mes derivative with LDA was reported to result in competing deprotonation of the mesityl group.[37] The weaker basicity of LiHMDS (reported pK_a of conjugate acid = 29.5, vs 35.7 for LDA in THF)[40] used by other groups may thus be an asset.

The sole reported route to **UC-C1** (Scheme 2.4)[5] involved reaction of **C1**·BF_4 with LiHMDS at 80 °C in toluene, and addition of **Ind-0** after 1 min. After 2 min, the reaction was worked up by filtering through a pad of Celite, and **UC-C1** was isolated by reprecipitating from CH_2Cl_2/CH_3NO_2. Reported yields were only ca. 60%. **UC-C1** is the only commercially-available example of this potentially large family of catalysts, though four others were described.[5]

Scheme 2.4 Synthesis of **UC-C1**

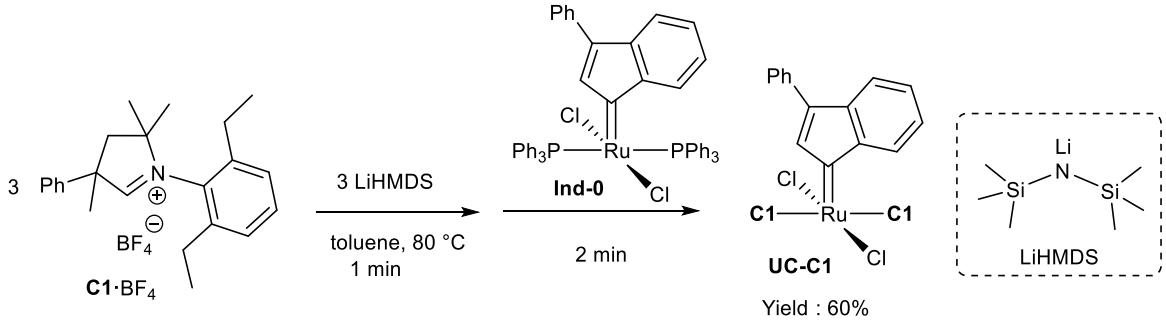

A one-pot route to **HII-C1** was described in 2015 by Bertrand, Grubbs and coworkers[4] (Scheme 2.5a), where **HI**, KHMDS and **C1**·BF_4 were stirred together at the same time. Yields were only about 45% (that is, the net yield of **HII-C1** from $RuCl_3 \cdot xH_2O$ using this route is 17%). This one-pot route was used because of the belief that the free carbene must be trapped immediately by the Ru complex.[36] The low yield could reflect competing reaction of KHMDS with the ruthenium chloride precursor and/or product. Skowerski reported yields close to 90% when he synthesized **HII-C1** from **UC-C1** (Scheme 2.5b), which has the CAAC ligands pre-installed. The reaction of **UC-C1** with β-methyl isopropoxystyrene (**6**) was reported to give **HII-C1** in 86% yield.[5] (That is, the net yield of **HII-C1** from $RuCl_3 \cdot xH_2O$ using this route is 38%).[5]

Scheme 2.5 Synthesis of **HII-C1**

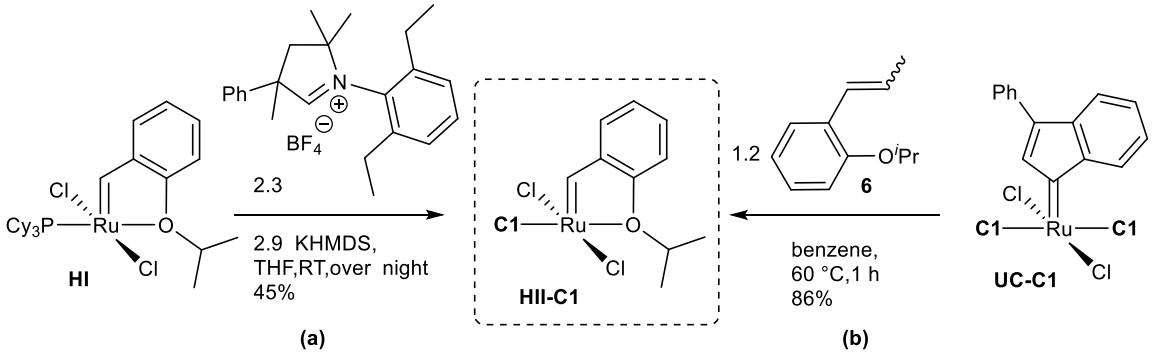

The Skowerski group reported the only synthetic route to **nG-C1** (Scheme 2.6).[6] This involved in situ synthesis of **UC-C1** at 60 °C, and then addition of the *p*-nitro substituted β-methyl isopropoxystyrene (**6'**) and CuCl. The one-pot synthesis is time-saving because isolation of **UC-C1** is not required. However, yields were poor (38%), perhaps because of incomplete conversion of **Ind-0** to **UC-C1** in the first step.

Scheme 2.6 One-pot synthesis of **nG-C1**

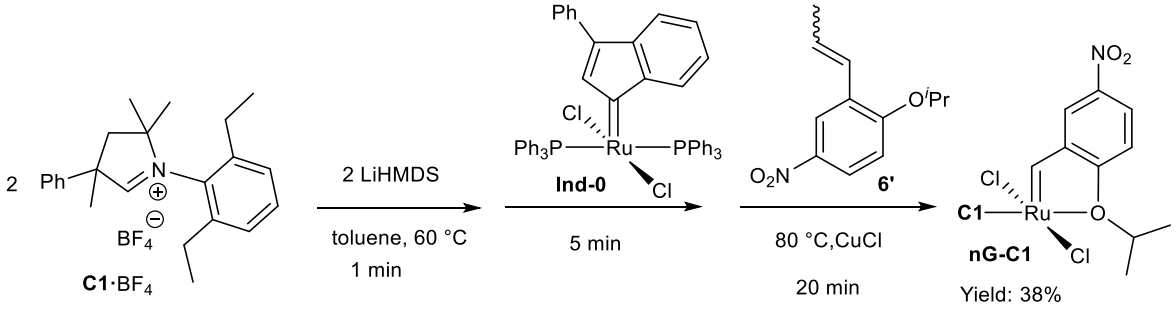

The above routes to high-performing Ru-carbene metathesis catalysts were explored in efforts to identify the most robust routes to high-purity catalysts for mechanistic study. Described below are these and modified methods for the production of the required ligands and Ru-CAAC catalysts, undertaken to identify the best routes for purity, yields, and reproducibility.

2.2 Results and Discussion

The major focus of this chapter is optimal routes to the phosphine-free catalysts. Clean synthesis of the styrenyl ether ligand is necessary for this purpose. The routes to these ligands were therefore an initial focus, and will be discussed first. An additional initial goal was synthesis of a ^{13}C-labelled derivative of the nitro-styrenyl ether **3'**, which was planned to support the mechanistic studies in Chapter 3.

2.2.1 Challenges in synthesis of the styrenyl ether ligands

Synthesis of the styrenyl ether ligand **3** and its *p*-nitro analogue **3'**, developed by Grela and co-workers,[41,42] starts with the salicylaldehydes (Scheme 2.7a). The initial alkylation of the phenol group in *o*-hydroxyaldehyde **1** to afford isopropoxy derivative **2** (Scheme 2.7a) gives very good to excellent yields (82-98%; Table 2.2, entry 1-4).[43] Good yields of the nitro derivative **2'** (Table 2.2, entry 4) can also be achieved, if care is taken to ensure efficient extraction of the product, which is more water-soluble because of the nitro group present.

In the ensuing Wittig reaction (Scheme 2.7b), a yield of 92% (Table 2.2, entry 6) was reported when nBuLi was used to deprotonate the methylphosphonium salt to form the ylide.[44] In contrast, Jennifer Bates of this research group observed only 62% yield (Table 2.2, entry 5).[45] Replacing nBuLi with KOtBu was more successful, giving up to 85% yield of **3** (Table 2.2, entry 7).

It should be noted that an important additional experimental parameter is the volatility of the product **3**, which can result in losses in yield when drying under vacuum, or even leaving too long on the rotary evaporator.

Scheme 2.7 Synthetic routes to styrenyl ether ligands **3** and **3'**

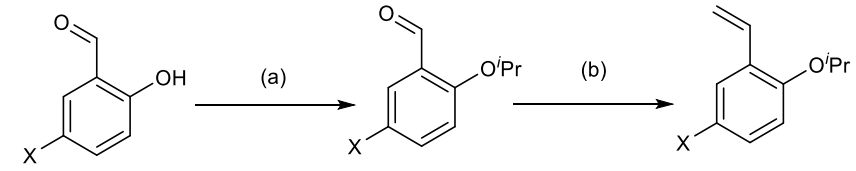

Table 2.2 Summary of reported yields and reproduced yields for Scheme 2.7

	Product	Condition	Yield (%)	Ref.
Step a		*Alkylation of the phenol*		
1	**2**	^{i}PrI, K_2CO_3, DMF, RT, 20 h	98	43 (see SI)
2	**2**	^{i}PrI, K_2CO_3, DMF, 45 °C, 16 h	90	this work
3	**2'**	^{i}PrI, K_2CO_3, Cs_2CO_3, DMF, 40 °C, 24-48 h (general procedure; specifics not given)	86	41
4	**2'**	^{i}PrI, K_2CO_3, DMF, 45 °C, 16-48 h	82[a] (one trial)	this work
Step b		*Wittig reaction of the aldehyde*		
5	**3**	nBuLi, PPh_3MeBr, -78 °C, THF, 16 h	62	45
6	**3**	nBuLi, PPh_3MeBr, -78 °C, THF, 12 h	92	44
7	**3**	KOtBu, PPh_3MeBr, 0 °C, THF, 16 h	85[b] (one trial)	this work
8	**3'**	nBuLi, PPh_3MeBr, -78 °C, THF 48 h	57	41
9	**3'**	nBuLi, PPh_3MeBr, -78 °C, THF,16 h	17-23 (two trials)	this work
10	**3'**	KOtPe, PPh_3MeBr, 0 °C, THF, 1 h	84	46
11	**3'**	KOtBu, PPh_3MeBr, 0 °C, THF, 16 h	60-65 (five trials)	this work

[a]An initial experiment gave only 60% yield, due to insufficient reaction time and insufficient extraction. [b]A yield of 64% in a first experiment was probably due to loss of the volatile product when drying under vacuum.

Synthesis of the nitro-functionalized analogue **3'** is more demanding. While Grela's 2004 report described 57% yield for the Wittig reaction using nBuLi (Table 2.2, entry 8),[41] in our hands, yields were consistently only 17-23% (Table 2.2, entry 9). This is possibly due to nucleophilic attack of nBuLi on the nitro substituent. Barbasiewicz and co-workers[46] utilized the less nucleophilic base KOtPe (potassium tert-pentoxide), with reported yields improving to 84% (Table 2.2, entry 10). In the present work, KOtPe was not used, given its steric and electronic similarity to KOtBu, and its 5-fold higher cost ($1320/mol for 2M KOtPe in THF, vs $259/mol for solid KOtBu). Instead, KOtBu was used, giving yields of 60-65% (Table 2.2, entry 11).

A further initial objective, as noted above, was the synthesis of Grela-class catalysts bearing a ^{13}C label at the benzylidene carbon. Other isotopically-labelled catalysts (specifically, **HII** and **GIIm**) have proved highly valuable in mechanistic studies.[22,47] Marciniec described a route to ^{13}C-labelled styrenyl ether ligand **3** (Scheme 2.8).[44] The biggest challenge is installing the labelled carbonyl group (indicated with an asterisk) on the bromobenzene compound **5**/**5'**. Synthesis of the "non-

nitro" derivative **2** by successive lithiation (nBuLi) and quenching with N,N-dimethylformamide (DMF) proceeded in 65% yield, consistent with the literature report.[44,45] However, the corresponding reaction of nitro-substituted analogue **5'** (carried out in single trial runs with non-labelled reagent) failed to yield the desired **2'**. Only unreacted DMF was isolated, probably because of the sensitivity of the nitro substituent to nBuLi mentioned above. Attempts to synthesize **2'** using the more functional-tolerant reagent ^{i}PrMgCl:LiCl[48] again yielded only DMF, and synthesis of labelled **3'** was therefore pursued no further.

Scheme 2.8 Potential route to ^{13}C-labelled **3** or **3'**, showing reported isolated yields and (brackets) yields found in the present work.

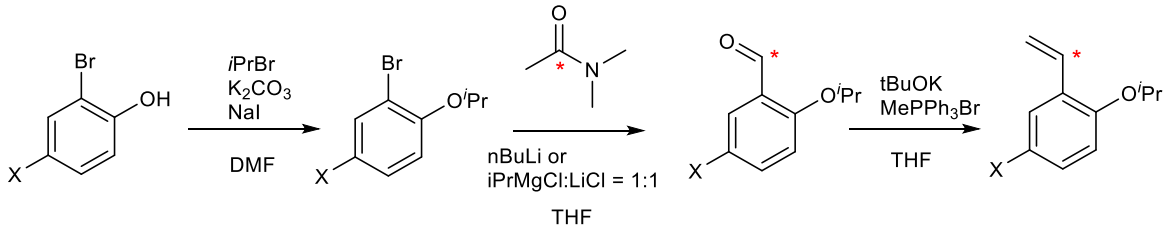

X = H	**4**	84% (85%) **5**	65% (65%) **2**	**3**
X = NO_2	**4'**	74% (75%) **5'**	None **2'**	**3'**

2.2.2 Analysis of routes to Hoveyda- and Grela-class catalysts bearing an H_2IMes ligand

Advantages and disadvantages of Hoveyda's original route to **HII** (Scheme 2.1a), including the need for CuCl, were discussed above. The Hoveyda report commented that CuCl-PCy_3 must be removed before chromatography, otherwise it complicates column in ways that were not specified.[11] The procedure for removing the CuCl-PCy_3 adduct (a molecularly ill-defined species) involved dissolving the crude product in 1:1 pentane/CH_2Cl_2, and loading onto the column by filtering through a Pasteur pipet containing a plug of cotton. On repeating this procedure (pending implementation of the Merrifield workup), the high solubility of CuCl-PCy_3 in CH_2Cl_2 was found to result in very poor separation from **HII**. Searching for a convenient solvent in which the CuCl-PCy_3 adduct is insoluble led to identification of EtOAc as suitable. Accordingly, separation of CuCl-PCy_3 was accomplished by dissolving the crude product in EtOAc and filtering through a fritted funnel before chromatography. Yields were then up to 75% (as compared to 85% in the original report). While the Merrifield route is clearly preferable, EtOAc is a good choice for removing the copper-phosphine adduct where CuCl must be used.

To overcome the low lability of the PCy_3 ligand in **Ind-II** at RT, synthesis of **HII** or **nG** was carried out at 75 °C (Scheme 2.9). Elevated temperatures always carry the risk of decomposition and reduced yields. Indeed, compared to the 72% yield in synthesis of **HII** from **Ind-II** (Scheme 2.1b), yields were 50-60%. While this work was in progress, the Grela group reported a solid-state mechanochemical method.[49] High purity and yields (94%) were described, but the equipment is not widely accessible. The possibility of using a ball mill in a research group in this department was explored, but the owner was concerned about possible metal residues in the reactor.

Scheme 2.9 Synthesis of **HII** and **nG** from **Ind-II**

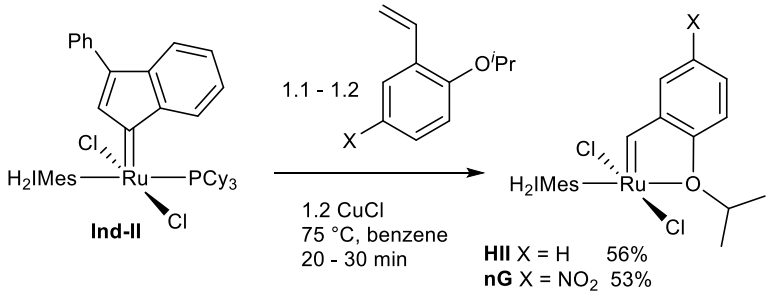

2.2.3 Analysis of synthetic routes to UC-C1

Developing a high-yield and clean synthetic route to **UC-C1** is important because this complex serves not only as a key CAAC catalyst in its own right, but also as a precursor to **HII-C1** or **nG-C1**. Attempts to reproduce the Skowerski procedure resulted in only 10-15% **UC-C1**, much lower than the reported yield of 60%. The poor yields could have several sources. First, the free **C1** may not have been fully generated, which would limit conversion of **Ind-0** to **UC-C1**. Alternatively, incomplete reaction could be due to the incomplete solubility of **C1**·BF_4 in aromatic solvents. Finally, the free CAAC ligand may decompose at elevated temperature. To test the last two points, synthesis of **UC-C1** was carried out at ambient temperature in THF, in which **C1**·BF_4 is partially soluble (Scheme 2.10). Free **C1** was generated in situ by mixing **C1**·BF_4 with LiHMDS for 10 min in THF (until the suspension turned clear). **Ind-0** was then added to free **C1** and stirred at ambient temperature for 2.5 h until ^{31}P NMR indicated no **Ind-0** left. The yield was improved to 32%, but this is still unsatisfactory.

Scheme 2.10 Modified synthesis of **UC-C1**

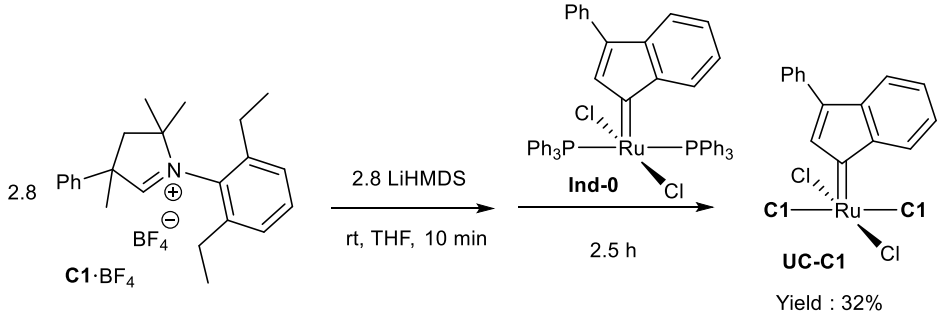

Isolation of **UC-C1** is also problematic. In the Skowerski report, **UC-C1** was reprecipitated from CH_2Cl_2 by addition of nitromethane, to remove free PPh_3 and the bis(trimethylsilyl)amine byproduct. In our hands, this procedure did not completely remove the phosphine. Purification of **UC-C1** by column chromatography using 19:1 hexanes/EtOAc as eluant was also unsuccessful in completely removing free PPh_3. (The Merrifield resin approach[13] was not used in this case, as PPh_3 was thought to be too poor a nucleophile to effect efficient S_N2 reaction with the CH_2I groups on the resin). Moreover, because **UC-C1** is hexanes-soluble, PPh_3 cannot be selectively extracted with hexanes. Reprecipitation using CH_2Cl_2/MeOH gave clean **UC-C1** but in only 32% yield.

2.2.4 Analysis of routes to Hoveyda- and Grela-class catalysts bearing a C1 ligand

An expected limitation of the Grubbs-Bertrand route is the competing reaction of KHMDS with **HI**, leading to unwanted byproducts. To examine whether this risk is real, and how fast it occurs, the NMR-scale reaction of **HI** with KHMDS was carried out in C_6D_6 (Scheme 2.11), with 1,3,5-trimethoxybenzene (TMB) as internal standard. A 42% decrease in the alkylidene signal for **HI** was observed within 30 min. Two new alkylidene signals accounted for 9% and 4% of the original charge of **HI**, meaning that total alkylidene loss is 29%. The new signals could be the structures shown in Scheme 2.11. Their identity was not pursued, but this clearly shows that competing reaction can occur, and that the majority product no longer contains a benzylidene ligand.

Scheme 2.11 Proposed reaction of KHMDS with **HI**

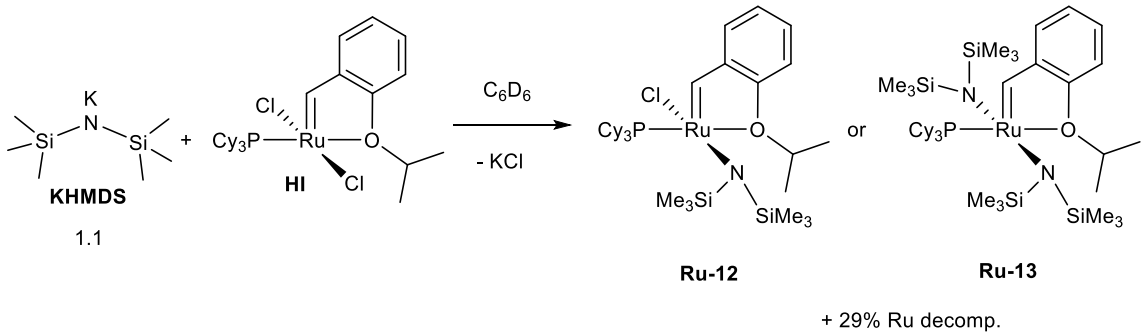

Synthesis of **HII-C1** was therefore carried out by adding **HI** to in situ-generated **C1** (that is, **C1** was generated in situ, then filtered through a pad of Celite to remove any residual base). However, yields remained only about 40% (38-43%). Utilizing **UC-C1** as precursor to **HII-C1** increased the yield to 52%, but the reported yield of 86% could not be reached.

Attempts to reproduce the Skowerski one-pot synthesis of **nG-C1** failed, proceeding in only 5% yield, as compared with the reported yield of 38%. A two-stage process, utilizing isolated **UC-C1** as precursor, is therefore preferred. Considering the low-yield synthesis of **UC-C1**, another approach was also tried, in which the first-generation Grela catalyst **nGI** was added to in-situ generated **C1** (Scheme 2.12). A slight excess of **C1**·BF_4 (1.25 equiv) was used to consume KHMDS (1.2 equiv). However, none of the desired product was isolated, probably because of nucleophilic attack of **C1** on the nitro substituent.

Scheme 2.12 Synthesis of **nG-C1** from **nGI**

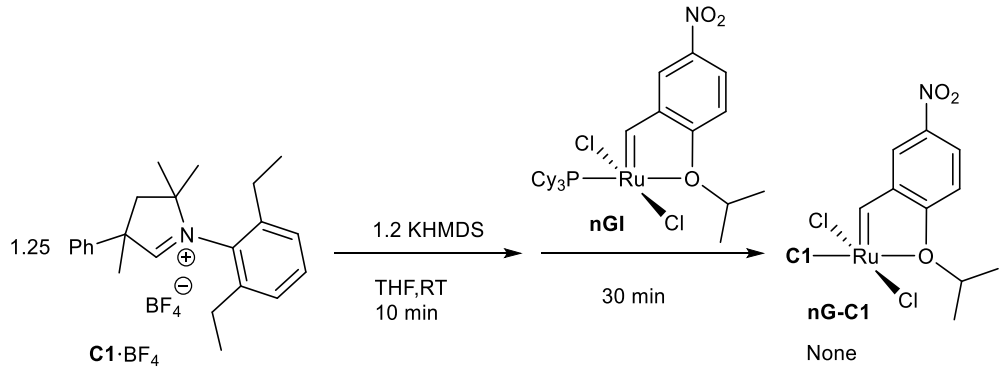

2.3 Conclusion and suggestions for future work

Discussed above are challenges and improvements to the most current, high-yield synthetic routes to second-generation Ru metathesis catalysts. While routes to catalysts bearing an H_2IMes ligand have been explored intensively, routes to CAAC catalysts have only begun to be explored. A key lesson in both the NHC and the CAAC chemistry is the impact on isolated yields of Hoveyda- or Grela-class catalysts of methods used to remove the free PCy_3. Both chromatography and extraction are tedious and reduce yields. Use of Merrifield resin as a phosphine scavenger is much more convenient. Alternatively, the route based on $RuCl_2$(*p*-cymene)(H_2IMes) is a clean and atom-economical entry point to **HII**, which offers very good yields and sidesteps the need for **GII**, which is expensive to buy or tedious to prepare. Although this route has not been applied to **nG**, it has great potential and should be explored.

In comparison, synthetic routes to CAAC catalyst are currently limited by moderate yields and poor reproducibility (as shown in Table 2.3), as well as tedious purification. Computational assessment of the pK_a of the aldiminium proton in the cyclic aldiminium salts, vs the benzylic protons in the N-diethylphenyl and N-mesityl groups, could be helpful in identifying an optimal base.

Table 2.3 Summary of current best routes to **C1** metathesis catalysts from various Ru precursors

Target	Precursor	Reported yield	Reproduced yield via literature route	Updated yield via modified route[a]	Ref.
UC-C1	**Ind-0**	60%	10-15%	32%	5
HII-C1	**UC-C1**	86%	52%	-	5
HII-C1	**HI**	45%	-	38-43%	4
nG-C1	**Ind-0**	38%	5%	-	6
nG-C1	**nGI**	N/A	N/A	0%	This work

[a] Reproduced in duplicate or triplicate in each case.

Base-free synthesis via CAAC·CO_2 salts is less promising, given that for NHC·CO_2, very high temperatures are required to liberate the free NHC, and chromatographic purification is still necessary. The CO_2 adducts have been reported with other CAACs,[50,51] but not with those of primary interest in olefin metathesis.

Development of free-CAAC routes should be considered a priority. The successful isolation of the free N-DIPP CAACs by the Bertrand group makes a case for isolation of free **C1** and other CAAC ligands that show maximum metathesis activity. Also promising is the development of a CAAC analogue to the $RuCl_2$(*p*-cymene)(NHC) complexes, which could allow installation of a benzylidene via reaction with $ArCHN_2$. This avenue is being explored by Eliza-Jayne Boisvert of the Fogg group.

2.4 Experimental

2.4.1 General procedures

The reactions were carried out under N_2 in a glovebox or Schlenk line unless otherwise noted. HPLC-grade solvents (C_6H_6, *n*-hexane, CH_2Cl_2, THF) dried and degassed using a Glass Contour solvent purification system, and stored under N_2 over 4 Å molecular sieves for at least 12 h prior to use. Ethyl acetate was distilled over $MgSO_4$ under N_2 protection, then brought into the glovebox and stored over 4 Å molecular sieves for at least 12 h prior to use. $CDCl_3$ and C_6D_6 (Cambridge Isotopes) were freeze/pump/thaw degassed and stored as above. The **C1**·BF_4 salt was synthesized according to literature methods.[6] Glassware was flame-dried, or oven-dried overnight. NMR spectra were recorded on Avance 300 NMR spectrometers at 23 ± 2 °C.

2.4.2 Two routes to O=CH-C_6H_4-2-O^{i}Pr (2)

A) The reaction was carried out using a slight modification to the Grela procedure.[41,42] To a two-neck round-bottom flask were added 15 mL anhydrous DMF, K_2CO_3 (1.658 g, 4 mmol, 3.0 equiv) and *o*-hydroxybenzaldehyde **1** (0.42 mL, 4 mmol, 1.0 equiv). The suspension was stirred for 10 min at RT, after which ^{i}PrI (0.81 mL, 8.0 mmol, 2.0 equiv) was injected. The reaction was stirred at 45 ºC for 16 h, then quenched with distilled water. The aqueous phase was extracted with Et_2O (3x). The organic layer was combined and washed with water, dried with $MgSO_4$ and filtered. The solvent was removed under vacuum to afford the product as a yellow oil (0.591 g, 90%). ^{1}H NMR data were consistent with literature values.[43] The key signal is specified below.

^{1}H NMR (300 MHz, $CDCl_3$): δ 10.48 (s, 1H, aldehyde C*H*O).

B) The reaction was carried out using the Marciniec procedure.[44] To a round-bottom Schlenk flask, *o*-isopropoxybromobenzene **4** (0.43 g, 2.0 mmol, 1.0 equiv) and 10 mL THF were added. nBuLi (2.61 M, 0.92 mL, 1.2 equiv) was injected into the Schlenk flask at -78 °C and stirred for 3 h. DMF (0.1754 g, 2.4 mmol, 1.2 equiv) in 2 mL THF was added dropwise. The suspension was stirred overnight, then quenched with saturated aqueous NH_4Cl and extracted with Et_2O (3x). The combined organic layers were washed with water, dried ($MgSO_4$), and filtered. The solvent was

removed under vacuum to afford the product as a yellow oil (0.24 g, 65%). ^{1}H NMR data were consistent with literature values;[43] the key signal is specified below.

^{1}H NMR (300 MHz, $CDCl_3$): δ 10.48 (s, 1H, aldehyde C*H*O).

2.4.3 Synthesis of CH_2=CH-C_6H_4-2-O^{i}Pr (3)

The reaction was carried out using Barbasiewicz's procedure with slight modification.[46] In a Schlenk flask, KOtBu (0.224 g, 2.0 mmol, 2.0 equiv), PPh_3MeBr (0.7145 g, 2.0 mmol, 2.0 equiv) and anhydrous 30 mL THF were added. The reaction was stirred at 0 °C for 90 min. *o*-isopropoxybenzaldehyde **2** (0.1642 g, 1.0 mmol, 1.0 equiv) was dissolved in 5 mL anhydrous THF, then dropwise added to the stirred reaction mixture. The reaction was stirred for 16 h then quenched with saturated solution of NH_4Cl, extracted with Et_2O (3x). The organic layer was combined and dried with $MgSO_4$. The solvent was removed under vacuum. The crude product was purified by chromatography (silica gel; hexanes : EtOAc = 10:1). Pale yellow oil was obtained (0.137 g, 85%). ^{1}H NMR data were consistent with literature values;[45] key signals are specified below.

^{1}H NMR (300 MHz, $CDCl_3$): δ 5.78 (dd, $^2J_{HH}$ = 1.5 Hz, $^3J_{HH}$ = 18 Hz, 1H, *trans*-C*H*$_2$=CHAr).

2.4.4 Synthesis of O=CH-C_6H_3-2-O^{i}Pr-5-NO_2 (2')

The reaction was carried out with a slight modification of the Grela procedure.[41,42] In a two-neck round-bottom flask, 20 mL anhydrous DMF, K_2CO_3 (3.32 g, 24.0 mmol, 2.0 equiv), Cs_2CO_3 (0.3 g, 0.96 mmol, 0.08 equiv), 2-hydroxy-5-nitrobenzaldehyde **1'** (2.0 g, 11.97 mmol, 1.0 equiv) were added. The reaction was stirred for 10 min at RT. ^{i}PrI in total (4.1 g, 24.1 mmol, 2.0 equiv) was injected several times over 72 h. The reaction was filtered through a fritted funnel, and the solid was rinsed with 20 mL water and 10 mL CH_2Cl_2. The filtrate was transferred into a separatory funnel. Et_2O was used to extract product (2x). Aqueous layer was then extracted with CH_2Cl_2 until organic layer was colorless. The organic layer was combined, dried with $MgSO_4$ and filtered. The solvent was removed under vacuum to afford the product as a yellow solid (2.05 g, 82%). ^{1}H NMR data were consistent with literature values.[41] The key signal is specified below.

^{1}H NMR (300 MHz, $CDCl_3$): δ 10.47 (s, 1H, aldehyde C*H*O).

2.4.5 Synthesis of CH_2=CH-C_6H_3-2-O^{i}Pr-5-NO_2 (3')

The reaction was carried out with a slight modification of the Barbasiewicz procedure.[46] In a Schlenk flask, KOtBu (0.168 g, 1.45 mmol, 1.5 equiv), PPh_3MeBr (0.54 g, 1.45 mmol, 1.5 equiv) and anhydrous 25 mL THF were added. The reaction was stirred at 0 °C for 90 min. A solution of 2-isopropoxy-5-nitrobenzaldehyde **2'** (0.2 g, 0.9 mmol, 1.0 equiv) in 5 mL anhydrous THF was added dropwise to the stirred reaction mixture. The reaction was stirred for 16 h then quenched with a saturated solution of NH_4Cl, extracted with Et_2O (3x). The organic layer was combined and dried with $MgSO_4$. The solvent was removed under vacuum. The crude product was purified using

column chromatography (silica gel; hexanes:EtOAc = 10:1). Pale yellow solid was obtained (0.112 g, 60%). ^{1}H NMR data were consistent with literature values.[41] The key signals are specified below.

^{1}H NMR (300 MHz, $CDCl_3$): δ 5.86 (dd, $^2J_{HH}$ = 1 Hz, $^3J_{HH}$ = 17.5 Hz, 1H, trans-C*H*$_2$=CHAr).

2.4.6 Synthesis of C_6H_4-1-O^{i}Pr-2-Br (5)

The reaction was carried out according to the literature with slight modification.[52] To a two-neck round-bottom flask, 30 mL anhydrous DMF, K_2CO_3 (6 g, 43.2 mmol, 3.0 equiv), *o*-hydroxybromobenzene **4** (2.5 g, 14.4 mmol, 1.0 equiv) and NaI (0.22 g, 1.44 mmol, 0.1 equiv) were added. The reaction was stirred for 10 min at RT. ^{i}PrBr (2.03 mL, 8.0 mmol, 2.0 equiv) was injected into the reaction mixture. The reaction was stirred at 45 ºC for 16 h. The reaction was quenched with distilled water. The aqueous phase was extracted with EtOAc (3x). The organic layer was combined and washed with water, dried with $MgSO_4$ and filtered. The solvent was removed under vacuum to afford the product as a yellow oil (2.63 g, 85%). ^{1}H NMR data were consistent with literature values.[52] The key signal is specified below.

^{1}H NMR (300 MHz, $CDCl_3$): δ 4.54 (sept, $^3J_{HH}$ = 6 Hz, 1H, OC*H*Me$_2$),

2.4.7 Synthesis of C_6H_4-1-O^{i}Pr-2-Br-4-NO_2 (5')

The reaction was carried out according to the literature with slight modification.[52] To a two-neck round-bottom flask, 10 mL anhydrous DMF, K_2CO_3 (0.415 g, 3.0 mmol, 3.0 equiv), 2-hydroxy-5-nitrobromobenzene **4'** (0.218 g, 1.0 mmol, 1.0 equiv) and NaI (15 mg, 0.1 mmol, 0.1 equiv) were added. The reaction was stirred for 10 min at RT. ^{i}PrBr (2.03 mL, 8.0 mmol, 2.0 equiv) was injected into the reaction mixture. The reaction was stirred at 45 ºC for 16 h. Solvent was removed under vacuum. Distilled water was added to reaction mixture. The aqueous phase was extracted with CH_2Cl_2 (3x). The organic layer was combined and washed with water, dried with $MgSO_4$ and filtered. The solvent was removed under vacuum to afford the product as a yellow solid (0.195 g, 75%).

^{1}H NMR (300 MHz, $CDCl_3$) δ 8.46 (d, $^4J_{HH}$ = 3 Hz, 1H, Ar), 8.17 (dd, $^3J_{HH}$ = 9 Hz, $^4J_{HH}$ = 3 Hz, 1H, Ar), 6.93 (dd, $^3J_{HH}$ = 9 Hz, $^5J_{HH}$ = 0.5 Hz, 1H, Ar), 4.71 (sept, $^3J_{HH}$ = 6 Hz, 1H, OC*H*Me$_2$), 1.44 (d, $^3J_{HH}$ = 6 Hz, 6H, CH(C*H*$_3$)$_2$).

2.4.8 Attempted synthesis of O=CH-C_6H_3-2-O^{i}Pr-5-NO_2 (2') from C_6H_4-1-O^{i}Pr-2-Br-4-NO_2 (5')

In the glovebox, 2-isopropoxy-5-nitrobromobenzene **5'** (0.1405 g, 0.538 mmol, 1.0 equiv) was dissolved in 15 mL THF in a Schlenk flask. The flask was carried out and connected to the Schlenk line. nBuLi (1.97 M, 0.32 mL, 1.2 equiv) was injected into the Schlenk flask at -78 °C. The reaction mixture was stirred at -78 °C for 1 hour. DMF (47 mg, 0.646 mmol, 1.2 equiv) was dissolved in 2 mL THF then, added to the reaction mixture dropwise and stirred overnight. The reaction was quenched with a saturated solution of NH_4Cl, then extracted with Et_2O (3x). The organic layer was combined, dried with $MgSO_4$ and filtered. Only unreacted DMF was isolated.

In the glovebox, 2-isopropoxy-5-nitrobromobenzene **5'** (0.238 g, 0.92 mmol, 1.0 equiv) was dissolved in 15 mL THF in a Schlenk flask. The flask was transferred to the Schlenk line, and ^{i}PrMgCl (1.3 M, 0.85 mL, 1.2 equiv) and anhydrous LiCl (42.8 mg, 1.104 mmol, 1.2 equiv) were mixed in a Schlenk flask. ^{i}PrMgCl:LiCl (1:1) solution was added to **5'** at -40 °C dropwise. The reaction mixture was stirred at -40 °C for 2 hours. DMF (80 mg, 1.104 mmol, 1.2 equiv) was injected into the reaction mixture dropwise and stirred for 1 hour. The reaction was quenched with a saturated solution of NH_4Cl, then extracted with Et_2O (3x). The organic layer was combined, dried with $MgSO_4$ and filtered. Only unreacted DMF was isolated.

2.4.9 Synthesis of HII from GII or Ind-II

The reaction was carried out using Hoveyda's procedure with slight modification. **GII** (0.335 g, 0.394 mmol, 1.0 equiv), CuCl (46.8 mg, 0.473 mmol, 1.2 equiv), and **3** (71 mg, 0.433 mmol, 1.1 equiv) were dissolved in 10 mL CH_2Cl_2. The reaction was stirred at 30 °C for 25 min. The solvent was removed under vacuum. The crude mixture was dissolved in 15-20 mL EtOAc, the filtered through a fritted funnel to remove CuCl-PCy_3 as white powder. Ethyl acetate was then removed under vacuum. The mixture was dissolved in benzene, then loaded on column (silica gel). Elution with hexanes/EtOAc (5:2) removes **HII** as a green band (0.184 g, 75%). ^{1}H NMR data were consistent with literature values.[11] The key signal is specified below.

^{1}H NMR (300 MHz, $CDCl_3$): δ 16.56 (s, 1H, [Ru]=C*H*Ar).

Ind-II (0.3 g, 0.316 mmol, 1.0 equiv), CuCl (44 mg, 0.44 mmol, 1.4 equiv) and **3** (61 mg, 0.376 mmol, 1.2 equiv) were dissolved in 10 mL benzene. The reaction mixture was stirred at 75 °C for 15 min. The solvent was removed under vacuum. The crude mixture was dissolved in EtOAc and filtered through a fitted funnel to remove CuCl-PCy_3. EtOAc was removed under vacuum. The crude mixture was dissolved in benzene then loaded on column (silica gel). Elution with hexanes/EtOAc (10:3) removes **HII** (110.1 mg, 56%) as a green bond. ^{1}H NMR data were consistent with literature values.[11] The key signal is specified below.

^{1}H NMR (300 MHz, $CDCl_3$): δ 16.56 (s, 1H, [Ru]=C*H*Ar).

2.4.10 Synthesis of nG from GII or Ind-II

The reaction was carried out with slight modifications of the Grela procedure. **GII** (0.13 g, 0.153 mmol, 1.0 equiv), CuCl (19 mg, 0.184 mmol, 1.2 equiv), and **3** (29 mg, 0.184 mmol, 1.2 equiv) were dissolved in 18 mL CH_2Cl_2. The reaction was stirred at 40 °C for 20 min with the glovebox lights turned off. The solvent was removed under vacuum. The crude mixture was dissolved in EtOAc, the filtered through a fritted funnel to remove CuCl-PCy_3 as white powder. Ethyl acetate was then removed under vacuum. The mixture was dissolved in benzene, then loaded on column (silica gel). Elution with hexanes/EtOAc (5:2) removes **nG** as a green band (72 mg, 70%). ^{1}H NMR data were consistent with literature values.[41] The key signal is specified below.

^{1}H NMR (300 MHz, $CDCl_3$): δ 16.47 (s, 1H, [Ru]=C*H*Ar).

Ind-II (0.3226 g, 0.34 mmol, 1.0 equiv), CuCl (47 mg, 0.475 mmol, 1.4 equiv) and **3'** (84.5 mg, 0.4078 mmol, 1.2 equiv) were dissolved in 10 mL benzene. The reaction mixture was stirred at 75 °C for 30 min. The solvent was removed under vacuum. The crude mixture was dissolved in EtOAc and filtered through a fitted funnel. EtOAc was removed under vacuum. The crude mixture was dissolved in benzene then loaded on column (silica gel). Elution with hexanes/EtOAc (10:3) removes **nG** (114.8 mg, 53%) as a green bond. ^{1}H NMR data were consistent with literature values.[41] The key signal is specified below.

^{1}H NMR (300 MHz, $CDCl_3$): δ 16.47 (s, 1H, [Ru]=C*H*Ar).

2.4.11 Synthesis of UC-C1

The reaction was carried out by slight modification of the Skowerski procedure.[5] **C1**·BF_4 (0.2347 g, 0.5825 mmol, 2.8 equiv) and LiHMDS (0.098 g, 0.5824 mmol, 2.8 equiv) were dissolved in 5 mL THF. The reaction mixture was stirred in a sealed 20 mL vial for 10 min. **Ind-0** (0.1846 g. 0.208 mmol, 1.0 equiv) was added to reaction mixture for 2.5 h. The reaction was filtered through a pad of Celite. The solvent was removed under vacuum. The crude mixture was dissolved in Et_2O, then filtered through a pad of Celite and dried under vacuum. The crude product was dissolved in a small amount of CH_2Cl_2, then cold MeOH was added. CH_2Cl_2 was removed under vacuum. The precipitate was filtered through a fritted funnel, then dried under vacuum overnight to yield a dark red powder. Yield 67 mg (32%). ^{1}H NMR data were consistent with literature values.[5] The key signal is specified below.

^{1}H NMR (300 MHz, C_6D_6): δ 9.59 (d, $^3J_{HH}$ = 7.5 Hz, 1H, [Ru]=CCCH of ind).

2.4.12 Synthesis of HII-C1 from HI or UC-C1

The reaction was carried out using Grubbs procedure with slight modification.[4] In a Schlenk flask, **C1**·BF_4 (0.52 g, 1.27 mmol, 1.3 equiv) and LiHMDS (0.213 g, 1.27 mmol, 1.3 equiv) were dissolved in 10 mL THF. The reaction mixture was stirred for 3 min, the filtered through a pad of Celite. **HI** (0.587 g, 0.977 mmol, 1.0 equiv) was added to free **C1**. The reaction was stirred for 1 hour. The crude ^{1}H NMR suggested **HI** was remained. Therefore, another 0.1 equiv free **C1** was added to reaction mixture. After stirring for another 2 h, reaction mixture was filtered through a pad of Celite. The solvent was removed under vacuum. **HII-C1** was isolated by chromatography (silica gel; hexanes:EtOAc = 10:1 to 5:2) as a dark green powder. Yield 0.269 g (43%). ^{1}H NMR data were consistent with literature values.[4] The key signals are specified below.

^{1}H NMR (300 MHz, $CDCl_3$): δ 17.72 (s, 0.29 H, [Ru]=C*H*Ar, minor isomer). δ 16.47 (s, 1H, [Ru]=C*H*Ar, major isomer).

The reaction was carried out using the Skowerski procedure with slight modification.[6] In a Schlenk flask, **UC-C1** (0.18 g, 0.18 mmol, 1.0 equiv), **3** (32 mg, 0.198 mmol, 1.1 equiv) and CuCl (26.7 mg, 0.216 mmol, 1.2 equiv) were mixed in 15 mL benzene. The reaction mixture was stirred at 75 °C for 25 min. Solvent was removed under vacuum. Crude mixture was dissolved in EtOAc,

the filtered through a pad of Celite. EtOAc was then removed under vacuum. **HII-C1** was isolated by column chromatography (silica gel; 5:1 hexanes:EtOAc eluant). ^{1}H NMR data were consistent with literature values.[4] The key signals are specified below.

^{1}H NMR (300 MHz, $CDCl_3$): δ 17.72 (s, 0.29 H, [Ru]=C*H*Ar, minor isomer). δ 16.47 (s, 1H, [Ru]=C*H*Ar, major isomer).

2.4.13 Attempted synthesis of nG-C1 from nGI

In a 20 mL vial, **C1**·BF_4 (61 mg, 0.15 mmol) and KHMDS (29 mg, 0.15 mmol, 1.2 equiv) were dissolved in 3 mL THF and stirred for 10 min. **nGI** (78 mg, 0.121 mmol) was added to the reaction mixture. The reaction was stirred for 20 min. ^{1}H NMR analysis of the crude material in protonic-THF showed no alkylidene signal for **nG-C1**.

2.4.14 Decomposition of HI by KHMDS

HI (8.2 mg, 0.0136 mmol, 1.0 equiv) and TMB (ca. 1 mg) were dissolved in 0.6 mL C_6D_6 in a J-Young NMR tube. A spectrum was taken to establish the initial ratio of TMB to **HI**, and the sample was returned to the glovebox. KHMDS (3 mg, 0.15 mmol, 1.1 equiv) was added, and the solution was mixed. ^{1}H NMR analysis after 30 min indicated a 42% decrease in the alkylidene signal for **HI**. Two new alkylidene signals accounted for 13% of the original charge of **HI**, meaning that total alkylidene loss is 29%.

^{1}H NMR (300 MHz, C_6D_6): δ 17.56 (s, unknown, 9%), 17.16 (d, $^3J_{HP}$ = 5.5 Hz, unknown, 4%), 17.37 (d, $^3J_{HP}$ = 4.5 Hz, **HI**, 58%). The spectrum is shown in the Appendices (Figure A1). The chemical shift for **HI** is in relatively good agreement with the reported value in $CDCl_3$ (δ 17.44, d, $^3J_{HP}$ = 4.5 Hz).[28]

2.5 References

(1) Grubbs, R. H.; Wenzel, A. G., *Handbook of Metathesis*. 2nd ed.; Wiley-VCH: Weinheim, 2015.

(2) Higman, C. S.; Lummiss, J. A. M.; Fogg, D. E., Olefin Metathesis at the Dawn of Uptake in Pharmaceutical and Specialty Chemicals Manufacturing. *Angew. Chem., Int. Ed.* **2016**, *55*, 3552–3565.

(3) Vougioukalakis, G. C.; Grubbs, R. H., Ruthenium-Based Heterocyclic Carbene-Coordinated Olefin Metathesis Catalysts. *Chem. Rev.* **2010**, *110*, 1746–1787.

(4) Marx, V. M.; Sullivan, A. H.; Melaimi, M.; Virgil, S. C.; Keitz, B. K.; Weinberger, D. S.; Bertrand, G.; Grubbs, R. H., Cyclic Alkyl Amino Carbene (CAAC) Ruthenium Complexes as Remarkably Active Catalysts for Ethenolysis. *Angew. Chem., Int. Ed.* **2015**, *54*, 1919–1923.

(5) Gawin, R.; Kozakiewicz, A.; Guńka, P. A.; Dąbrowski, P.; Skowerski, K., Bis(Cyclic Alkyl Amino Carbene) Ruthenium Complexes: A Versatile, Highly Efficient Tool for Olefin Metathesis. *Angew. Chem., Int. Ed.* **2017**, *56*, 981–986.

(6) Gawin, R.; Tracz, A.; Chwalba, M.; Kozakiewicz, A.; Trzaskowski, B.; Skowerski, K., Cyclic Alkyl Amino Ruthenium Complexes—Efficient Catalysts for Macrocyclization and Acrylonitrile Cross Metathesis. *ACS Catal.* **2017**, *7*, 5443–5449.

(7) Nascimento, D. L.; Gawin, A.; Gawin, R.; Guńka, P. A.; Zachara, J.; Skowerski, K.; Fogg, D. E., Integrating Activity with Accessibility in Olefin Metathesis: An Unprecedentedly Reactive Ruthenium-Indenylidene Catalyst Bearing a Cyclic Alkyl Amino Carbene. *J. Am. Chem. Soc.* **2019**, *141*, 10626–10631.
(8) Nascimento, D. L.; Fogg, D. E., Origin of the Breakthrough Productivity of Ruthenium-CAAC Catalysts in Olefin Metathesis (CAAC = Cyclic Alkyl Amino Carbene). *J. Am. Chem. Soc.* **2019**, *141*, 19236–19240.
(9) Scholl, M.; Ding, S.; Lee, C. W.; Grubbs, R. H., Synthesis and Activity of a New Generation of Ruthenium-Based Olefin Metathesis Catalysts Coordinated with 1,3-Dimesityl-4,5-dihydroimidazol-2-ylidene Ligands. *Org. Lett.* **1999**, *1*, 953–956.
(10) Trnka, T. M.; Morgan, J. P.; Sanford, M. S.; Wilhelm, T. E.; Scholl, M.; Choi, T.-L.; Ding, S.; Day, M. W.; Grubbs, R. H., Synthesis and Activity of Ruthenium Alkylidene Complexes Coordinated with Phosphine and N-Heterocyclic Carbene Ligands. *J. Am. Chem. Soc.* **2003**, *125*, 2546–2558.
(11) Garber, S. B.; Kingsbury, J. S.; Gray, B. L.; Hoveyda, A. H., Efficient and Recyclable Monomeric and Dendritic Ru-Based Metathesis Catalysts. *J. Am. Chem. Soc.* **2000**, *122*, 8168–8179.
(12) Sauvage, X.; Demonceau, A.; Delaude, L., Imidazol(in)ium-2-carboxylates as N-Heterocyclic Carbene Precursors for the Synthesis of Second Generation Ruthenium Metathesis Catalysts. *Adv. Synth. Catal.* **2009**, *351*, 2031–2038.
(13) Nascimento, D. L.; Davy, E. C.; Fogg, D. E., Merrifield Resin-Assisted Routes to Second-Generation Catalysts for Olefin Metathesis. *Catal. Sci. Technol.* **2018**, 1535–1544.
(14) Day, C. S.; Fogg, D. E., High-Yield Synthesis of a Long-Sought, Labile Ru-NHC Complex and Its Application to the Concise Synthesis of Second-Generation Olefin Metathesis Catalysts. *Organometallics* **2018**, *24*, 4551–4555.
(15) Weskamp, T.; Schattenmann, W. C.; Spiegler, M.; Herrmann, W. A., A Novel Class of Ruthenium Catalysts for Olefin Metathesis. *Angew. Chem., Int. Ed.* **1998**, *37*, 2490–2493.
(16) Scholl, M.; Trnka, T. M.; Morgan, J. P.; Grubbs, R. H., Increased Ring Closing Metathesis Activity of Ruthenium-Based Olefin Metathesis Catalysts Coordinated with Imidazolin-2-Ylidene Ligands. *Tetrahedron Lett.* **1999**, *40*, 2247–2250.
(17) Huang, J.; Stevens, E. D.; Nolan, S. P.; Petersen, J. L., Olefin Metathesis-Active Ruthenium Complexes Bearing a Nucleophilic Carbene Ligand. *J. Am. Chem. Soc.* **1999**, *121*, 2674–2678.
(18) Bantreil, X.; Nolan, S. P., Synthesis of N-heterocyclic carbene ligands and derived ruthenium olefin metathesis catalysts. *Nature Protoc.* **2011**, *6*, 69–77.
(19) Lummiss, J. A. M.; Higman, C. S.; Fyson, D. L.; McDonald, R.; Fogg, D. E., The Divergent Effects of Strong NHC Donation in Catalysis. *Chem. Sci.* **2015**, *6*, 6739–6746.
(20) Lummiss, J. A. M.; Perras, F. A.; Bryce, D. L.; Fogg, D. E., Sterically-Driven Metathesis: The Impact of Alkylidene Substitution on the Reactivity of the Grubbs Catalysts. *Organometallics* **2016**, *35*, 691–698.
(21) Hong, S. H.; Wenzel, A. G.; Salguero, T. T.; Day, M. W.; Grubbs, R. H., Decomposition of Ruthenium Olefin Metathesis Catalysts. *J. Am. Chem. Soc.* **2007**, *129*, 7961–7968.
(22) Lummiss, J. A. M.; Beach, N. J.; Smith, J. C.; Fogg, D. E., Targeting an Achilles Heel In Olefin Metathesis: A Strategy For High-Yield Synthesis of Second-Generation Grubbs Methylidene Catalysts. *Catal. Sci. Technol.* **2012**, *2*, 1630–1632.

(23) Lummiss, J. A. M.; Botti, A. G. G.; Fogg, D. E., Isotopic Probes for Ruthenium-Catalyzed Olefin Metathesis. *Catal. Sci. Technol.* **2014**, *4*, 4210–4218.
(24) McClennan, W. L.; Rufh, S. A.; Lummiss, J. A. M.; Fogg, D. E., A General Decomposition Pathway for Phosphine-Stabilized Metathesis Catalysts: Lewis Donors Accelerate Methylidene Abstraction. *J. Am. Chem. Soc.* **2016**, *138*, 14668−14677.
(25) Lummiss, J. A. M.; Ireland, B. J.; Sommers, J. M.; Fogg, D. E., Amine-Mediated Degradation in Olefin Metathesis Reactions that Employ the Second-Generation Grubbs Catalysts. *ChemCatChem* **2014**, *6*, 459–463.
(26) Lummiss, J. A. M.; McClennan, W. L.; McDonald, R.; Fogg, D. E., Donor-Induced Decomposition of the Grubbs Catalysts: An Intercepted Intermediate *Organometallics* **2014**, *33*, 6738–6741.
(27) Bailey, G. A.; Fogg, D. E., Acrylate Metathesis via the Second-Generation Grubbs Catalyst: Unexpected Pathways Enabled by a PCy_3-Generated Enolate. *J. Am. Chem. Soc.* **2015**, *137*, 7318–7321.
(28) Kingsbury, J. S.; Harrity, J. P. A.; Bonitatebus, P. J.; Hoveyda, A. H., A Recyclable Ru-Based Metathesis Catalyst. *J. Am. Chem. Soc.* **1999**, *121*, 791–799.
(29) Gessler, S.; Randl, S.; Blechert, S., Synthesis and Metathesis Reactions of a Phosphine-Free Dihydroimidazole Carbene Ruthenium Complex. *Tetrahedron Lett.* **2000**, *41*, 9973–9976.
(30) Leitgeb, A.; Szadkowska, A.; Michalak, M.; Barbasiewicz, M.; Grela, K.; Slugovc, C., Unequal siblings: Adverse characteristics of naphthalene-based hoveyda-type second generation initiators in ring opening metathesis polymerization. *J. Polym. Sci. A* **2011**, *49*, 3448–3454.
(31) Delaude, L., The Chemistry of Azolium-Carboxylate Zwitterions and Related Compounds: a Survey of the Years 2009–2020. *Adv. Synth. Catal.* **2020**, *362*, 3259– 3310.
(32) Sauvage, X.; Zaragoza, G.; Demonceau, A.; Delaude, L., Mixed Isobutylphobane/N-Heterocyclic Carbene Ruthenium-Indenylidene Complexes. *Adv. Synth. Catal.* **2010**, *352*, 1934–1948.
(33) van Lierop, B. J.; Reckling, A. M.; Lummiss, J. A. M.; Fogg, D. E., High-Yield, High-Purity Routes to Second-Generation Ru Metathesis Catalysts from Commercially Available Precursors. *ChemCatChem* **2012**, *4*, 2020–2025.
(34) Yu, B.; Luo, Z.; Hamad, F. B.; Leus, K.; van Heckec, K.; Verpoort, F., Effect of the Bulkiness of Indenylidene Moieties on the Catalytic Initiation and Efficiency of Second Generation Ruthenium-Based Olefin Metathesis Catalysts. *Catal. Sci. Technol.* **2016**, *6*, 2092–2100.
(35) Frey, G. D.; Dewhurst, R. D.; Kousar, S.; Donnadieu, B.; Bertrand, G., Cyclic (alkyl)(amino)carbene gold(I) complexes: A synthetic and structural investigation. *J. Organomet. Chem.* **2008**, *693*, 1674–1682.
(36) Soleilhavoup, M.; Bertrand, G., Cyclic (Alkyl)(Amino)Carbenes (CAACs): Stable Carbenes on the Rise. *Acc. Chem. Res.* **2015**, *48*, 256–266.
(37) Melaimi, M.; Jazzar, R.; Soleilhavoup, M.; Bertrand, G., Cyclic (Alkyl)(amino)carbenes (CAACs): Recent Developments. *Angew. Chem., Int. Ed.* **2017**, *56*, 10046–10068.
(38) Lavallo, V.; Canac, Y.; Sang, C. P.; Donnadieu, B.; Bertrand, G., Stable Cyclic (Alkyl)(Amino)Carbenes as Rigid or Flexible, Bulky, Electron-Rich Ligands for

Transition-Metal Catalysts: A Quaternary Carbon Atom Makes the Difference. *Angew. Chem., Int. Ed.* **2005**, *44*, 5705–709.
(39) Bailey, G. A.; Jensen, V. R.; Fogg, D. E., Oxidation-State Paradigms in Olefin Metathesis. Submitted.
(40) Fraser, R. R.; Mansour, T. S., Acidity Measurements with Lithiated Amines: Steric Reduction and Electronic Enhancement of Acidity. *J. Org. Chem.* **1984**, *49*, 3442–3443.
(41) Michrowska, A.; Bujok, R.; Harutyunyan, S.; Sashuk, V.; Dolgonos, G.; Grela, K., Nitro-Substituted Hoveyda-Grubbs Ruthenium Carbenes: Enhancement of Catalyst Activity through Electronic Activation. *J. Am. Chem. Soc.* **2004**, *126*, 9318–9325.
(42) Bieniek, M.; Michrowska, A.; Gulajski, L.; Grela, K., A Practical Larger Scale Preparation of Second-Generation Hoveyda-Type Catalysts. *Organometallics* **2007**, *26*, 1096–1099.
(43) Rouen, M.; Chaumont, P.; Barozzino-Consiglio, G.; Maddaluno, J.; Harrison-Marchand, A., Chiral Lithium Amido Zincates for Enantioselective 1,2-Additions: Auto-assembling Reagents Involving a Fully Recyclable Ligand. *Chem. Eur. J.* **2018**, *24*, 9238–9242.
(44) Marciniec, B.; Rogalski, S.; Potrzebowski, M. J.; Pietraszuk, C., *ChemCatChem* **2011**, *3*, 904–910.
(45) Bates, J. M. Ruthenium Catalysts for Olefin Metathesis: Understanding the Boomerang Mechanism and Challenges Associated with Stereoselectivity. M.Sc. Dissertation, University of Ottawa, Ottawa, ON, 2014.
(46) Basak, T.; Grudzień, K.; Barbasiewicz, M., Remarkable Ability of the Benzylidene Ligand To Control Initiation of Hoveyda–Grubbs Metathesis Catalysts. *Eur. J. Inorg. Chem.* **2016**, 3513–3523.
(47) Bates, J. M.; Lummiss, J. A. M.; Bailey, G. A.; Fogg, D. E., Operation of the Boomerang Mechanism in Olefin Metathesis Reactions Promoted by the Second-Generation Hoveyda Catalyst. *ACS Catal.* **2014**, *4*, 2387−2394.
(48) Krasovskiy, A.; Knochel, P., A LiCl-Mediated Br/Mg Exchange Reaction for the Preparation of Functionalized Aryl- and Heteroarylmagnesium Compounds from Organic Bromides. *Angew. Chem., Int. Ed.* **2004**, *43*, 3333–3336.
(49) Mukherjee, N.; Marczyk, A.; Szczepaniak, G.; Sytniczuk, A.; Kajetanowicz, A.; Grela, K., A Gentler Touch: Synthesis of Modern Ruthenium Olefin Metathesis Catalysts Sustained by Mechanical Force. *ChemCatChem* **2019**, *11*, 5362–5369.
(50) Kuchenbeiser, G.; Soleilhavoup, M.; Donnadieu, B.; Bertrand, G., Reactivity of Cyclic (Alkyl)(amino)carbenes (CAACs) and Bis(amino)cyclopropenylidenes (BACs) with Heteroallenes: Comparisons with their N-Heterocyclic Carbene (NHCs) Counterparts. *Chem. Asian J.* **2009**, *4*, 1745–1750.
(51) Lieske, L. E.; Freeman, L. A.; Wang, G.; Dickie, D. A.; Gilliard, Jr.; R, J.; Machan, C. W., Metal-Free Electrochemical Reduction of Carbon Dioxide Mediated by Cyclic(Alkyl)(Amino) Carbenes. *Chem. Eur. J.* **2019**, *25*, 6098–6101.
(52) Keenan, M.; Abbott, M. J.; Alexander, P. W.; Armstrong, T.; Best, W. M.; Berven, B.; Botero, A.; Chaplin, J. H.; Charman, S. A.; Chatelain, E.; Geldern, T. W. v.; Kerfoot, M.; Khong, A.; Nguyen, T.; McManus, J. D.; Morizzi, J.; Ryan, E.; Scandale, I.; Thompson, R. A.; Wang, S. Z.; White, K. L., Analogues of Fenarimol Are Potent Inhibitors of *Trypanosoma cruzi* and Are Efficacious in a Murine Model of Chagas Disease. *J. Med. Chem.* **2012**, *55*, 4189−4204.

Chapter 3. Entry into and Exit from the Active Cycle for Hoveyda- and Grela-Class Catalysts*

3.1 Introduction

As noted in the thesis introduction, the key factors that control catalyst productivity are initiation, deactivation, and decomposition. Decomposition pathways common to the active species were described in Chapter 1.[1-9] Chapter 2 considered *deactivation* of the Grubbs-class precatalysts and methylidenes, a consequence of the low lability of PCy_3 (Chart 3.1).[10,11] In this chapter, the discussion will turn to initiation and deactivation of the phosphine-free catalysts. A particular focus is the Hoveyda catalyst **HII**, the corresponding catalyst **HII-C1**, in which the H_2IMes ligand is replaced by the CAAC ligand **C1**, and **nG-C1**, the faster-initiating nitro-Grela analogue of **HII-C1**. **HII**-class catalysts containing other CAAC ligands were shown by Grubbs and Bertrand to deliver record-breaking turnover numbers in ethenolysis (ca. 340,000),[12] although Skowerski found it to perform less well than **GII** in macrocyclization via ring-closing metathesis (mRCM).[13]

The faster-initiating **nG-C1** catalyst has been shown by the Skowerski group and our own[13-15] to confer very high productivity in important metathesis reactions, including ethenolysis and macrocyclization. This work in this chapter was aimed at evaluating the impact of the carbene ligand on the rates at which these catalysts enter the catalytic cycle, and recapture the styrenyl ether ligand, via a systematic study of **HII**, **HII-C1**, and **nG-C1**.

Chart 3.1 Catalysts and carbene discussed

* "A Paradigm Inversion in Ru-Catalyzed Olefin Metathesis: Enhancing Metathesis Productivity by Slowing Catalyst Initiation." X. Ou, D. L. Nascimento, G. Occhipinti, V. R. Jensen and D. E. Fogg, Manuscript in Preparation.

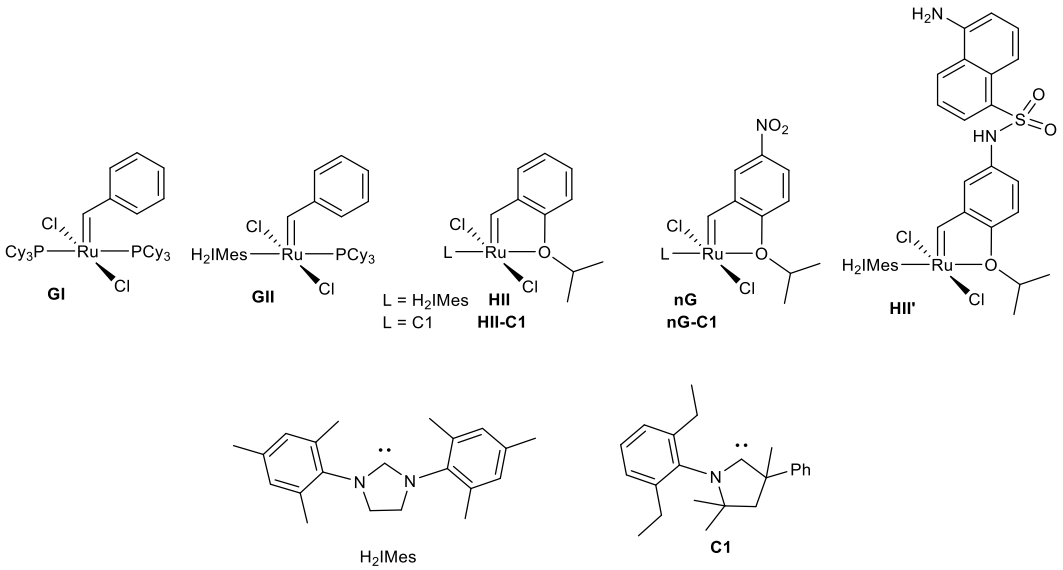

To set the context for examining initiation of the Hoveyda catalysts, it is important to start with a discussion of the Grubbs catalysts, which were studied more thoroughly at an earlier stage. Grubbs and coworkers originally attributed the higher reactivity of their second-generation catalysts (such as **GII**) to the high trans influence of the NHC ligand, and its ability to labilize the PCy_3 ligand.[16] In 2001, however, an important study by Sanford and Grubbs corrected this suggestion, instead showing evidence that the **GII** initiates 150× slower than **GI**. The higher metathesis activity of **GII** was suggested to be due to its bias toward reaction with olefin in preference to rebinding PCy_3.

In this 2001 study, the initiation mechanism for Grubbs catalysts was also discussed. Several vinyl ethers (as specified below) were utilized as substrates to explore the kinetics of initiation. The advantages of using vinyl ethers as substrates are their rapid and irreversible metathesis, and the fact that the Fischer carbenes thus produced do not engage in further metathesis. Such experiments offer a convenient means of measuring initiation rates from the disappearance of precatalyst. The initiation rate constant for **GII** was shown to be independent of ethyl vinyl ether (EVE) concentration over a range of 0.17-1 M (Scheme 3.1). In contrast, for **GI**, saturation kinetics emerged only at 3.0 M, consistent with the much higher lability of the PCy_3 ligand in the first-generation complex. The initiation rate constants for **GII** were found to be essentially identical for EVE, 1-ethoxy-1-propene, dihydrofuran, and dihydropyran (ca. 4.6×10^{-4} s^{-1} at 35 °C). This insensitivity to substrate structures, as well as the positive activation entropy (13 kcal/mol) and large activation enthalpy (27 kcal/mol) observed with EVE are all consistent with a dissociative (D) mechanism.

Scheme 3.1 Initiation mechanism of **GII**

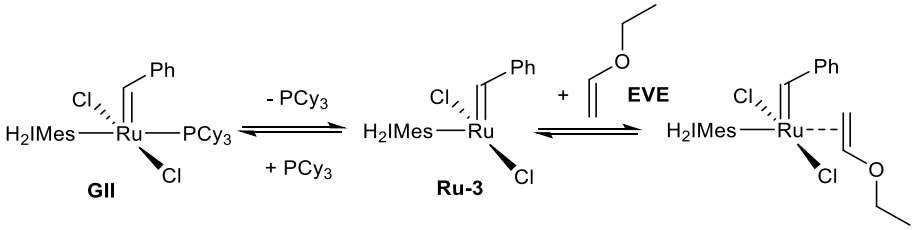

The mechanism of initiation for phosphine-free catalysts such as **HII** has been extensively studied.[17-24] Hoveyda and co-workers originally suggested that **HII** initiates by dissociation of the chelated benzylidene ether ligand donor, by analogy to the chemistry of **GII**. In 2009, an interesting study by Dorta reported that **HII**-type complexes exhibit faster metathesis at higher substrate concentration, meaning that the mechanism must have some associative component.[25] This observation was consistent with an earlier Grubbs study[19] that showed a linear dependence of initiation rates on the concentration of n-butyl vinyl ether (nBuVE) for **HII**-type complexes, with negative activation entropies (-19 to -32 kcal/mol). Indeed, Grubbs had proposed an associative mechanism (Scheme 3.2a) with olefin binding being rate-limiting. In principle, this could be consistent with fast ether dissociation, followed by rate-limiting olefin binding to a four-coordinate species with a dangling benzylidene-ether ligand (**Ru-14**, Scheme 3.2b). However, the robustness of **HII** to solution thermolysis and chromatography in air[17] strongly suggests low ether lability. This tends to support an associative initiation pathway, though it does not indicate whether the rate-determining step is indeed olefin binding, as suggested, or cycloaddition.

In 2011, Plenio reported that **HII** and **nG** initiate via an interchange-associative mechanism (I_A; Scheme 3.2c). This study used EVE and diethyl diallyl malonate (DDM) as substrates (Table 3.1, entry 1 and 10). The initiation rate showed a linear dependence on olefin concentration. Moreover, the rate was ca. 3x faster with EVE than DDM, and 10-100x slower activation with electron-deficient dichloroethylene. From the dependence on the nature and concentration of olefin, the D mechanism was viewed as unlikely. However, the dissociating ether ligand (e.g., the presence of the electron-withdrawing *p*-NO_2 group in **nG**) is also known to have a significant effect on rates of metathesis.[26] In metathesis with EVE, for example, initiation was 3x faster for **nG** in toluene. Plenio concluded that **HII** and **nG** initiate via interchange, rather than dissociative or purely associative pathways, but that it was difficult to distinguish between an I_A or an I_D mechanism. Given the slow rate for the electron-deficient olefin, however, the I_A mechanism was suggested to be more likely.

Similarly, Percy and coworkers[27,28] concluded that interchange (whether I_A or I_D was not specified) or associative mechanisms are favoured over dissociative pathways, in a combined experimental and computational analysis of **HII** and **nG** with EVE[22-24] (Table 3.1, entry 2). They reached the same conclusion in a computational study of ethene, propylene, and 1-hexene (Table 3.1, entry 3 and entry 5-6). That is, in each case, they concluded that an associative or interchange mechanism is favored.[24]

In a 2012 report, again focused on **HII** and **nG**, but with an expanded range of substrates, the Plenio group reported that whether initiation proceeds via interchange-associative or dissociative pathways depends on substrate bulk. For small substrates (e.g. n-butyl vinyl ether (nBuVE), 1-hexene; Table 3.1, entry 7-9), initiation rates showed a linear dependence on substrate concentration at high olefin concentrations (although the dependence was weak at low concentrations). However, saturation kinetics were claimed for bulky substrates such as styrene, DDM and neohexene (Table 3.1, entry 11-13). (The published plots of k_{obs} vs [olefin] show continued increases in k_{obs} even at concentrations approaching 2 M DDM).[21] The authors suggested that this indicates that **HII**-type catalysts initiate via a combination of dissociative and interchange-associative mechanisms.

After Plenio's 2012 report, the idea that **HII**-type catalysts initiate through both dissociative and interchange-associative mechanisms seemed to be widely accepted, with a D pathway being favoured for bulky substrates.

Scheme 3.2 (a) Associative, (b) dissociative and (c) interchange mechanisms for initiation of **HII**

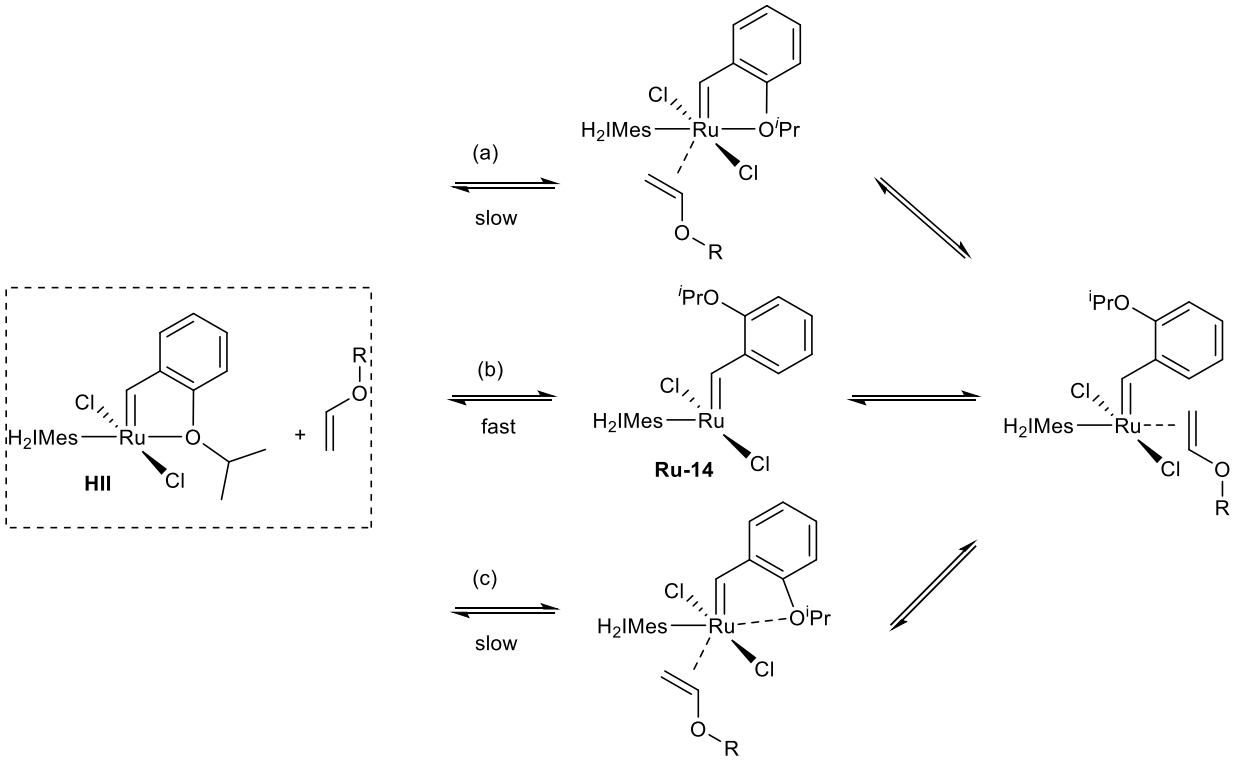

Table 3.1 Summary of proposed initiation mechanisms for **HII** and **nG** catalysts

Entry	Cat.	Substrate	Inferred	Method	PI, Year	Ref.
1	**HII/nG**	EVE	I_A	Experimental	Plenio, 2010	20
2	**HII/nG**	EVE	A or I	Experimental	Percy, 2011, 2013	22,24

3	**HII/nG**	Ethylene	A or I	Computational	Percy, 2013	24
4	**HII/nG**	Ethylene	I_A *	Experimental	Plenio, 2019	29
5	**HII/nG**	Propylene	A or I	Computational	Percy, 2013	24
6	**HII/nG**	1-Hexene	A or I	Computational	Percy, 2013	24
7	**HII/nG**	1-Hexene	I_A *	Experimental	Plenio, 2012	21
8	**HII/nG**	1-Hexene	I_A *	Experimental	Plenio, 2019	29
9	**HII/nG**	nBuVE	I_A *	Experimental	Plenio, 2012	21
10	**HII/nG**	DDM	I_A	Experimental	Plenio, 2010	20
11	**HII/nG**	DDM	D	Experimental	Plenio, 2012	21
12	**HII/nG**	Styrene	D	Experimental	Plenio, 2012	21
13	**HII/nG**	Neohexene, $^tBuCH=CH_2$	D	Experimental	Plenio, 2012	21

*At "low" olefin concentrations (0.01–0.3 M), Plenio suggested that the D pathway dominates.

Additional factors that affect catalyst productivity are deactivation (that is, inhibition) or decomposition. For **HII**-type catalysts, a major deactivating effect is recapture of styrenyl ether ligand (Scheme 3.3). This recapture process (widely described as "boomerang" recapture) was originally proposed by Hoveyda to prolong catalyst lifetime.[17] Since then, there has been debate about whether the boomerang mechanism is operative and how it affects catalyst productivity.

Scheme 3.3 Recapture of styrenyl ether **3** or **3'**

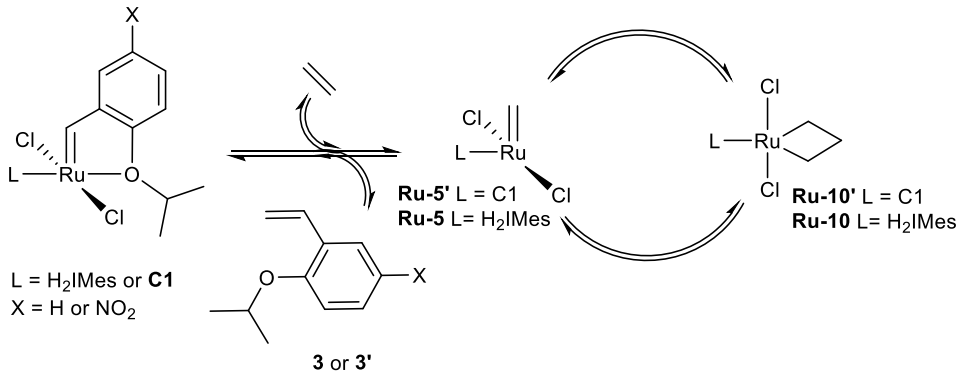

Hoveyda's initial suggestion was based on the discovery that **HII** could be recovered in up to 98% yield after RCM reactions.[30] However, given the high catalyst loadings (5 mol%), the evidence for recapture is weak. That is, if only small portion of the original precatalyst initiated, the rest may simply remain as precatalyst. A subsequent study from Grela and co-workers suggested that labelling studies provide evidence for re-uptake of the styrenyl ether ligand.[31] In these experiments, 1 equiv of the protio-styrenyl ether **3** was added to an RCM reaction in which deuterium-labelled **HII-*d*** was used as catalyst (Scheme 3.4a). After RCM, the recovered catalyst showed only ca. 40% of the *d*-label remaining (**HII-*d***:**HII** = 41:59). A control reaction indicated slow background exchange of **HII-*d*** with styrenyl ether in the absence of substrate. Similar behaviour was observed

for **nG**. From this, Grela inferred that **HII** and **nG** fully initiated in the RCM reaction, then efficiently recaptured the styrenyl ether ligand **3**: that is, boomerang was suggested to be operative for both **HII** and **nG**. As we subsequently noted, however, a flaw in the experiment is the ease with which adventitious **H-D** exchange can "wash out" the label.[32]

A 2010 fluorescence labelling study by the Plenio group[33] instead utilized catalyst **HII'** (Scheme 3.4b), which bears a dansyl tag at the para position of the benzylidene ring. Fluorescence by the dansyl group is quenched in the proximity of the metal, but observed when the styrenyl ether ligand is released. The authors reported observation of strong fluorescence following RCM. This implies that the fluorophore-tagged styrenyl ether is not recaptured, and the authors therefore concluded that the boomerang mechanism is not operative. However, it should be pointed out that fluorophore tag is bound to the styrenyl ether via an electron-withdrawing group, and **HII'** should hence be regarded as a Grela-class, rather than a Hoveyda-class catalyst. Recapture of the styrenyl ether ligand is expected to be less efficient in consequence. Moreover, a major experimental weakness is retention of the ethylene coproduct of metathesis. Ethylene is well known to trigger decomposition of Ru-phosphine and Ru-NHC metathesis catalysts[34-36] via the pathways described in Chapter 1, and this too would prevent recapture of the styrenyl ether ligand.

Scheme 3.4 Studies probing the boomerang mechanism

(a) Grela deuterium-labelling study (graphic reproduced from ref 32)

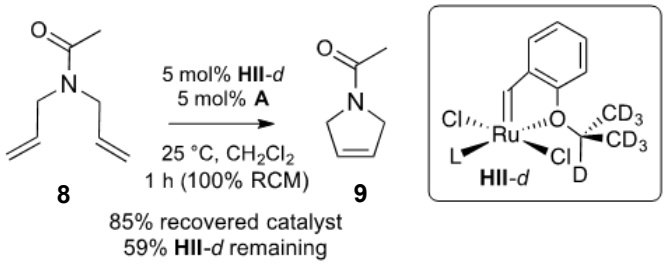

(b) Plenio fluorescence study (graphic reproduced from ref 32)

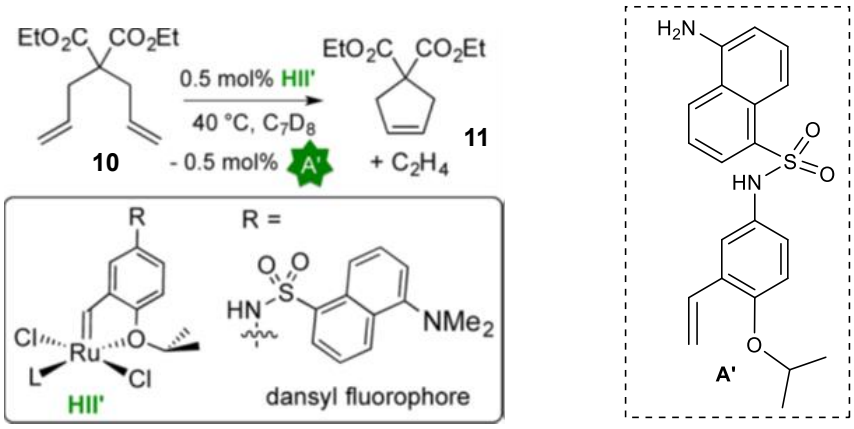

In a more recent report, Jennifer Bates of the Fogg group[32] adopted an isotopic labelling approach building on that of Grela shown in Scheme 3.4 above, but utilizing an α-^{13}C-labelled styrenyl ether to ensure unambiguous isotopic labelling. The alkylidene signal of non-labelled **HII** is a singlet, whereas that for **HII-^{13}C** (^{13}C labelled at the alkylidene carbon) is a doublet arising from $^{1}J_{CH}$ coupling. Two metathesis reactions were undertaken in the presence of one equivalent of labelled **3** per Ru. To establish whether the boomerang mechanism operates within the relatively demanding contexts in which **HII** is arguably most valuable, challenging 1,1- and 1,2-disubstituted olefins were chosen for study. Competition experiments involving metathesis in the presence of added ^{13}C-**3** (Scheme 3.5) showed rate inhibition by **3**, and near-equilibrium proportions of the doublet benzylidene signal within the early stages of reaction. These experiments provide unambiguous evidence for the boomerang mechanism in these demanding metathesis reactions. Whether it is also operative with 1-olefin substrates with more conventional steric and electronic parameters, however, is a question considered in Section 3.2.2 below.

Scheme 3.5 Recapture of ^{13}C-labelled styrenyl ether **3** during (a) RCM of a 1,1-olefin, and (b) cross-metathesis of anethole with methyl acrylate

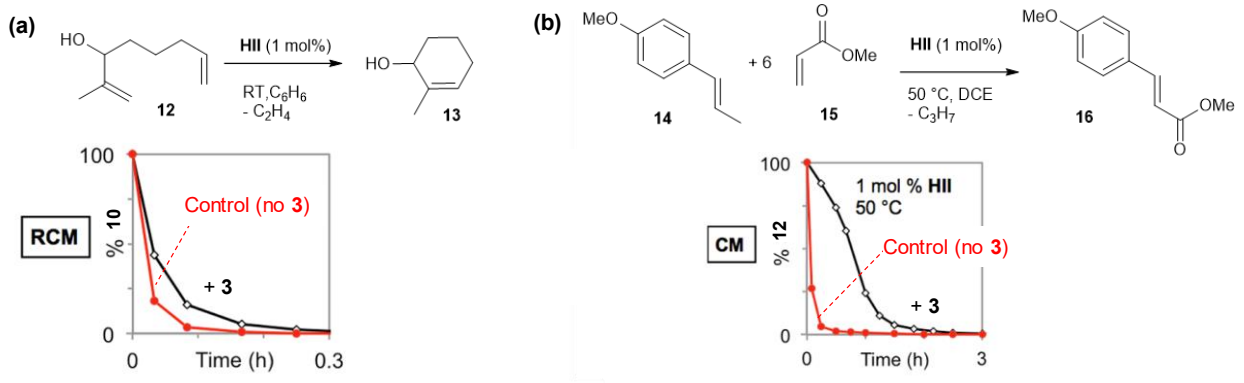

3.2 Results and Discussion

Two lines of study were pursued. Considered first are initiation rates for leading CAAC catalysts containing the C1 ligand, for comparison with the H_2IMes benchmark catalyst **HII**. The second question focuses on re-uptake of the styrenyl ether ligand during conditions of catalysis for sterically accessible 1-olefins.

3.2.1 Assessing initiation rates

In light of Plenio's report that **HII**-type catalysts initiate via primarily a dissociative mechanism in reactions with bulky substrates, we chose tert-butyl vinyl ether (tBuVE; Scheme 3.6) to examine the impact of the carbene ligand on initiation rates. The ruthenium species studied, as noted above, were the **HII-C1** and **nG-C1** catalysts and, for comparison, the H_2IMes system **HII**.

Scheme 3.6 Reaction of Hoveyda- and Grela-class catalysts with tBuVE

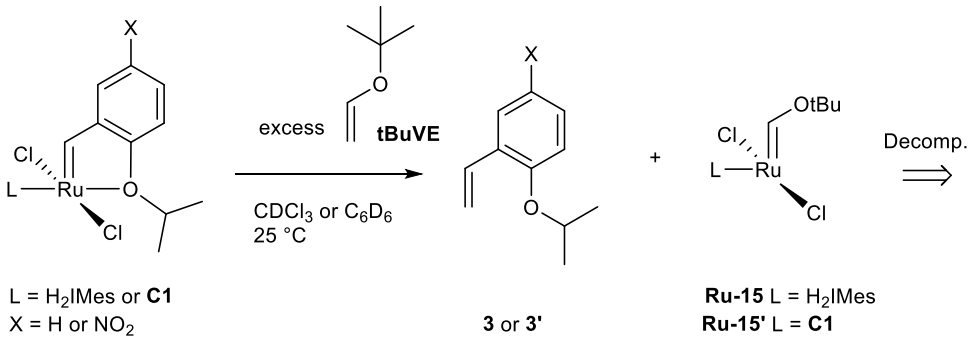

The rates of initiation of these catalysts were examined by NMR spectroscopy at a probe temperature of 25 °C. For each kinetics run, a stock solution was made up of catalyst (38 mM Ru) and an appropriate internal standard. In each case, 0.40 mL of this stock solution was transferred to an NMR tube, and diluted with $CDCl_3$ or C_6D_6 so that the final reaction volume (with the volume of tBuVE taken into account) would be 0.60 mL total. That is, the Ru concentration was maintained at 25 mM for all experiments.

Reactions were carried out in Parafilm-sealed screw-capped NMR tubes, so that the tBuVE reagent could be injected in the NMR room. Samples were permitted to equilibrate in the NMR probe at 25 °C for 10 min, over which time the initial ratio of alkylidene signal against internal standard was measured. Neat tBuVE was then injected, a stopwatch was immediately started, and the sample was rapidly returned to the probe (< 40s) after shaking the tube to effect mixing. The excess of tBuVE used in reactions with **HII** was 20-80 equiv (0.5-2.0 M), or 20-100 equiv (0.5-2.5 M) for **nG-C1**. Because the reaction with **HII-C1** was very slow at 20 equiv tBuVE, rates were instead measured at 40-100 equiv tBuVE (concentration range 1.0-2.5 M). The reaction rate curves are shown in Appendix **B** section.

Pseudo-first order rate constants k_{obs} were obtained by integrating the alkylidene signal vs internal standard over time for at least three half-lives. The pseudo-first order plots for **HII**, **HII-C1**, and **nG-C1** in $CDCl_3$ and C_6D_6 are shown in Figure 3.1-3.3. Shown in Figure 3.4 are the second-order rate plots for all three catalysts. Collected in Table 3.1 are the values of k_1 extracted from the slopes of these second-order plots.

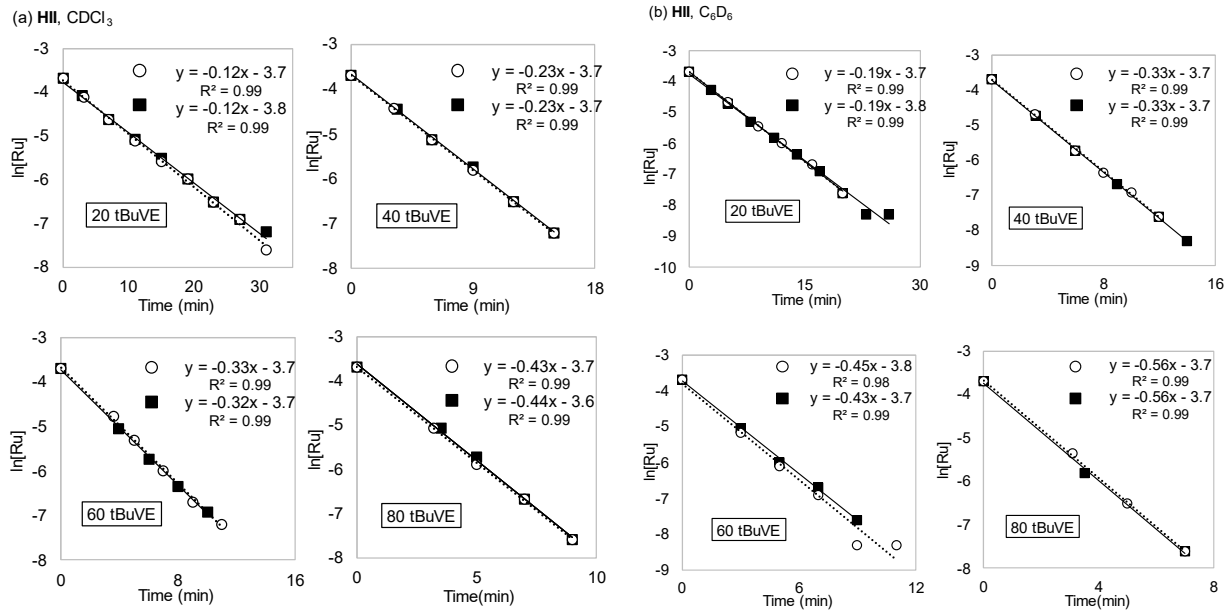

Figure 3.1 Pseudo-first-order plots for **HII** at 25 °C. (a) In $CDCl_3$. (b) In C_6D_6.

(a) **nG-C1**, $CDCl_3$

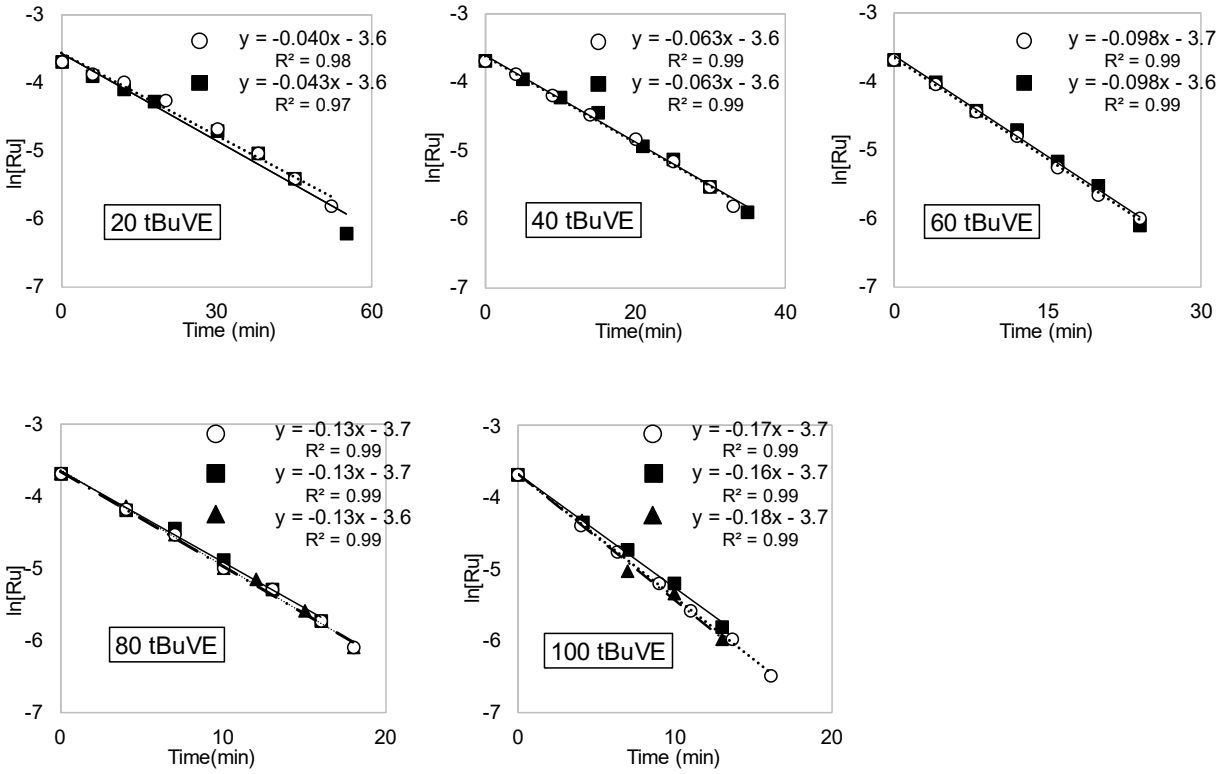

Figure 3.2 Pseudo-first-order plots for **nG-C1** at 25 °C. (a) In $CDCl_3$. (Continued next page).

(b) **nG-C1**, C_6D_6

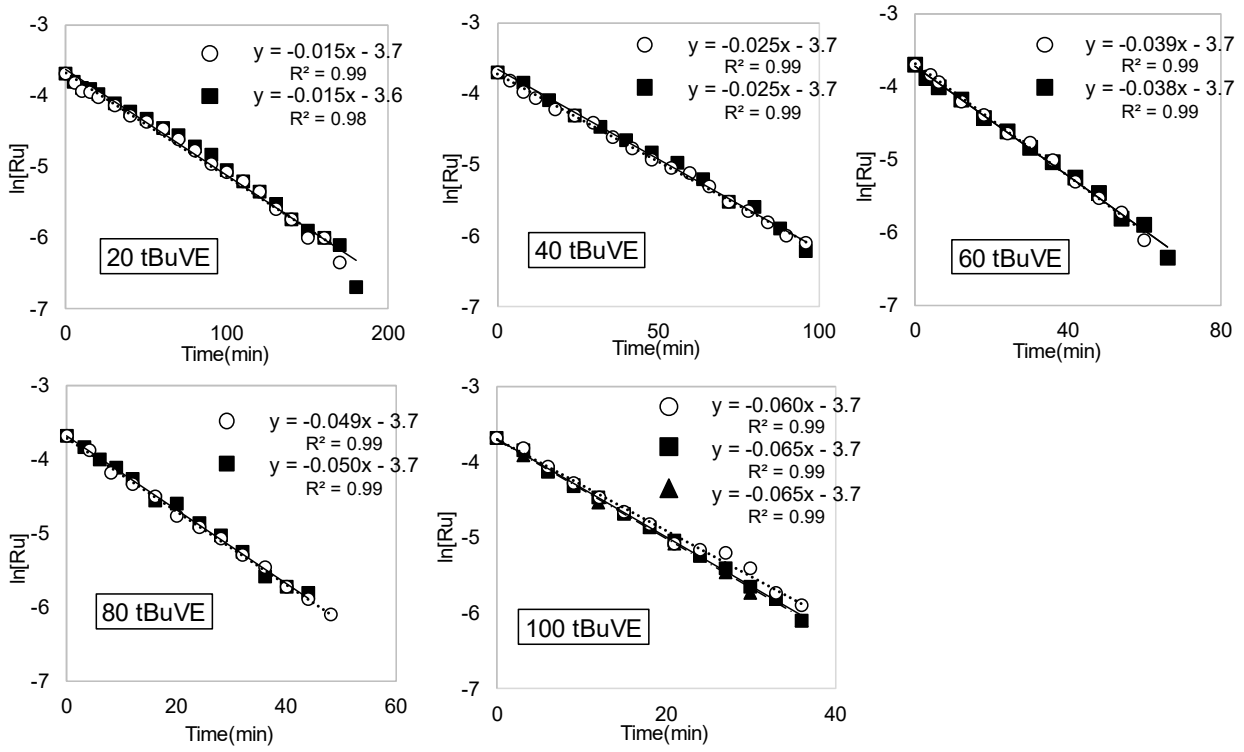

Figure 3.2 Pseudo-first-order plots for **nG-C1** at 25 °C. (Continued from previous page). (b) In C_6D_6.

(a) **HII-C1**, $CDCl_3$

(b) **HII-C1**, C_6D_6

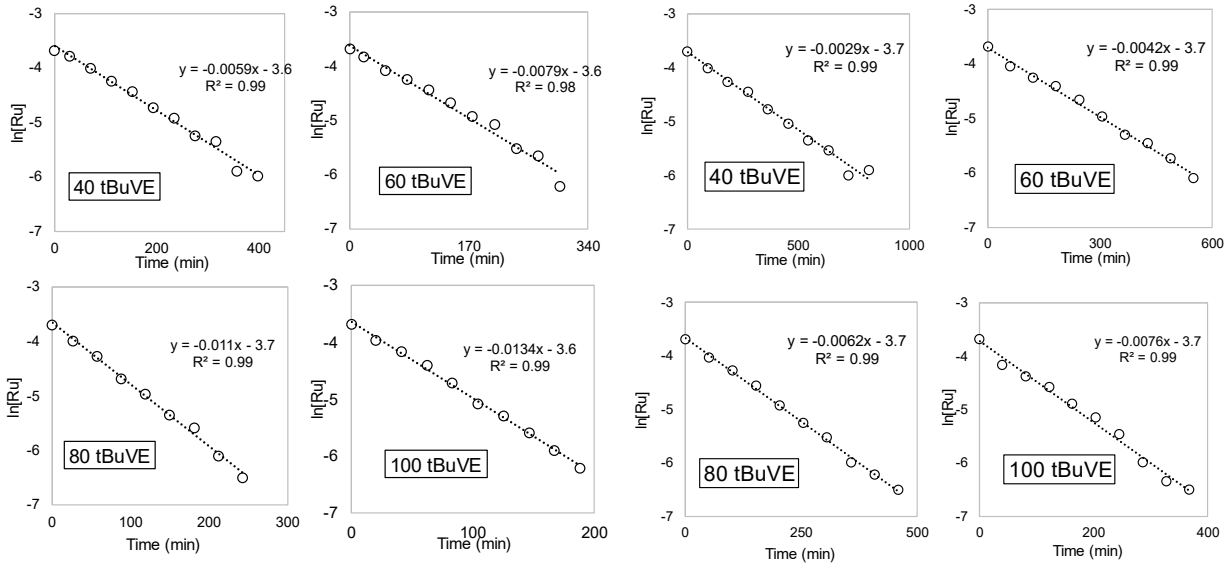

Figure 3.3 Pseudo-first-order plots for **HII-C1** at 25 °C. (a) In $CDCl_3$. (b) In C_6D_6.

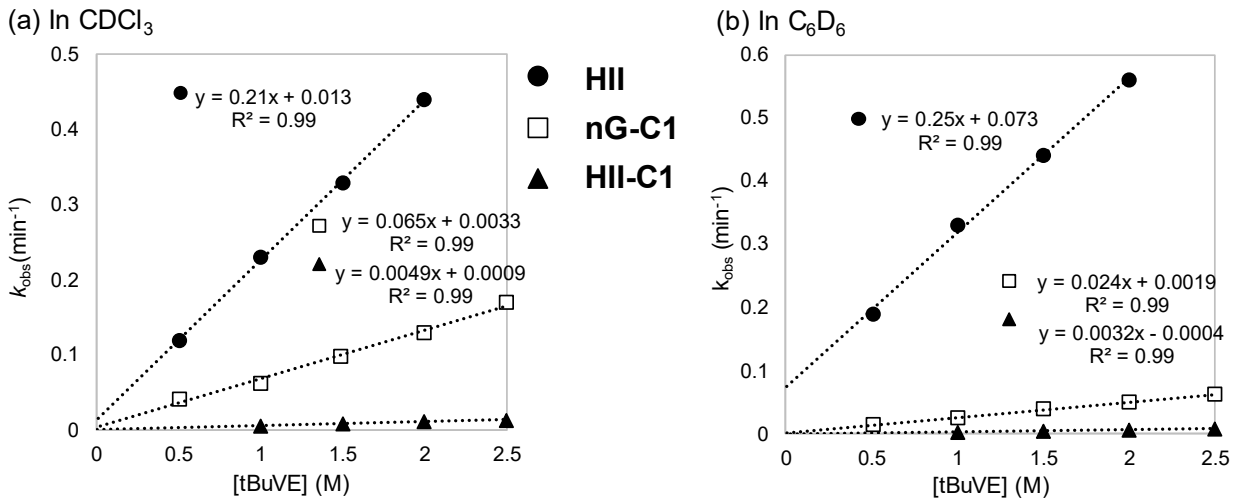

Figure 3.4 Extracting second-order rate constants for metathesis with tBuVE at 25 °C by **HII**, **nG-C1**, and **HII-C1**: $k_{obs} = k_1$[tBuVE]. (a) In $CDCl_3$. (b) In C_6D_6.

Table 3.2 Tabulated initiation rate constants (all experiments at 25 °C)

Entry	Cat.	Substrate	Solvent	k_1 ($s \cdot mol^{-1}L^{-1}$)	k_{rel}	ref
1	**HII**	tBuVE	$CDCl_3$	3.5×10^{-3}	66	this work
2	**HII-C1**	tBuVE	$CDCl_3$	8.2×10^{-5}	1.5	this work
3	**nG-C1**	tBuVE	$CDCl_3$	1.1×10^{-3}	20	this work
4	**HII**	tBuVE	C_6D_6	4.2×10^{-3}	79	this work
5	**HII-C1**	tBuVE	C_6D_6	5.3×10^{-5}	1	this work
6	**nG-C1**	tBuVE	C_6D_6	4.0×10^{-4}	7.5	this work
7	**HII**	EVE	$CHCl_3$	2.31×10^{-2}	-	23
8	**HII**	EVE	C_6H_6	4.60×10^{-2}	-	23

We anticipated that the steric bulk of tBuVE would promote dissociative reaction, enabling clean first-order kinetics. Unexpectedly, however, a linear dependence of k_{obs} on the concentration of tBuVE was evident over a wide concentration range (e.g., 0.5–2.5 M, in the case of **nG-C1**). This is consistent with initiation via an interchange-associative pathway, as is the observed sensitivity of reaction rates to substrate bulk. Thus, for **HII**, the reported rate constants are ca. 7× higher for reaction with EVE than tBuVE (Table 3.2, entry 7 vs 1; 25 °C, $CHCl_3$).[23] Similarly, **HII** initiates 11× faster with EVE than with tBuVE (entry 8 vs 4; 25 °C in benzene).[23] Faster initiation with smaller substrates is consistent with an associative or interchange-associative reaction. However, these data do not distinguish whether initiation or MCB formation is rate-limiting

Of note is the faster initiation of the H_2IMes catalyst relative to the CAAC catalysts. In both $CDCl_3$ and C_6D_6, the trend is **HII** > **nG-C1** > **HII-C1**. In practical terms, **HII** is only 3.3× faster than **nG-C1** (Table 3.2, entry 1 vs 3), meaning that broadly similar initiation rates can be attained for the CAAC and NHC catalysts. Importantly, however, comparison of identical platforms for **HII** and **HII-C1** shows that the latter initiates 43× slower (Table 3.2, entry 1 vs 2) in $CDCl_3$. **nG-C1** initiates 13× faster than **HII-C1** in $CDCl_3$ (Table 3.2, entry 2 vs 3). The difference accords closely with that reported for the H_2IMes analogues: specifically, **nG** is reported to initiate 12× faster than **HII** in CH_2Cl_2 at 25 °C.[24]

While **HII** initiates slightly faster in C_6D_6 than $CDCl_3$, the rates for the CAAC catalysts in the aromatic solvent drop to approximately half. In consequence, the rate difference between **HII** and **HII-C1** is nearly doubled in C_6D_6, with **HII** initiating 79× faster (Table 3.2 entry 4 vs 5). At the same time, the difference between **nG-C1** and **HII-C1** is slightly compressed, from 12× to 7.5× (Table 3.2, entry 5 vs 6).

It may be noted that in toluene, the H_2IMes analogues **nG** and **HII** initiate at surprisingly comparable rates: **nG** is reported to react only 2–3× faster than **HII**, over temperatures ranging from 10–40 °C. In short, differences between the Hoveyda and Grela platforms are dwarfed by differences resulting from the nature of the carbene, and the slower initiation of the **C1** catalysts relative to H_2IMes is particularly dramatic in the aromatic solvent. The reason why CAAC catalysts are faster in chlorinated solvent than aromatic solvent is not clear.

An important question that emerges from these studies is the basis for the intrinsically slower initiation of the CAAC catalysts. Computational data from our Norwegian collaborators (Jensen group, Bergen) indicate that the steric parameters are not very different for H_2IMes and **C1**. Instead, the decisive parameter appears to be the high trans influence of the CAAC ligands,[37] which in the case of the **C1** catalysts explored above inhibits binding of ligands trans to **C1**. While this might at first glance be expected to *accelerate* initiation, it should be recognized that initiation requires not only loss of the styrenyl ether ligand to open a binding site trans to the carbene ligand, but subsequent olefin binding and cycloaddition.

3.2.2 Assessing recapture rates

Prior work by Ms. Jennifer Bates of this research group confirmed recapture of styrenyl ether **3** during **HII**-mediated olefin metathesis, as described in Section 3.1.[32] Uptake of the ^{13}C-labelled isotopologue ^{13}C-**3** was confirmed from the emergence of the characteristic ^{1}H NMR doublet for the [Ru]=^{13}C*H*Ar group, and the inhibiting effect of **3** on metathesis. A weakness, however, was the use of demanding 1,1- or 1,2-disubstitued olefins to test this behaviour. The cross-metathesis reaction of Scheme 3.5b, for example, employed a sterically deactivated 1,2-trans-disubstituted phenylpropene, and an electronically deactivated acrylate. Uptake of the styrenyl ether ligand **3** may thus be strongly favoured.

In the present work, our original plan was to carry out key metathesis reactions, such as RCM of

the prolactone **17** (Scheme 3.7) in the presence of ^{13}C-labelled **3** and **3'**, with the intention of assessing recapture for **HII**, **HII-C1** and **nG-C1**. The use of RCM to synthesize macrocycles is arguably the most topical current application of olefin metathesis in pharma, where mRCM methodologies can give more efficient routes to important antiviral drugs.[38] CAAC catalysts have recently been shown to be extremely productive in mRCM, as noted in the Introduction,[13] and the potential role of ligand re-uptake in their strong performance is thus of compelling interest. Given the challenges in accessing ^{13}C-labelled **3'** described in Chapter 2, however, an alternative approach was adopted to probe uptake. Inhibition of the rate of metathesis by added styrenyl ether offers direct evidence of recapture, and a measure of the capacity of **3** (or **3'**) to compete for reaction with the metal center.

Macrocyclization of prolactone **17** was therefore undertaken in the presence of 1 equivalent of the styrenyl ether ligands relative to the Ru catalyst (Scheme 3.7). The observed rate inhibitions (Figure 3.5) indicate that recapture of **3** and, more unexpectedly, its *p*-nitro analogue **3'**, is operative for **HII**, **HII-C1** and **nG-C1**. The inhibiting effect decreases in the order **HII** > **HII-C1** > **nG-C1**. That is, recapture is more pronounced for the H_2IMes catalyst than the CAAC catalysts, as expected from the higher trans influence of **C1**, which will retard olefin binding. For mRCM in the presence of **3**, **HII** exhibited a 60% drop in mRCM yield at 2 h, vs 39% for **HII-C1**. In comparison, a negligible 7% drop was seen for **3'** + **nG-C1**, consistent with the weaker binding of **3'** with its electron-withdrawing *p*-nitro group.

Scheme 3.7 Probing the inhibiting effect of **3 or 3'** on macrocyclization

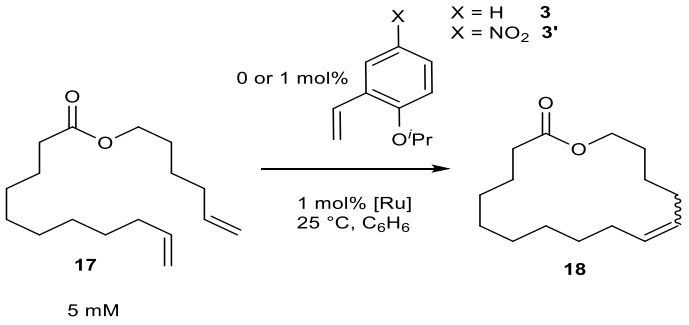

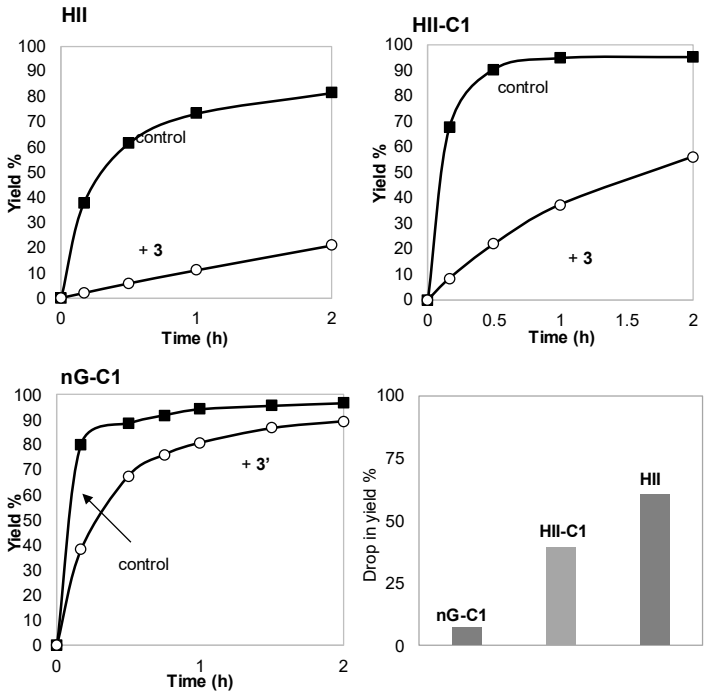

Figure 3.5 Inhibiting effect of added styrenyl ether **3** or nitrostyrenyl ether **3'** on macrocyclization.

Also of note is the ability of added **3** to preserve the catalyst from bimolecular decomposition,[5] consistent with Hoveyda's original proposal[39] that the boomerang mechanism to extends catalyst lifetime. This is evident with the data for **HII-C1**: the control experiment shows a plateau in mRCM from 1-2 h, consistent with complete catalyst decomposition. In contrast, yields continue to increase in the experiment with added **3**, although the rate is slower.

3.3 Conclusions

In the first section, the H_2IMes catalysts were shown to initiate much faster than CAAC catalysts, via an interchange-associative pathway. The reason why CAAC catalysts initiate slower than H_2IMes catalysts has been traced in parallel work to the high trans influence of the CAAC ligand. In the second section, the boomerang mechanism was shown to be operative for both Hoveyda and Grela-class catalysts bearing H_2IMes or the CAAC ligand **C1**. Recapture, as inferred from the rate retardations in mRCM reactions in the presence of styrenyl ether ligand **3**, was most pronounced for the NHC catalyst **HII**, but was also seen for **HII-C1** and, to a small extent, for **nG-C1**. The reduced rate of recapture for **HII-C1** is again consistent with the higher trans influence of the CAAC ligand. Although recapture of **3** slows down metathesis rates, it can also preserve the catalyst from bimolecular decomposition.

In summary, the higher productivity of the CAAC catalysts in mRCM is due to their slow initiation, which inhibits bimolecular decomposition, and their lower affinity for the styrenyl ether ligand, which allows CAAC catalysts to spend more time in the productive catalytic cycle.

3.4 Experimental Details

3.4.1 General procedures

Reactions were carried out under N_2 in a glovebox or Schlenk line unless otherwise noted. HPLC-grade solvents (C_6H_6, *n*-hexane, CH_2Cl_2) were dried and degassed using a Glass Contour solvent purification system, and stored under N_2 over 4 Å molecular sieves for at least 12 h prior to use. NMR solvents ($CDCl_3$ and C_6D_6, Cambridge Isotopes) were freeze/pump/thaw degassed and stored as above. tBuVE was purchased from Sigma-Aldrich (98%), freeze-pump-thaw degassed, and stored in the glovebox freezer (-35 °C). KTp was purchased from TCI (98%). **nG-C1** was kindly supplied by Apeiron Synthesis. Metathesis catalysts **HII** and **HII-C1** were prepared by literature methods, as were diene **17**[40] and macrocycle **18** (the latter being required for GC-FID calibration).[41] NMR experiments were recorded on an AVANCE III 500 MHz NMR spectrometer.

3.4.2 Experimental procedure for catalyst initiation experiments with tBuVE

For the kinetics experiments below, solid catalysts and internal standard were weighed outside the glovebox using an analytical balance for mass accuracy, then transferred into the glovebox.

For **HII** and **nG-C1**, stock solutions of catalyst were made up in 1.00 mL of the NMR solvent. Each stock solution was sufficient for experiments using two different tBuVE ratios. For **HII-C1**, stock solutions of catalyst were made up in 0.50 mL of the NMR solvent. A catalyst stock solution with internal standard was prepared in a screw-capped NMR tube sealed with Parafilm. The initial ratio of alkylidene signal against internal standard was measured. Then, tBuVE (20-100 equiv) was injected into catalyst stock solution neat (final [Ru] = 25 mM). The pseudo-first order rate constants k_{obs} were obtained by integrating the alkylidene signal for the precatalyst against internal standard over time. Each kinetic experiment was monitored over at least three half-lives.

3.4.3 Representative procedure for catalyst initiation in $CDCl_3$

In the glovebox, a stock solution of **HII** (23.5 mg, 0.038 mmol) and anthracene (ca. 1.7 mg, 0.010 mmol, 0.25 equiv) were dissolved in 1.00 mL $CDCl_3$ (stock solution, 38 mM Ru). An aliquot (0.40 mL) was transferred to a NMR tube and another 0.16 mL of $CDCl_3$ was added. After homogenization, the NMR tube was capped with a screw-cap containing a septum and wrapped with parafilm. Then, it was brought outside the glovebox and inserted into the spectrometer, which was set to 25 °C. After thermal equilibration (10 min), the initial ratio between **HII**:anthracene was measured. tBuVE (40 μL, 0.30 mmol, 20 equiv) was injected via a gas-tight syringe and the septum was quickly sealed with Parafilm (final volume: 0.60 mL, [Ru] = 25 mM). The NMR tube was shaken and the timer was immediately started. The decrease in integration of the well-isolated alkylidene signal against the internal standard peak was recorded periodically.

The procedure above was carried out with the other catalysts, with the minor exceptions indicated: **nG-C1 (**25.7 mg, 0.038 mmol), with 1,3,5-trimethoxybenzene (TMB, ca. 1.6 mg, 0.010 mmol, 0.25 equiv**)** as internal standard.

HII-C1 (12.0 mg, 0.0188 mmol), with TMB (ca. 1.5 mg, 0.009 mmol, 0.5 equiv) in 0.50 mL of $CDCl_3$. To a 0.40 mL aliquot diluted with 121 µL of $CDCl_3$ was injected tBuVE (79 µL, 0.60 mmol, 40 equiv) via a gas-tight syringe. The reaction was monitored using the program "kinetic_t_norga".

3.4.4 Catalyst Initiation Experiments in C_6D_6

HII: the procedure described in Section 3.4.3 was carried out in C_6D_6 with dimethyl terephthalate (DMT) as the internal standard, as the aromatic signal of TMB overlaps with the olefinic signal for tBuVE in C_6D_6. **HII** (23.5 mg, 0.038 mmol), DMT (ca. 1.6 mg, 0.008 mmol, 0.21 equiv).

nG-C1: as above. **nG-C1** (25.7 mg, 0.038 mmol); DMT (ca. 0.8 mg, 0.004 mmol, 0.11 equiv).

HII-C1: as above. **HII-C1** (12.0 mg, 0.0188 mmol); TMB (ca. 0.3 mg, 0.002 mmol, 0.1 equiv).

3.4.5 Representative procedure for mRCM (control experiments)

In the glovebox, a stock solution of pro-lactone **17** (100 mg, 0.375 mmol, 1.0 equiv) and dodecane (85 µL, 0.374 mmol, 1.0 equiv) in C_6H_6 (1.81 mL; 2.00 mL in total, 0.188 M) was prepared. An aliquot was removed for GC-FID analysis to establish the starting ratio of substrate to dodecane. 0.40 mL (0.075 mmol) of substrate stock solution was diluted to 15.0 mL (5 mM) in C_6H_6. Catalyst stock solution was prepared as **nG-C1** (8.4 mg, 0.0123 mmol) in 1.00 mL C_6H_6 ([Ru]=12.3 mM).

Then to the stirred substrate solution, 61 µL (0.00075 mmol) of **nG-C1** stock solution was added, and the timer was started. Aliquots were removed periodically from the stirred reaction, quenched with KTp stock solution (10 mg/mL), and analyzed by GC-FID.

3.4.6 Representative procedure for mRCM: styrenyl ether inhibition experiments

The procedure was carried out as in the control experiment, with addition of a solution of **3'** prior to catalyst. From a stock solution of **3'** (19.9 mg, 0.096 mmol) in 1.00 mL of C_6H_6 ([**3'**] = 96 mM) was added a 7.8 µL aliquot (0.00075 mmol, 1.0 equiv to Ru) to the stirred substrate solution, then 61µL of catalyst stock solution (0.00075 mmol) was injected. Aliquots were removed periodically from the stirred reaction, quenched with KTp stock solution (10 mg/mL), and analyzed by GC-FID.

3.5 References

(1) Lummiss, J. A. M.; McClennan, W. L.; McDonald, R.; Fogg, D. E., Donor-Induced Decomposition of the Grubbs Catalysts: An Intercepted Intermediate. *Organometallics* **2014**, *33*, 6738–6741.

(2) McClennan, W. L.; Rufh, S. A.; Lummiss, J. A. M.; Fogg, D. E., A General Decomposition Pathway for Phosphine-Stabilized Metathesis Catalysts: Lewis Donors Accelerate Methylidene Abstraction. *J. Am. Chem. Soc.* **2016**, *138*, 14668−14677.

(3) Amoroso, D.; Yap, G. P. A.; Fogg, D. E., Deactivation of Ruthenium Metathesis Catalysts via Facile Formation of Face-Bridged Dimers. *Organometallics* **2002**, *21*, 3335–3343.

(4) Amoroso, D.; Snelgrove, J. L.; Conrad, J. C.; Drouin, S. D.; Yap, G. P. A.; Fogg, D. E., An Attractive Route to Olefin Metathesis Catalysts: Facile Synthesis of a Ruthenium Alkylidene Complex Containing Labile Phosphane Donors. *Adv. Synth. Catal.* **2002**, *344*, 757–763.

(5) Bailey, G. A.; Foscato, M.; Higman, C. S.; Day, C. S.; Jensen, V. R.; Fogg, D. E., Bimolecular Coupling as a Vector for Decomposition of Fast-Initiating Olefin Metathesis Catalysts. *J. Am. Chem. Soc.* **2018**, *140*, 6931–6944.

(6) Janse van Rensburg, W.; Steynberg, P. J.; Meyer, W. H.; Kirk, M. M.; Forman, G. S., DFT Prediction and Experimental Observation of Substrate-Induced Catalyst Decomposition in Ruthenium-Catalyzed Olefin Metathesis. *J. Am. Chem. Soc.* **2004**, *126*, 14332–14333.

(7) Romero, P. E.; Piers, W. E., Direct Observation of a 14-Electron Ruthenacyclobutane Relevant to Olefin Metathesis. *J. Am. Chem. Soc.* **2005**, *127*, 5032–5033.

(8) Romero, P. E.; Piers, W. E., Mechanistic Studies on 14-Electron Ruthenacyclobutanes: Degenerate Exchange with Free Ethylene. *J. Am. Chem. Soc.* **2007**, *129*, 1698–1704.

(9) Engel, J.; Smit, W.; Foscato, M.; Occhipinti, G.; Törnroos, K. W.; Jensen, V. R., Loss and Reformation of Ruthenium Alkylidene: Connecting Olefin Metathesis, Catalyst Deactivation, Regeneration, and Isomerization. *J. Am. Chem. Soc.* **2017**, *139*, 16609–16619.

(10) Lummiss, J. A. M.; Perras, F. A.; Bryce, D. L.; Fogg, D. E., Sterically-Driven Metathesis: The Impact of Alkylidene Substitution on the Reactivity of the Grubbs Catalysts. *Organometallics* **2016**, *35*, 691–698.

(11) Lummiss, J. A. M.; Higman, C. S.; Fyson, D. L.; McDonald, R.; Fogg, D. E., The Divergent Effects of Strong NHC Donation in Catalysis. *Chem. Sci.* **2015**, *6*, 6739–6746.

(12) Marx, V. M.; Sullivan, A. H.; Melaimi, M.; Virgil, S. C.; Keitz, B. K.; Weinberger, D. S.; Bertrand, G.; Grubbs, R. H., Cyclic Alkyl Amino Carbene (CAAC) Ruthenium Complexes as Remarkably Active Catalysts for Ethenolysis. *Angew. Chem., Int. Ed.* **2015**, *54*, 1919–1923.

(13) Gawin, R.; Tracz, A.; Chwalba, M.; Kozakiewicz, A.; Trzaskowski, B.; Skowerski, K., Cyclic Alkyl Amino Ruthenium Complexes—Efficient Catalysts for Macrocyclization and Acrylonitrile Cross Metathesis. *ACS Catal.* **2017**, *7*, 5443–5449.

(14) Nascimento, D. L.; Gawin, A.; Gawin, R.; Guńka, P. A.; Zachara, J.; Skowerski, K.; Fogg, D. E., Integrating Activity with Accessibility in Olefin Metathesis: An Unprecedentedly Reactive Ruthenium-Indenylidene Catalyst Bearing a Cyclic Alkyl Amino Carbene. *J. Am. Chem. Soc.* **2019**, *141*, 10626–10631.

(15) Blanco, C.; Sims, J.; Nascimento, D. L.; Goudreault, A. Y.; Steinmann, S. N.; Michel, C.; Fogg, D. E., The Impact of Water on Ru-Catalyzed Olefin Metathesis: Potent Deactivating Effects Even at Low Water Concentrations. *ACS Catal.* **2021**, *11*, 893−899.

(16) Scholl, M.; Ding, S.; Lee, C. W.; Grubbs, R. H., Synthesis and Activity of a New Generation of Ruthenium-Based Olefin Metathesis Catalysts Coordinated with 1,3-Dimesityl-4,5-dihydroimidazol-2-ylidene Ligands. *Org. Lett.* **1999**, *1*, 953–956.

(17) Garber, S. B.; Kingsbury, J. S.; Gray, B. L.; Hoveyda, A. H., Efficient and Recyclable Monomeric and Dendritic Ru-Based Metathesis Catalysts. *J. Am. Chem. Soc.* **2000**, *122*, 8168–8179.

(18) Vieille-Petit, L.; Luan, X.; Gatti, M.; Blumentritt, S.; Linden, A.; Clavier, H.; Nolan, S. P.; Dorta, R., Improving Grubbs' II Type Ruthenium Catalysts by Appropriately Modifying the N-Heterocyclic Carbene Ligand. *Chem. Commun.* **2009**, 3783–3785.

(19) Vougioukalakis, G. C.; Grubbs, R. H., HII associative. *Chem. – Eur. J.* **2008**, *14*, 7545–7556.

(20) Vorfalt, T.; Wannowius, K. J.; Plenio, H., Probing the Mechanism of Olefin Metathesis in Hoveyda and Grela Type Complexes. *Angew. Chem., Int. Ed.* **2010**, *49*, 5533 –5536.

(21) Thiel, V.; Hendann, M.; Wannowius, K.-J.; Plenio, H., On the Mechanism of the Initiation Reaction in Grubbs-Hoveyda Complexes. *J. Am. Chem. Soc.* **2012**, *134*, 1104–1114.

(22) Ashworth, I. W.; Hillier, I. H.; Nelson, D. J.; Percy, J. M.; Vincent, M. A., What is the initiation step of the Grubbs-Hoveyda olefin metathesis catalyst? *Chem. Commun.* **2011**, *47*, 5428–5430.

(23) Ashworth, I. W.; Nelson, J. D.; Percy, J. M., Solvent effects on Grubbs' pre-catalyst initiation rates. *Dalton Trans.* **2013**, *42*, 4110-4113.

(24) Ashworth, I. W.; Hillier, I. H.; Nelson, D. J.; Percy, J. M.; Vincent, M. A., Olefin Metathesis by Grubbs–Hoveyda Complexes: Computational and Experimental Studies of the Mechanism and Substrate-Dependent Kinetics. *ACS Catal.* **2013**, *3*, 1929-1939.

(25) Gatti, M.; Vieille-Petit, L.; Luan, X.; Mariz, R.; Drinkel, E.; Linden, A.; Dorta, R., Impact of Solvent Concentration on Ru-Catalyzed RCM. *J. Am. Chem. Soc.* **2009**, *131*, 9498–9499.

(26) Michrowska, A.; Bujok, R.; Harutyunyan, S.; Sashuk, V.; Dolgonos, G.; Grela, K., Nitro-Substituted Hoveyda-Grubbs Ruthenium Carbenes: Enhancement of Catalyst Activity through Electronic Activation. *J. Am. Chem. Soc.* **2004**, *126*, 9318–9325.

(27) Engle, K. M.; Lu, G.; Luo, S.-X.; Henling, L. M.; Takase, M. K.; Liu, P.; Houk, K. N.; Grubbs, R. H., Origins of Initiation Rate Differences in Ruthenium Olefin Metathesis Catalysts Containing Chelating Benzylidenes. *J. Am. Chem. Soc.* **2015**, *137*, 5782−5792.

(28) Griffiths, J. R.; Keister, J. B.; Diver, S. T., From Resting State to the Steady State: Mechanistic Studies of Ene−

Yne Metathesis Promoted by the Hoveyda Complex. *J. Am. Chem. Soc.* **2016**, *138*, 5380−5391.

(29) Peschek, N.; Wannowius, K.-J. r.; Plenio, H., The Initiation Reaction of Hoveyda−Grubbs Complexes with Ethene. *ACS Catal.* **2019**, *9*, 951−959.

(30) Van Veldhuizen, J. J.; Garber, S. B.; Kingsbury, J. S.; Hoveyda, A. H., A recyclable chiral Ru catalyst for enantioselective olefin metathesis. Efficient catalytic asymmetric ring-opening/cross metathesis in air. *J. Am. Chem. Soc.* **2002**, *124*, 4954–4955.

(31) Bieniek, M.; Michrowska, A.; Usanov, D. L.; Grela, K., An Attempt to Provide a User's Guide to the Galaxy of Benzylidene, Alkoxybenzylidene, and Indenylidene Ruthenium Olefin Metathesis Catalysts. *Chem. – Eur. J.* **2008**, *14*, 806–818.

(32) Bates, J. M.; Lummiss, J. A. M.; Bailey, G. A.; Fogg, D. E., Operation of the Boomerang Mechanism in Olefin Metathesis Reactions Promoted by the Second-Generation Hoveyda Catalyst. *ACS Catal.* **2014**, *4*, 2387−2394.

(33) Vorfalt, T.; Wannowius, K. J.; Thiel, V.; Plenio, H., How Important Is the Release–Return Mechanism in Olefin Metathesis? *Chem. – Eur. J.* **2010**, *16*, 12312–12315.

(34) Monfette, S.; Eyholzer, M.; Roberge, D. M.; Fogg, D. E., Getting RCM Off the Bench: Reaction-Reactor Matching Transforms Metathesis Efficiency in the Assembly of Large Rings. *Chem. – Eur. J.* **2010**, *16*, 11720–11725.

(35) Lysenko, Z.; Maughon, B. R.; Mokhtar-Zadeh, T.; Tulchinsky, M. L., Stability of the First-Generation Grubbs Metathesis Catalyst in a Continuous Flow Reactor. *J. Organomet. Chem.* **2006**, *691*, 5197–5203.

(36) Burdett, K. A.; Harris, L. D.; Margl, P.; Maughon, B. R.; Mokhtar-Zadeh, T.; Saucier, P. C.; Wasserman, E. P., Renewable Monomer Feedstocks via Olefin Metathesis: Fundamental Mechanistic Studies of Methyl Oleate Ethenolysis with the First-Generation Grubbs Catalyst. *Organometallics* **2004**, *23*, 2027–2047.

(37) Nascimento, D. L.; Foscato, M.; Occhipinti, G.; Jensen, V. R.; Fogg, D. E., Bimolecular Coupling in Olefin Metathesis: Correlating Structure and Decomposition for Leading and Emerging Ruthenium-Carbene Catalysts. *J. Am. Chem. Soc.* **2021**, 143, 11072-11079.

(38) (a) Higman, C. S.; Lummiss, J. A. M.; Fogg, D. E. *Angew. Chem., Int. Ed.* **2016**, *55*, 3552–3565. (b) Farina, V.; Horváth, A., Ring-Closing Metathesis in the Large-Scale Synthesis of Pharmaceuticals. In *Handbook of Metathesis*, Grubbs, R. H.; Wenzel, A. G., Eds. Wiley-VCH: Weinheim, 2015; Vol. 2, pp 633–658. (c) Fandrick, K. R.; Savoie, J.; Jinhua, N. Y.; Song, J. J.; Senanayake, C. H., Challenges and Opportunities for Scaling the Ring-Closing Metathesis Reaction in the Pharmaceutical Industry. In *Olefin Metathesis – Theory and Practice*, Grela, K., Ed. Wiley: Hoboken, 2014; pp 349-366.

(39) Kingsbury, J. S.; Harrity, J. P. A.; Bonitatebus, P. J.; Hoveyda, A. H., A Recyclable Ru-Based Metathesis Catalyst. *J. Am. Chem. Soc.* **1999**, *121*, 791–799.

(40) Bates, J. M. Ruthenium Catalysts for Olefin Metathesis: Understanding the Boomerang Mechanism and Challenges Associated with Stereoselectivity. M.Sc. Dissertation, University of Ottawa, Ottawa, ON, 2014.

(41) Monfette, S. From Analysis of Ligands Effects to Reactor Design: A Rational Approach to Efficient Macrocyclization via Ring-Closing Metathesis. Ph.D., University of Ottawa, Ottawa, 2010.

Chapter 4. Conclusions and Future Work

The past few years have seen tremendous advances in both synthesis and applications of ruthenium catalysts for olefin metathesis. The Grubbs-class phosphine-stabilized catalysts, despite their groundbreaking role in putting metathesis methodologies into the hands of organic chemists, have now largely been displaced by phosphine-free catalysts. This change is due to a large body of mechanistic and synthetic work demonstrating that the nucleophilic, non-labile PCy_3 ligand limits catalyst productivity. The phosphine-free second generation Hoveyda and Grela catalysts (**HII** and **nG**) have become popular catalyst platforms in consequence. However, over the past six years, catalysts bearing the new cyclic alkyl amino carbene (CAAC) ligands – in particular, **HII-C2** and **nG-C1** – have drawn much attention for their breakthrough productivity in ethenolysis and macrocyclization.

The key difference between the Hoveyda and Grela catalyst lies in the nature of the H_2C=CHAr "styrenyl ether" ligand. In the Hoveyda catalysts, the Ar ligand is C_6H_4-2-O^{i}Pr (**3**); in the Grela catalysts, an NO_2 substituent is *para* to the ether oxygen. A major question in this thesis was the impact of these two styrenyl ether ligands on entry into the active cycle for the CAAC vs the H_2IMes catalysts, and recapture of the four-coordinate methylidene active species by the free styrenyl ether, H_2C=CHAr to regenerate the precatalyst.

The first part of this thesis assesses the strengths and weaknesses of the synthetic methods required to produce high yielding, pure Hoveyda- and Grela-class catalysts, including their **C1** derivatives. The first part of Chapter 2 focused on the synthetic routes used to access the key styrenyl ether ligands H_2C=CHAr, and the potential to extend these routes to synthesis of the α-^{13}C isotopologues. The latter would enable synthesis of an **nG** isotopologue bearing a ^{13}C label at the alkylidene carbon. Use of ^{13}C-labelled **nG** was envisioned as a means of probing both catalyst initiation and recapture (the subject of Chapter 3), using an approach developed by Jennifer Bates of the Fogg group with ^{13}C-labelled **HII**.

The most widely used route to **3/3'** involves an alkylation-Wittig sequence beginning with 2-hydroxybenzaldehyde (Scheme 4.1a). Despite the virtue of its brevity and its good overall yield for **3** (ca. 70%; 50% for **3'**), it cannot be used to access the isotopically-labelled analogues, as the ^{13}C-labelled 2-hydroxybenzaldehyde is not commercially available.

Scheme 4.1 Routes to **3** or **3'** (X = H or NO_2; ^{13}C label indicated with an asterisk)

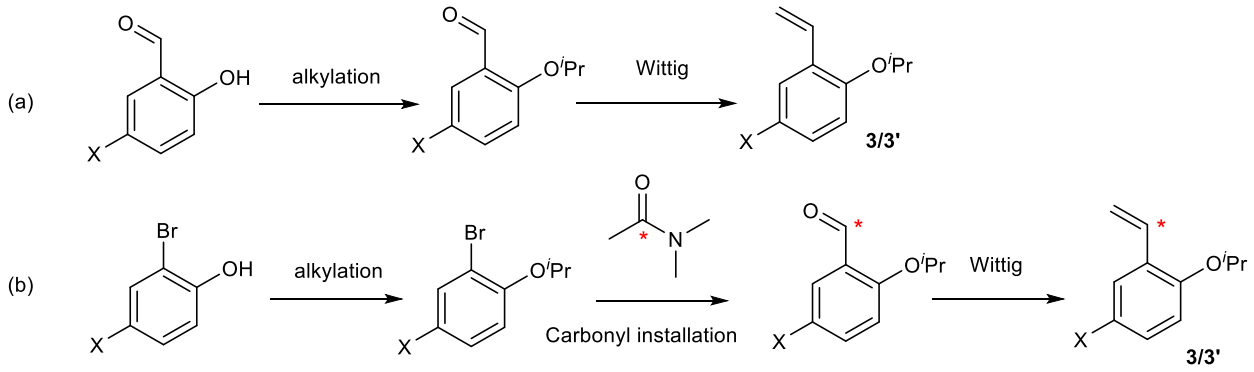

Preparation of the latter was therefore undertaken, via alkylation of 2-hydroxybromobenzene, installation of the carbonyl group using DMF (this permitting, in principle, extension of ^{13}C-DMF) and finally the Wittig reaction (Scheme 4.1b). While this route was successfully used to access **3** in 45% overall yield, extension to **3'** failed, owing to the sensitivity of the nitro substituent to the *n*-BuLi required for carbonyl installation. Attempts to use a less aggressive reagent (^{i}PrMgCl/LiCl) also failed. In the interests of time, synthesis of ^{13}C-labelled **3'** was therefore abandoned, and an alternative approach was ultimately used to tackle the questions of initiation and recapture in Chapter 3. Future work could involve synthesis from 2-isopropoxy-5-nitrobenzaldehyde (**5'**) utilizing a Grignard reagent such as PhMgCl to install the carbonyl group and access **2'** (Scheme 4.2).

Scheme 4.2 Potential alternative synthesis of ^{13}C-labelled **2'** (^{13}C label indicated with an asterisk)

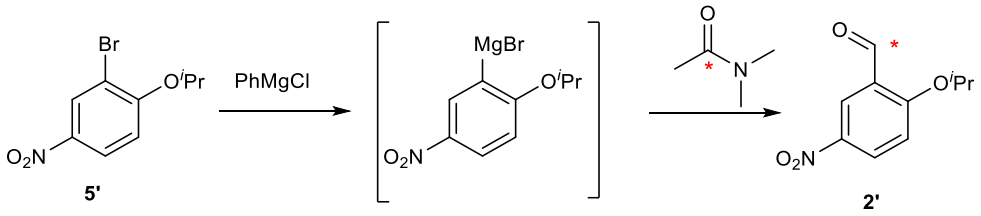

The second half of Chapter 2 focused on analysis of the common routes used to synthesize **HII** and **nG**, and their **C1** analogues. Common routes to H_2IMes catalysts begin with the PCy_3 complexes **GII** and the indenylidene complex **Ind-II**, which are subjected to cross-metathesis and ligand exchange with **3** or **3'**. The need for workup via column chromatography is both inconvenient, and unsatisfactory in terms of losses of material. In the present work, this approach resulted in yields of ca. 75% and 55% for **GII** and **Ind-II**, respectively. The lower yield for the latter is likely due to the low lability of PCy_3 in **Ind-II**, which requires use of higher temperatures (75 °C, vs 30 °C for **GII**), increasing risk of catalyst decomposition. These findings reinforce the advantages of a workup procedure developed by members of our group, in which a Merrifield resin is used to scavenge free PCy_3 ligand. **GII** is a convenient precursor when (as at the outset of the

present study) it is available in abundance. However, greater net efficiency in synthesis of **HII** is attainable using a route developed concurrently with the study above, in which the dimer [$RuCl_2$(*p*-cymene)]$_2$ is treated with free H_2IMes and diazo-styrenyl ether ligand. Extension of that chemistry to the CAAC derivatives is under study by Ms. Eliza-Jayne Boisvert of this research group.

Current routes to the CAAC analogues, in contrast, commence with the indenylidene precursor $RuCl_2(PPh_3)_2$(Ind), rather than Grubbs-class catalysts. Grubbs-class catalysts bearing a CAAC ligand have not been reported: instead, attempts to install a CAAC yield the bis-CAAC indenylidene complex $RuCl_2(CAAC)_2$(Ind) (e.g., **UC-C1**). The latter complexes are reported to serve as precursors to Hoveyda- and Grela-class catalysts bearing CAAC ligands. However, great difficulties were encountered in attempting to reproduce the literature route involving transformation of **Ind-0** to **UC-C1**. The published route relies on generation of free **C1** at 80 °C in toluene. Even after optimization (including generating **C1** at ambient temperature in THF), yields of **UC-C1** were limited to ca. 35%, compared to reported yields of 60%.

The reported routes to **HII-C1** involve ligand exchange of **HI** with in-situ generated **C1**, or cross-metathesis of **UC-C1** with **3**. Both were found to proceed in moderate yields of ca. 40%. For **nG-C1**, the corresponding ligand-exchange reaction of **nGI** to **nG-C1** was shown to fail, probably because free **C1** attacks the nitro substituent on **nGI**, triggering decomposition. The sole route to **nG-C1** is thus the literature route via cross-metathesis of **UC-C1** with **3'**, despite the limitations in reliability and yield noted above. Problems in the synthesis of CAAC catalysts inferred in Chapter 2 include the following. First, impurities associated with in situ generation of the free CAAC may cause decomposition of the Ru precursor. Second, the requirement of chromatography for workup may cause loss of product. Another weakness in the synthesis of CAAC catalysts is the identification of fully generation of the free CAAC. It is more reasonable to monitor the CAAC salt deprotonation by NMR. Development of an improved route to the CAAC catalysts would be a significant advance. Particularly attractive would be transformation of the *p*-cymene Ru dimer into $RuCl_2$(*p*-cymene)(CAAC) derivatives. A potential problem with this route is the instability of free CAACs for the ligands of interest. Isolation of leading CAAC ligands such as **C1** and **C2** has not been reported, although the Bertrand group has described the successful isolation of bulkier CAACs, which were found to exhibit impressive stability as the free CAACs. The protocols described may aid in isolating **C1** or **C2** in future work. As a minor but important point, deliberate synthesis of the carbene dimers should be undertaken to identify their NMR signatures. Similarly, their decomposition products on exposure to water should be characterized. With these NMR data in hand, it will be much easier to identify the reason for failed reactions: that is, whether more rigorous drying is required, or whether CAAC dimerization is the problem. As well, the Merrifield resin route holds potential in the current routes: using the resin to trap PCy_3 would avoid column chromatography and associated losses in yield during workups.

The second part of this thesis examined how the alkylidene and carbene ligands (the latter including both CAAC and NHC ligands) affect entry and exit of Hoveyda- and Grela-class

catalysts from the active cycle. Chapter 3 turns to the question about how initiation and recapture of the styrenyl ether ligan affect catalyst productivity. In the first part of Chapter 3, the initiation of **HII, HII-C1, and nG-C1** was examined. Chosen for study was the bulky substrate *tert*-butyl vinyl ether (tBuVE), to test if dissociative mechanism is operative for Hoveyda- and Grela-class catalysts. The linear dependence of k_{obs} on [tBuVE], as well as the impact of the *p*-nitro substituent on initiation rate, support an interchange-associative (I_A) mechanism. A systematic comparison of initiation rate constants in chlorinated and aromatic solvents ($CDCl_3$, C_6D_6) indicated that **HII-C1** initiates 40x times slower than **HII**, and **nG-C1** initiates 3x times slower than **HII** in $CDCl_3$. In C_6D_6, the difference was magnified (being 79x slower for **HII-C1** than **HII**, and 10x slower for **nG-C1** than **HII**), for reasons that are not yet clear.

The second part of Chapter 3 examined recapture of **3** or **3'** for **HII**, **HII-C1** and **nG-C1**. Specifically, the inhibiting effect of **3** or **3'** in mRCM of prolactone **17** was examined. The kinetic plots of control and inhibition experiments suggest that "boomerang" recapture of the styrenyl ether ligand is operative for both Hoveyda- and Grela-class catalysts. The inhibiting effect decreases in the order **HII** > **HII-C1** > **nG-C1**. That is, recapture is more pronounced for the H_2IMes catalyst than the CAAC catalysts, meaning the latter spend more time in their active form. This contributes to the higher productivity of the CAAC catalysts than NHC catalysts. Slower initiation may be an important asset for the CAAC catalysts, preserving them from bimolecular decompostion.

Future work could involve first, examining initiation rate constants and inhibition effects for **nG.** Second, the initiation experiments do not distinguish whether the rate-limiting step is ether de-chelation, olefin binding or cycloaddition. To probe this question, computational study might be helpful. Third, the reason why CAAC catalysts initiates more slowly than NHC catalysts and why CAAC catalysts exhibit lower affinity to **3** or **3'** is an important point. This appears almost certainly due to the high trans effect of the CAAC ligand, as described in studies by Occhipinti, Jensen, and Fogg.

Direct NMR evidence for the "boomerang" recapture of the styrenyl ether ligand for the Grela catalyst was not obtained in this thesis work, because of the failed attempts to synthesize ^{13}C-labelled **3'**. An alternative method could involve synthesis of a ^{13}C-labelled styrenyl ether ligand bearing another electron-withdrawing group in place of the nitro group.

5. Appendices

A. NMR Spectra

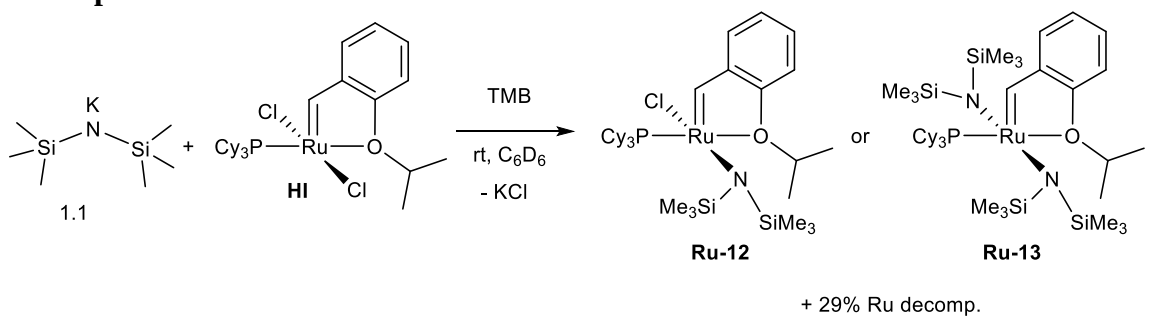

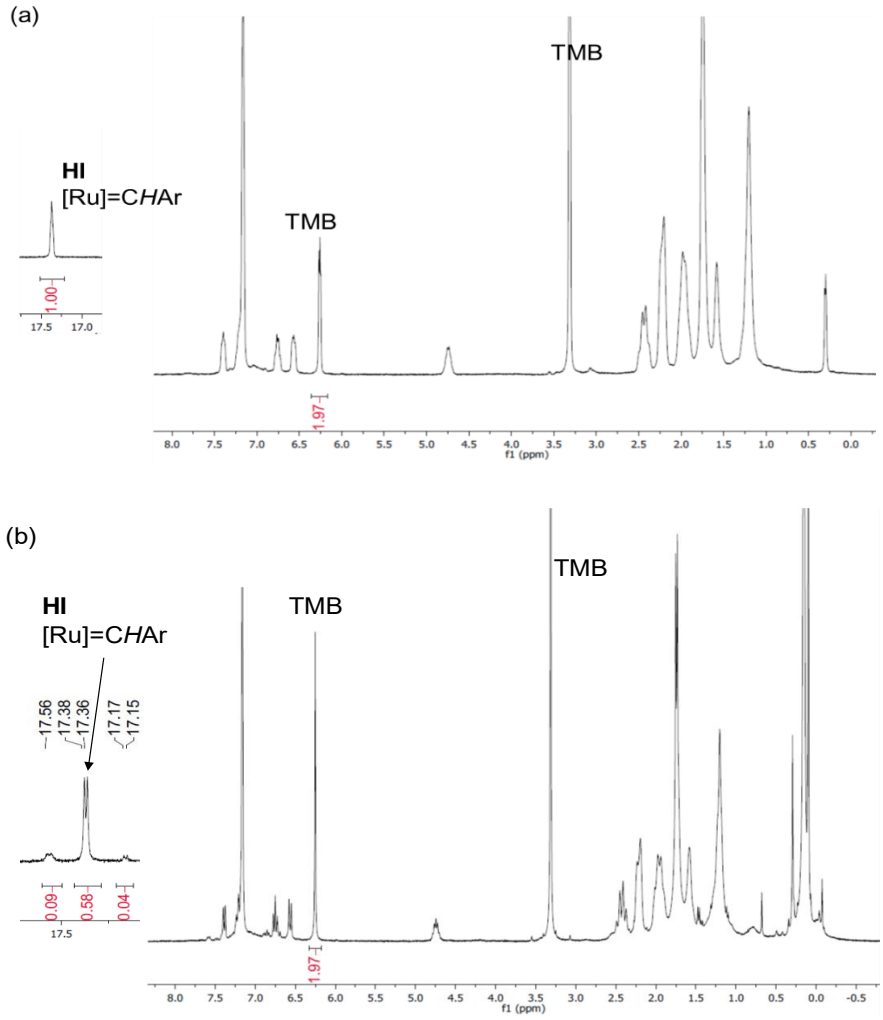

Figure A1. ^{1}H NMR spectra (300 MHz, C_6D_6) Decomposition of **HI** by KHMDS (a) Initial spectrum, before adding KHMDS. (b) Spectrum taken 30 min after adding KHMDS, showing only 58% **HI** remaining (The other two signals account for 9% and 4% respectively, were not assigned).

B. Rate curves

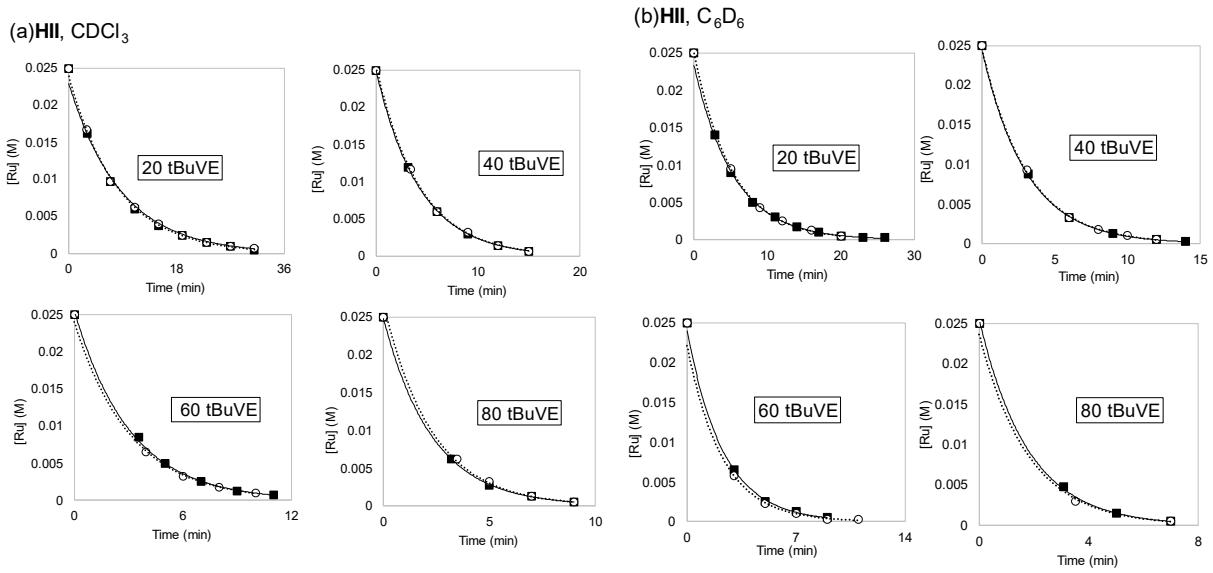

Figure B1. Initiation rate curves for **HII** at 25 °C. (a) In $CDCl_3$. (b) In C_6D_6.

(a)**nG-C1**, $CDCl_3$

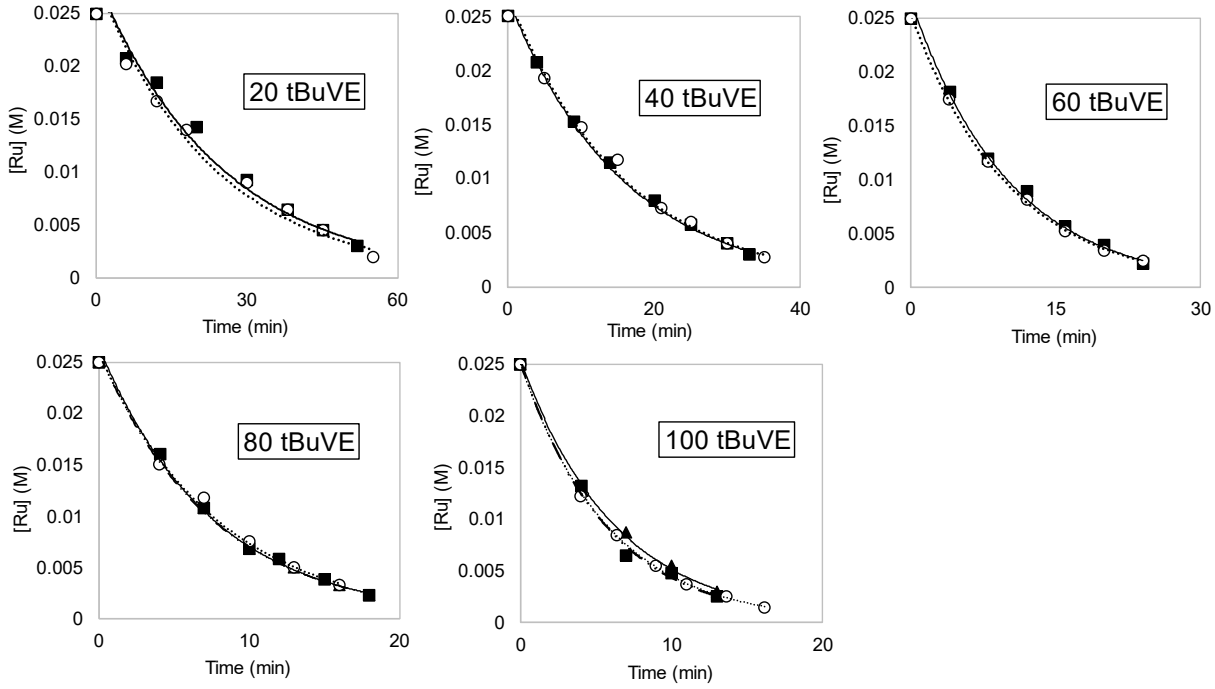

Figure B2. Initiation rate plots for **nG-C1** at 25 °C. (a) In $CDCl_3$. (Continued next page).

(b)**nG-C1**, C_6D_6

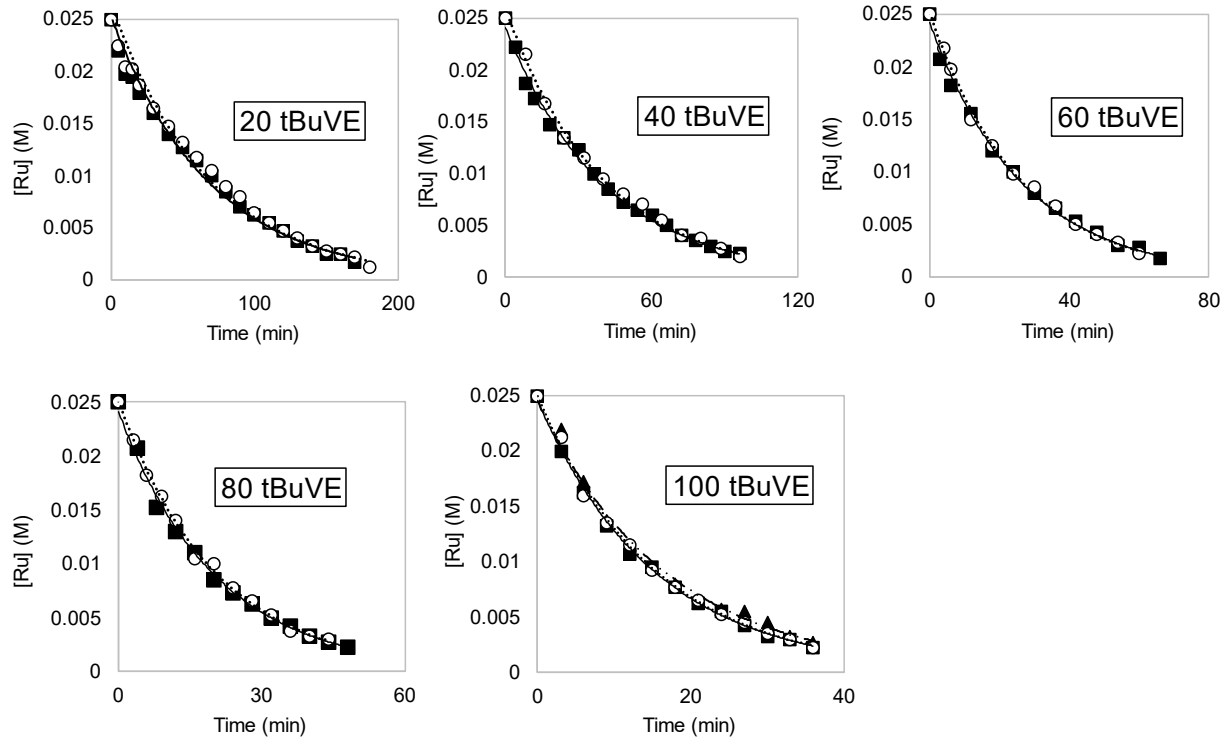

Figure B2. Initiation rate curves for **nG-C1** at 25 °C. (Continued from previous page). (b) In C_6D_6.

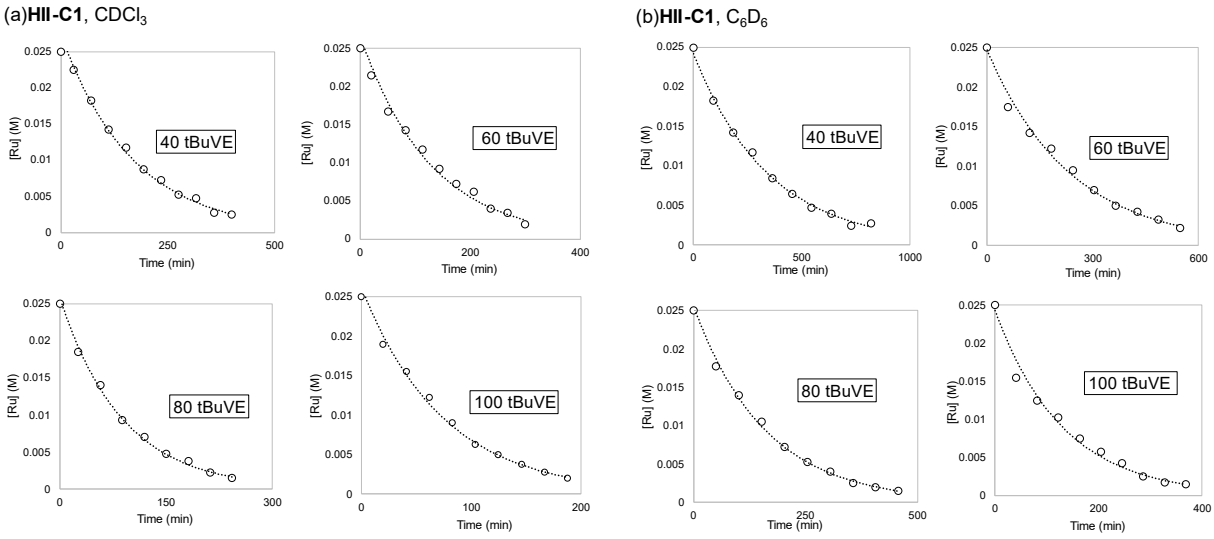

Figure B3. Initiation rate curves for **HII-C1** at 25 °C. (a) In $CDCl_3$. (b) In C_6D_6.